SPARC newsletter n° 21
2003
July
STRATOSPHERIC PROCESSES AND THEIR ROLE IN CLIMATE
A Project of the World Climate Research Programme

Report on the 23rd Session of the Joint Scientific Committee (JSC) for the World Climate Research Programme (WCRP)

Reading, United Kingdom, March 17-21, 2003

Alan O'Neill, Data Assimilation Research Centre, Reading, UK (alan@met.reading.ac.uk)

The JSC of the World Climate Research Programme held its 23rd annual meeting during 17-21 March at the University of Reading, UK. The co-chairs of SPARC, A. O'Neill and A.R. Ravishankara, attended on behalf of SPARC. The meeting was an especially important one for SPARC to air its views, since the scientific direction and structure of WCRP was being considered. The meeting considered a major new effort on the prediction and predictability of seasonal to interdecadal climate variations, reaffirming WCRP's original aims: to determine to what extent climate can be predicted; and to determine the extent of man's influence on climate. It was also proposed the JSC should investigate the feasibility of a Global Climate Experiment. Specifically, the idea for a decade long observational programme was proposed to exploit to the full all the new satellite instruments that are, or soon will be, available.

SPARC's new scientific themes fit in very well with the proposed evolution of WCRP. They recognise the need for a closely integrated effort with other projects in WCRP. **A. O'Neill** opened SPARC's presentation to the JSC by emphasising the science-oriented nature of SPARC's activities, and the responsiveness of SPARC to the needs of international bodies, such as WMO/UNEP and the IPCC. He noted that recent achievements included the completion of a SPARC reference climatology (led by **W. Randel**), and strong participation in the WMO/UNEP Ozone Assessment 2002.

He then outlined SPARC's future themes: stratospheric chemistry and climate; detection and attribution of past stratospheric changes; and stratosphere-troposphere coupling. These scientific themes are underpinned by targeted supporting activities: model development, process studies and data. Working groups are being established to advance these themes. The SPARC Data Center will continue to be an important resource for the community, linking in with the developing activities of the SPARC Data Assimilation Working Group. **A. O'Neill** expressed the sadness felt by the SPARC community about the tragic death of **P. Udelhofen**, who had done so much to place the SPARC Data Center on a secure footing.

He noted that the SPARC Office provided essential support for the project, and mentioned that discussions are under way to relocate the Office when the long-standing support provided by CNRS ends in spring 2004.

His presentation continued with a summary of the links between SPARC and other WCRP projects. Existing links with WGNE (e.g. on data assimilation) and WGCM (e.g. on coupled chemistry-climate modelling) are being strengthened, and closer links are needed with CLIVAR (e.g. on predictability), GEWEX

Contents

(on water vapour, the hydrological cycle and radiation), ACSYS/CliC (on studies of polar regions) and WGSIP (on seasonal and inter-annual prediction). SPARC is playing an active role in strengthening these links. **A. O'Neill** noted that the SPARC 3rd General Assembly in 2004, Victoria (BC), Canada, was located, and will be structured, to encourage participation of the wider climate community.

A.R. Ravishankara delivered the second part of the SPARC presentation to the JSC, focusing on the new theme of chemistry-climate interactions, and a joint venture in this area with the IGBP Global Atmospheric Chemistry (IGAC) project. The list of topics that would benefit from such a collaboration is large, including: the role of aerosols and clouds in chemistry and climate, the role of convection in controlling UT/LS water and chemical constituents, and the extent and role of stratosphere-troposphere exchange in controlling the abundances of ozone and other species in UT/LS region. **A.R. Ravishankara** noted the success of a current SPARC-IGAC collaboration on laboratory data, which led to a peer-reviewed paper. He mentioned that a joint SPARC-IGAC workshop was planned in April 2003, at Giens, France, to further define the programme, and that the main recommendations of this workshop were presented at the joint meeting of the AGU and EGS in Nice later in the month.

The SPARC presentations were very well received by the JSC. The JSC approved the new formulation of SPARC and its science goals. It welcomed the ongoing efforts in the joint IGBP/WCRP atmospheric chemistry-climate initiative, and supported the planned efforts in this direction, including the joint SPARC/IGAC workshop in April 2003. The JSC further recommended that its members help identify financial support for the SPARC 3rd General Assembly (1-6 August 2004, Victoria, Canada).

Highlights from the Joint SPARC-IGAC Workshop on Climate-Chemistry Interactions

Giens, France, 02-06 April, 2003

A.R. Ravishankara, NOAA, Boulder, USA (ravi@noaa.gov)
S. Liu, Institute of Earth Science, Taipei Tawain, China (shawliu@earth.sinica.edu.tw)
With inputs from **I. Bey, K. Carslaw, M. Chipperfield, A. Douglass, D. Hauglustaine, C. Mari, K. Rosenlof, T. Shepherd, and P. Simon**

Participants at the "Joint SPARC-IGAC Workshop on Climate-Chemistry Interactions, in Giens, France.

Many agents force Earth's climate. Changes in these agents or forcings can perturb the climate significantly. Atmospheric chemistry plays a critical role in the perturbation of climate by controlling the magnitudes and distributions of a large number of important climate forcing agents. For example, abundances and distributions of methane and ozone depend critically on the atmospheric chemistry. According to IPCC (2001), these two trace gases are the second and third most important greenhouse gases (GHGs) that have increased due to anthropogenic activities since the industrial revolution.

Effects of anthropogenic aerosols on the climate could be even greater, with a potential to cancel the positive radiative forcing of GHGs. Aerosols can alter atmospheric radiation directly by scattering and absorbing radiation. This direct effect depends critically on the chemical composition and mixing state of aerosols. Aerosols can also have an indirect effect *via* their interactions with clouds by acting as cloud condensation nuclei (CCN). Further, clouds can modify aerosols, their optical properties, their size distributions, and their ability to act as CCN. The indirect effect, which is a strong function of the chemical and physical properties of aerosols, can change clouds and even the hydrological cycle, two pivotal components of the climate system. In fact, atmospheric water vapour, a central link of the hydrological cycle, is by far the most important GHG. Any changes in water vapour due to GHGs and aerosols have a large indirect lever on climate.

Changes in climate can also affect the atmospheric chemistry significantly. For example, a change in water vapour due to change in temperature can alter the oxidation capacity of the atmosphere. A change in temperature or relative humidity can change the chemical and physical properties of aerosols. Changes in temperature also alter rates of chemical reactions and, thus, composition. These interactions and feedback processes are complex and poorly understood. Therefore, clear understanding of the processes acting in the climate system is essential. Because of their variability in

space and time, even the current contributions of short-lived species to radiative forcing cannot be easily evaluated *via* their atmospheric observations alone. At present, there is a great deal of emphasis on the short-lived species because of the possibility of a quick "return" upon some policy action. Furthermore, these short-lived species are also the "pollutants" that need to be addressed for human health and other concerns. Therefore, clear understanding of the processes that connect emissions (source, precursors) to abundances and the processes that connect the abundances to the climate forcings are essential for an accurate prediction of the future climate and an assessment of the impact of climate change and variations on the earth system **(Figure 1)**.

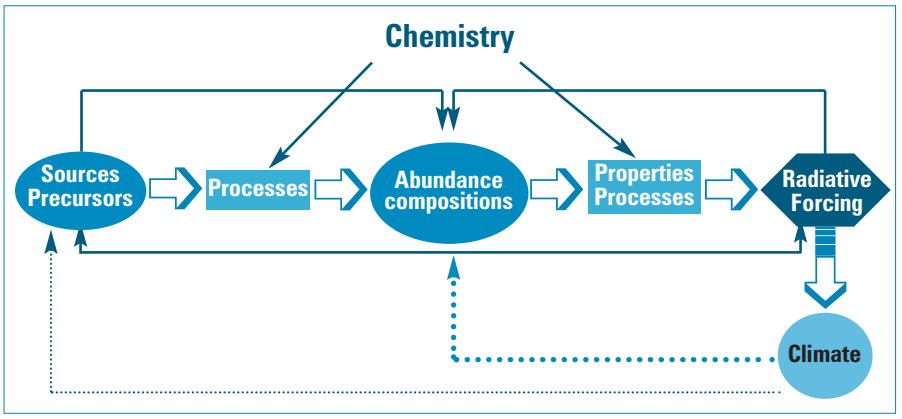

Figure 1. A schematic depiction of the connections between sources and the atmospheric abundances of radiatively important species and climate. The central role played by processes is indicated in the figure. Indirect effects and feedbacks are also indicated as arrows. Accurate inclusion of these processes, which include chemical, microphysical, radiative, and dynamical processes, is key for understanding climate and for succesfully predicting climate. [From A. Ravishankara]

To assess the current state of our understanding on some of the key issues related to climate-chemistry interactions, a joint SPARC-IGAC workshop was held in Giens, France, on 2-6 April 2003. The specific goal of the meeting was to identify, discuss and prioritise outstanding issues related to the interactions between climate and chemistry that could be attacked jointly by the two research communities. SPARC is a project of the WCRP and IGAC (International Global Atmospheric Chemistry) is a core project of the International Geosphere-Biosphere Program (IGBP).

A. R. Ravishankara and **S. Liu,** the co-organizers of the joint initiative between SPARC and IGAC, co-chaired the workshop. Other members of the organizing committee were **U. Platt, A. O'Neill, T. Bates, S. Fuzzi,** and **C. Granier.** The excellent local organization for the meeting was provided by **C. Michaut** of the SPARC Office. The meeting went extremely smoothly because **C. Michaut** (SPARC), **C. Burgdorf** (NOAA) and **K. Thompson** (Computer Sciences Corporation) handled the logistic extremely well.

The workshop was divided into five main sessions **(Table 1),** each with a speaker who summarized the issues pertaining to that session. The talk was followed by short presentations and discussions. The chair of each session organized the discussions and two rapporteurs summarized the findings from the session. In the last session of the workshop, the rapporteurs (with help from the session chairs) summarized the findings to the attendees. The rapporteurs' presentations were followed by further discussion. After the workshop, the rapporteurs (with help from the chairs and other key participants, when necessary) summarized the findings in writing. This written summary is the basis for the highlights given below and will also serve as an input for the white paper that will be generated in 2003.

Many major issues related to climate and chemistry in general, and climate-chemistry interactions in particular, were discussed. Special attention was paid to identifying uncertainties. All discussions and presentations are summarized in the rapporteurs' report, which will be available at a later date. A few highlights of the workshop are given below to indicate some of the main issues and uncertainties. This is not a comprehensive list, nor is it prioritised at this time; but it serves to give a flavour of the workshop proceedings.

Aerosols, Chemistry, and Climate

Involvement of aerosols in climate, as well as their special role in coupling chemistry with climate, centres around the following issues: (1) transformation and aging processes that affect aerosol composition and properties; (2) chemical processes that determine the global distribution of various aerosols; (3) the radiative impact of aerosols as a function of their chemical composition; (4) the interactions between aerosols and clouds and how they are determined and altered by chemical processes; (5) the role of aerosols in altering the chemical composition of the atmosphere *via* heterogeneous and multiphase reactions in/on aerosols; and (6) the response of the climate to changes in aerosol abundance and properties.

Here we give two examples of the kinds of issues that were discussed. **(a)** The regional/local nature of the aerosol abundance, properties, and hence their forcings requires calculating these forcings and impacts using very high-resolution models. The global impact can be accurately assessed only after calculating them using high-resolution models. Further, the impacts of climate change due to aerosols will be felt on a regional basis and, hence, understanding them on a regional (smaller) scale is essential. For example, even though the radiative forcing due to long-lived GHGs is longitudinally symmetric, the forcing due to

Table 1. Details of the sessions at the Giens workshop

Sessions	Rapporteurs	Session Chair	Main Speaker
Session 1 - Aerosols, chemistry, and climate	K. Carslaw, P. Quinn	T. Bates	F. Dentener
Session 2 - Water vapour and clouds	C. Mari, K. Rosenlof	T. Peter	U. Lohmann
Session 3 - Lower stratospheric ozone and its changes	M. Chipperfield, P. Simon	U. Platt	J. Pyle
Session 4 - Tropospheric ozone and other Chemically Active Greenhouse Gases (CAGGs)	D. Hauglustaine, I. Bey	S. Liu	D. Derwent
Session 5 - Stratosphere-troposphere coupling	T. Shepherd, A. Douglass	A. O'Neill	R. Rood
Session 6 - Final Summary Session	All participants		

aerosols is very inhomogeneous (see Figures in the IPCC Third Assessment Report). Further, the cooling by sulfate and warming by carbonaceous aerosols are spatially inhomogeneous and do not overlap. So, there will be a very large amount of spatial structure attributed to aerosol forcing. Even on a global scale, the influences can be isolated to some regions, as in the case of cirrus clouds and its primary forcing being in the upper troposphere (UT). The impacts of aerosols in changing the tropospheric composition can also be regional in scale. For example, the interesting and important tropospheric halogen chemistry shown by phenomenon such as the "bromine explosion" in the Arctic is regional and seasonal. Similarly, the impacts can be regional as in the case of the changes due to aerosol emissions by aircraft in the UT/LS. **(b)** The indirect effects of aerosols are complex processes involving interactions between aerosols, dynamics, cloud microphysics and both gas and heterogeneous phase chemistry. It demands a coupled high-resolution model that incorporates all the above pathways for changes. **Figure 2** exemplifies this coupled nature of the indirect effect and the various connections that need to be considered to assess this effect.

There are some commonalities between aerosols and tropospheric ozone (discussed in the session 4 on Tropospheric Ozone and other CAGGs). Both tropospheric ozone and aerosols are climatically and chemically important constituents, both are important in the context of public health, both are short-lived (and thus lead to regional scale forcings), and both are being altered by anthropogenic influences. Also while the impact of long-lived GHGs, which are reasonably well mixed in the atmosphere, is generally well constrained, aerosols and ozone have relatively short lifetimes and their radiative impact is still highly uncertain. The difficulties in incorporating the processes that affect aerosol and ozone abundance in global climate models arise from the high spatial scale resolutions that are needed and the poor state of our understanding of many of these processes. Examples of the spatial variability were also discussed in session 4.

Water Vapour and Clouds

Water vapour is a major climate gas by itself. However, its ability to magnify the contributions of other forcing agents heightens its role. Because water vapour is present in all three of its phases in the atmosphere, it poses a formidable challenge. Water interacts with radiation, changes properties of other forcing agents, provides an important pathway for energy transport and alters the dynamics of the atmosphere. Lastly, water is one of the most important variables of direct concern to life on Earth. Changes in its available amounts, physical state and rate of precipitation are some of the most important predictions needed from climate models. To do so, the climate models have to accurately represent the role of water in the climate system.

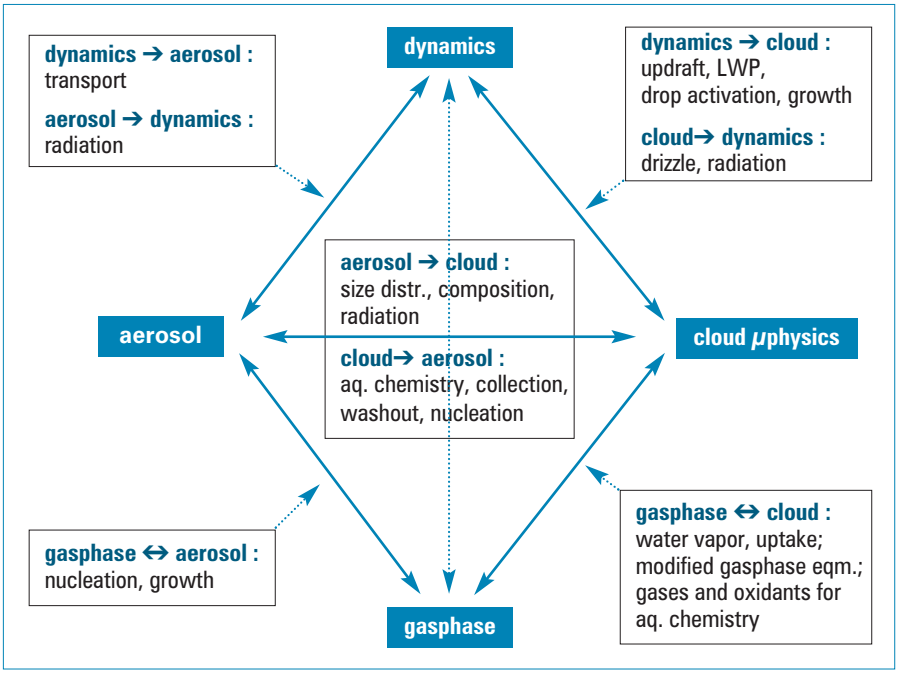

Figure 2. The interconnections between various types of processes that need to be included in assessing the direct and indirect effects of aerosols on climate, especially the indirect effect of aerosols arising from their influence on clouds. [From G. Feingold]

The major issues from the point view of global climate systems were noted and discussed: (1) the observation of increases of relative humidity with altitude in the UT; (2) the importance of including water vapour feedback in climate modelling; (3) hemispheric differences in water vapour; (4) homogeneous and heterogeneous freezing of water and their impacts; (5) water vapour trends in the troposphere and the stratosphere; (6) chemistry in clouds.

Two examples of the types of questions that were brought up for discussions in this session are given here. **(a)** What mechanism actually controls the humidity of the UT and the stratosphere and what processes control the long-term trends in water vapour? **Figure 3** captures the variation of relative humidity as a function of altitude and clearly shows that often there is vapour present with a super saturation greater than unity. The repercussions of and the processes that lead to such profiles were topics of discussions. **(b)** How do anthropogenic aerosols affect clouds and, hence, radiation? The key to evaluating and understanding the role of anthropogenic emissions is elucidating how anthropogenic aerosols can alter cloud properties, distributions, etc. **Figure 4** (p. I) shows the dramatic changes that can occur due to anthropogenic aerosols, which can have different properties of hygroscopicity and cloud condensation capabilities than natural aerosols. Clearly, large-scale changes in water vapour and clouds can be brought about by anthropogenic aerosols and, thus, have a major impact on climate and precipitation.

Tropospheric Ozone and Chemically Active Greenhouse Gases (CAGGs)

A great current policy challenge in tropospheric chemistry is to quantify accurately the future global radiative forcings of climate by methane and ozone. These are the major CAGGs in the troposphere, the others, such as CFCs and N_2O, are longer-lived and are removed predominantly in the stratosphere. Recently, concern has also been raised about the possible impact of climate change on tropospheric chemistry and, in turn, on regional air quality in the future. Therefore, variation of the abundances and lifetimes of CAGGs in the future atmosphere is of interest. These variations will depend on the details of the chemistry in the troposphere and, therefore, climate assessments demand an accurate representation of tropospheric chemistry in climate models.

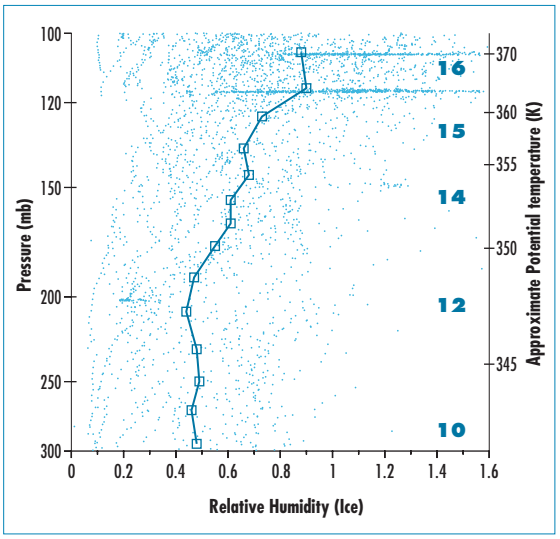

Figure 3. Vertical profiles of relative humidity in the troposphere. Clearly, there are instances where the relative humidity is above unity. The presence of RH greater than unity and the consequences of such values to earth's climate is of great interest in climate science. [From I. Folkins et al.]

The main questions that need to be addressed in relation to the role of ozone and other CAGGs on climate are: (1) How does tropospheric chemistry affect climate? (2) How does climate change affect tropospheric chemistry? (3) What are the current uncertainties in tropospheric chemistry? (4) What is the role of UT/LS, a key region for climate-chemistry interactions? (5) What type of model is needed to study climate-chemistry interactions? (6) How should one evaluate complex coupled models?

One of the examples that highlight the importance of the above needs is the effect of feedback on calculated future abundance of ozone. The amounts of HO_x, and consequently ozone photochemical production and destruction, are highly sensitive to climate changes and variations. This is particularly true for HO_x because of the large changes in the abundance of H_2O due to climate change. **Figure 5** shows the ozone abundances calculated using the STOCHEM model for a future climate and for today's climate. These changes arise primarily due to changes in HO_x brought about by climate change. Such interactions between climate change and changes in the abundances of tropospheric species need to be quantified and compared among models and to other processes as changes in dynamics and weather patterns occur due to changes in climate forcing.

Another example is the resolution dependence of measured and calculated abundances of species responsible for the production or destruction of O_3 in the troposphere. **Figure 6** (p. I) shows the measured amounts of NO_2 from two satellites with two different resolutions. Clearly, the satellite with the higher resolution shows larger peak amounts in NO_2. Because ozone abundances are non-linearly dependent on NO_x (= NO + NO_2) abundance, such differences due to spatial variations will lead to differences in the calculated concentrations of ozone. Resolution is an issue not only for modelling, but also for emissions and measurements of short-lived atmospheric species, such as ozone and aerosols.

The horizontal and vertical resolutions needed in future global models are certainly important issues to be considered. High resolution is required in source regions to provide a better representation of surface emissions, to account for non-linear effects in atmospheric chemistry and to better represent sub-grid scale processes, such as convection or boundary layer mixing. Such high resolution is also crucial for many other issues.

Lower Stratospheric Ozone and its Changes

Ozone in the lower stratosphere (LS) influences climate and vice-versa. Changes in LS O_3 will affect tropospheric climate (as well as LS climate) and climate change will affect LS O_3. As LS O_3 is partly controlled by chemical processes and partly by dynamics (which are again influenced by the chemical composition of the atmosphere), atmospheric chemistry and climate change are intricately linked together. Therefore, climate change models (i.e., GCMs) should include a realistic description of LS O_3, and models aiming to simulate the future composition of the stratosphere should include climate change. The major issues involved in the two-way coupling between chemistry and climate from the perspective of the LS are: (1) transport to the LS, (2) modelling of LS ozone, (3) remote effect of mid-stratosphere changes, and (4) uncertainties due to GCMs.

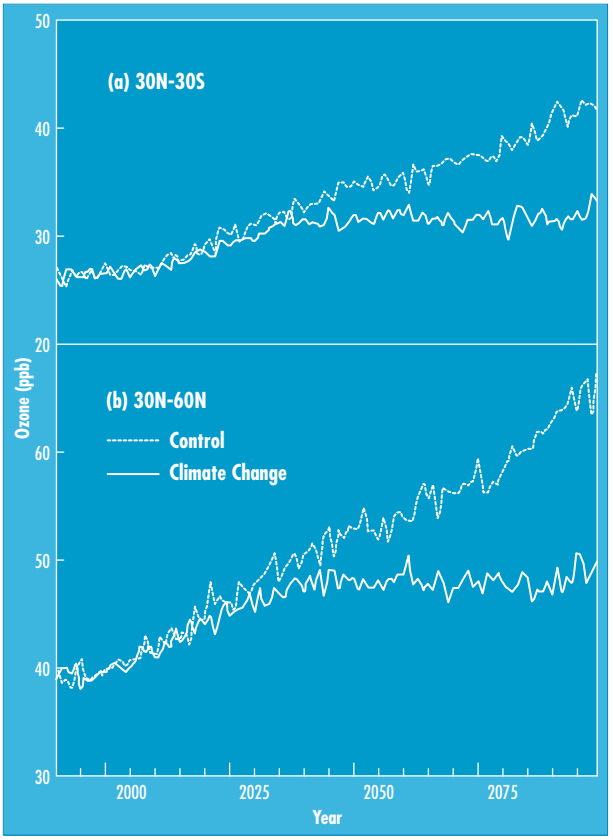

*Figure 5. Abundances of ozone calculated for equatorial region (**panel a**) and extratropics (**panel b**) from the STOCHEM model where the climate is assumed to be invariant with time (control run, dashed line) and where climate changes are included (solid line). These differences arise primarily because of changes in HO_x abundances between the control runs calculations where climate changes with time. [From Johnson et al.]*

Source gases (pollutants) reaching the stratosphere are believed to enter mainly at the tropical tropopause. The details of this transport are not fully understood (e.g. the role of the TTL and the processes that take place in this region are major sources of uncertainty). Even though detailed understanding of this region is not critical for long-lived pollutants (e.g. CFCs), what happens in this region is critical for short-lived source gases (e.g. bromine/ iodine species). Therefore, we must understand the role of convection/ TTL in transporting species to the stratosphere and how it may change in the future (see session on Stratosphere-Troposphere Interactions). In addition to the TTL, the wave driving and chemistry in the troposphere will affect how much and what species reach the stratosphere from the troposphere.

Ozone is chemically long-lived in the LS and its abundance is controlled by both dynamics and relatively slow chemistry (outside of the polar regions in the spring). Both gas-phase and heterogeneous chemistry are important under these cold conditions. We need to improve our understanding of the gas-phase chemistry at low temperature, the surfaces present in the LS/lowermost stratosphere, the heterogeneous chemistry that occurs on these surfaces and the transport for accurately describing LS O_3. Stratospheric O_3 is expected to increase ('recover') as the stratospheric halogen loading declines. Stratospheric cooling is expected to increase mid-stratospheric O_3. LS ozone may also increase, but the situation here is more complicated and harder to predict. Increased stratospheric ozone will reduce the UV flux and may decrease tropospheric OH. Therefore, coupled chemistry/climate change calculations must include important feedbacks and extend the model domain high enough to cover the important processes.

In addition to uncertainties in the understanding of processes, ther are some major issues related to models. Predictions of future changes in the atmospheric chemical composition will necessarily make use of meteorological forcing fields (temperature, winds, water vapour, convective fluxes, etc.) from GCM simulations. It is therefore of vital importance to have a clear idea of the ability of those GCMs to predict with reasonable accuracy the future climate changes.

Examples of key model-related issues are temperature biases in the models and the resultant effects on processes in the LS, especially those that depend non-linearly on temperature and/or have threshold temperatures for initiation of certain processes. The modelling calculations carried out so far show that significant biases exist in most models: for instance, temperature biases in the LS can reach several K, which is known to have a strong potential impact on high latitude winter ozone loss, specially in the Arctic. Such biases are shown in **Figure 7** (p. II). These biases will affect the amount of chemical loss calculated through, for example, different amounts of denitrification, which is shown in **Figure 8** (p. II). Mean meridional transport can also be largely different from model to model, either because of physical reasons (gravity waves, convection, etc., leading to different Brewer-Dobson circulations) or simply because of numerical reasons (location of the upper boundary of the model, numerical algorithms, etc.). Major problems also appear in the models' water vapour fields, especially in the UT/LS region. The consequences of differing temperatures lead to different predictions.

Stratosphere-Troposphere Coupling

The classical picture of stratospheric transport, in which material enters the stratosphere in the tropics, is transported poleward and downward and finally exits the stratosphere at middle and high latitudes, was proposed to explain observations of stratospheric water vapour [Brewer, 1949] and ozone [Dobson, 1956]. This conceptual model has since been refined but not drastically altered. Holton *et al.* (1995) pointed out that this Brewer-Dobson circulation is controlled by stratospheric wave drag (quantified by the Eliassen-Palm flux divergence), sometimes coined the "extratropical pump", with the circulation at any level being controlled by the wave drag above that level. However, the wave drag can be difficult to compute accurately and it is common to diagnose the mean circulation from the diabatic heating. It is possible to estimate the net mass flux across a given isentropic surface from the diabatic heating (for example, the 380 K potential temperature surface, which is nearly coincident with the tropical tropopause and which marks the upper boundary of the lowermost stratosphere). On the other hand, transport of material along isentropic surfaces, such as that between the tropical UT and the lowermost stratosphere, is more difficult to quantify - especially the net transport of a given species that results from the two-way mixing. Observations show that the composition of the lowermost stratosphere varies with season, and suggest a seasonal dependence in the balance between the downward transport of air of stratospheric character and the horizontal transport of air of UT character. For any time period, the integrated mass flux to the troposphere at middle and high latitudes is the sum of the mass flux across the 380 K potential temperature surface, the net mass transported between the tropical UT and the lowermost stratosphere, plus (minus) the mass decrease (increase) of the lowermost stratosphere [Appenzeller *et al.,* 1996]. The first quantity is straightforward to compute, but the last two quantities are sensitive to small-scale processes, including synoptic-scale disturbances and convection.

There are many issues and uncertainties in the stratosphere-troposphere interactions that need to be addressed to have an accurate climate model that couples chemistry and climate. They include: (1) dynamical coupling, (2) tropical stratosphere-troposphere exchange, the TTL, and dehydration, (3) extra-tropics and stratosphere-to-troposphere flux, (4) extra-tropics and troposphere-to-stratosphere flux, and (5) upscaling our knowledge/information, namely to link what we learn from case studies to the representation of various processes in global models, to determine global budgets and to understand their contribution to global change.

Because of these uncertainties, the model range for the O_3 flux from the stratosphere to the troposphere, shown in **Table 2,** is too high. There are not sufficient observational constraints to judge these models. In addition to the net mass flux, it is important to understand longitudinal variations in the

Table 2. Tropospheric O_3 budgets for circa 1990 conditions from a sample of global 3D-CTMs

	Tg/yr					Tg
CTM-ref	**STE**	**Prod**	**Loss**	**P-L**	**SURF-dep**	**Burden**
MATCH-a	**1440**	2490	3300	- 810	620	
MATCH-MPIC-b	**1103**	2334	2812	- 478	621	
TM3-c	**768**	3979	4065	- 86	681	311
TM3-d	**740**	2894	3149	- 255	533	266
HARVARD-e	**400**	4100	3680	+ 420	820	310
GCTM-f	**696**			+ 128	825	298
UIO-g	**846**			+ 295	1178	370
ECHAM4-h	**459**	3425	3350	+ 75	534	271
MOZART-i	**391**	3018	2511	+ 507	898	193
STOCHEM-j	**432**	4320	3890	+ 430	862	316
KNMI-k	**1429**	2864	3719	- 855	574	
UCI-l	**473**	4229	3884	+ 345	812	288
NEW						
Synoz-m	550±140					
GISS II	790					
GISS II'	421					
Oslo/EC	458					

These budgets do not always balance exactly (STE+P-L=SURF)

stratosphere-to-troposphere flux, as these will be important for short-lived species and for tropospheric chemistry. Such fluxes need to be assessed not only for today's atmosphere, but also for an atmosphere of the future with a different climate. Measurements are needed to examine both seasonal and spatial variability of species in the lowermost stratosphere, using a range of tracers with a spectrum of lifetimes.

The classical picture of the stratosphere-troposphere coupling has evolved over the last few years. The modification of the Holton diagram for the assessment of the transport of short-lived species to the stratosphere is shown in **Figure 9** (p. II). Such developments and "tuning" are essential for a good description of processes that are important for climate-chemistry coupling.

Summary

These highlights, along with the details of all the other presentations and discussions, form the basis for assessing the current state of climate-chemistry interactions and recommending the research needed to address the unresolved issues. This task will be taken up by the organizing committee in collaboration with a few members of the scientific community to write and publish a white paper that will be released later this year, with **A.R. Ravishankara** (SPARC Co-Chair, SSG) and **S. Liu** (IGAC Co-Chair, SSC) as the lead authors.

◆

Report on the SPARC Workshop on the Role of the Stratosphere in Tropospheric Climate

Whistler (BC), Canada, 29 April – 2 May, 2003.

Nathan P. Gillett, University of Victoria (BC), Canada (gillett@uvic.ca)
Mark P. Baldwin, Northwest Research Associates (WA), USA
David W.J. Thompson, Colorado State University (CO), USA
Emily F. Shuckburgh, University of Cambridge, UK
Warwick A. Norton, University of Oxford, UK
Jessica L. Neu, NOAA Climate Monitoring and Diagnostics Laboratory (CO), USA

Overview

Is the stratosphere important for predicting changes in weather and climate? Do perturbations to the stratosphere have a significant influence on the climate in the troposphere? These were the key questions addressed at a recent SPARC workshop in Whistler, British Columbia, sponsored by SPARC, NASA, NOAA, NSF, ESA and the Risk Prediction Institute. A total of 56 scientists participated, with 43 invited talks and 3 posters. Papers presented at the workshop explored observational evidence of stratosphere-troposphere coupling, the theory behind possible coupling mechanisms and the simulation of such coupling using a range of models, from simple mechanistic models to full GCMs. The meeting format allowed for ample discussion after each talk, with a summary/discussion session on the last day.

It has long been known that conditions in the stratosphere are controlled by wave driving from the troposphere, but traditionally it has been assumed that the stratosphere has little effect on the troposphere. Stratospheric variations, especially variations in the strength of the polar vortex, appear to be involved in feedback processes that in turn alter weather patterns in the troposphere. Stratospheric variations are largest during the winter season in the NH (and spring in the SH), and they are influenced by changes in solar irradiance, volcanic aerosols, changes in greenhouse gases, ozone depletion and the phase of the Quasi Biennial Oscillation (QBO).

A major focus of the meeting was the mechanisms by which stratospheric circulation anomalies affect the troposphere. Stratospheric circulation anomalies are caused mainly by wave forcing from the troposphere. Stochastic variations in the troposphere during NH winter lead to high-frequency changes in the planetary wave flux upwards into the stratosphere. When these waves break, they deposit momentum in the stratosphere, slowing the zonal-mean wind and weakening the polar vortex. The interaction of the waves with the mean flow tends to draw these zonal wind anomalies downward through the stratosphere. Our understanding of this process is incomplete, but in some ways it is analogous to the process by which zonal wind anomalies descend in the QBO.

The lowermost stratosphere has a long radiative timescale during winter, causing anomalies to persist there for several weeks. Thus, the lower stratosphere (LS) acts as an integrator of tropospheric variations, leading to longer-lasting anomalies in this region. Observational and modelling evidence suggests that LS anomalies are associated with circulation anomalies in the troposphere. This dynamical coupling occurs in the NH winter, when strong polar vortex anomalies in the stratosphere are followed, on average, by long-lived anomalies in the Northern Annular Mode (NAM) near Earth's surface. The NAM is similar to the North Atlantic Oscillation, and NAM anomalies are associated with strong westerly winds in the mid-latitudes, and mild wet winters over Northern Europe and much of the U.S. In the SH the dynamical coupling occurs during spring, when the stratospheric polar vortex is most variable. Surface effects are seen in the Southern Annular Mode (SAM).

Synopsis of Presentations

Based on a cross-spectral analysis of annular mode variations at the surface and in the LS, **D. Stephenson** demonstrated that the surface annular mode shows stronger variations on timescales of ~60 days than would be expected if it were forced solely by high frequency weather noise, and that this increased variability on monthly timescales is associated with variations in the LS. This apparent downward influence may allow improved seasonal predictions beyond the ~10-day limit of deterministic forecasts. **M. Baldwin** showed that statistical forecasts of the monthly-mean surface

NAM can be improved by using stratospheric data, and **A. Charlton** demonstrated that knowledge of stratospheric conditions gives some additional skill in forecasts of 15-20 days by using a medium-range weather forecasting model. **W. Norton** demonstrated that if stratospheric variability is artificially suppressed in a GCM, the timescale of the surface NAM is decreased, and **D. Thompson** showed a range of evidence for stratospheric influence on the tropospheric annular mode.

Observed stratosphere-troposphere links are not, however, limited solely to the extra-tropics: **M. Hitchman** and **M. Giorgetta** presented evidence that the equatorial QBO in stratospheric winds and temperatures can influence the surface *via* induced changes in tropopause conditions, which in turn can alter tropical convection. **K.-K. Tung** also presented statistical evidence that the influence of the QBO is manifested in tropospheric geopotential height. **R. Quadrelli** and **K. Kodera** presented evidence that the coupling between annular mode anomalies over the pole may be modulated by the phase of the El Niño/Southern Oscillation (ENSO), the warm ENSO phase being associated with stronger stratosphere-troposphere coupling in the extra-tropics. **H. Graf** also demonstrated that wave driving of the polar stratosphere is correlated with the phase of ENSO in observations.

Observational studies, thus, show that the strength of the zonal circulation in the troposphere is correlated with that in the stratosphere and based on the lag found between surface anomalies and those in the stratosphere, we might hypothesize that the influence is downwards. How might we test the direction of causality more conclusively, and find what mechanisms underlie the coupling? These questions were addressed by theoretical and model-based studies. Several presenters demonstrated that simple mechanistic models exhibit changes in the strength of the zonal circulation in the troposphere when conditions in the stratosphere are perturbed (**P. Kushner, W. Robinson, M. Taguchi)**. Several other presenters pointed out that full GCMs show an apparent downward propagation of annular mode anomalies similar to that observed (**R. Garcia, B. Boville, K. Hamilton**). These studies generally concluded that stratospheric sudden warmings are preceded by an increase in the upward flux of planetary wave energy from the troposphere and they are followed, on a timescale of 1-2 months, by a weakening of the zonal circulation in the troposphere. P**. Newman** showed that the Antarctic polar vortex of 2002 was anomalously warm and disturbed due to stratospheric wave driving and not due to reduced photochemical ozone depletion. **M. Salby** demonstrated that anomalous wave driving of the stratosphere accounts for almost all the variability in polar stratospheric temperatures. **D. Waugh** further showed that much of the variability in the strength of the stratospheric vortex could be explained by changes in the upward wave flux near the tropopause. It remains an open question what determines the upward flux of wave activity into the stratosphere, but it is becoming clear that the configuration of the stratosphere itself is important – and that tropospheric patterns by themselves are not sufficient to cause an upward flux of wave activity (**R. Scott**).

Several presenters discussed possible mechanisms by which anomalies in the zonal flow of the stratosphere might have a downward influence. The simplest and most direct is that anomalies in the LS have non-local dynamical effects in the troposphere (much as an electric charge has non-local effects on the surrounding electric field) (**P. Haynes, R. Black**). However, this effect by itself is unlikely to be large enough to explain the observed downward influence. A consensus emerged that a positive feedback mechanism in the troposphere is required to explain the strength of the observed coupling. One likely mechanism involves positive feedbacks on the subtropical jets due to baroclinic eddies (**A. Plumb, T. Shepherd, T. Dunkerton, W. Robinson**). Baroclinic eddies extend into the LS, providing a region of overlap where stratospheric anomalies can influence tropospheric eddies. **G. Vallis** described a related mechanism underlying tropospheric variability, whereby a NAM-like mode is a natural consequence of stirring by baroclinic eddies in the mid-latitudes. The tropospheric and stratospheric flows may also be coupled by other mechanisms, as for example the reflection of upward-propagating planetary-scale Rossby waves from the stratosphere back to the troposphere (**J. Perlwitz, N. Harnik, D. Ortland**). Analagous wave-mean flow interactions were demonstrated in a laboratory setting by **P. Rhines**.

Coupling between the stratosphere and troposphere may have important implications for our understanding of the climatic response to greenhouse gas (GHG) increases and stratospheric ozone depletion. GHGs are expected to have a radiative cooling effect on the stratosphere, though in some models this effect is outweighed in the Arctic polar vortex by an increase in upward planetary wave flux, which has a warming effect (**E. Manzini**). Stratospheric ozone depletion cools the polar vortex in the spring due to the reduced absorption of UV radiation. Persistent changes in the strength of the stratospheric polar vortex of either hemisphere might be expected to influence the tropospheric circulation. **B. Christiansen** showed that a significant change has occurred in the frequency of occurrence of strong and weak stratospheric vortex states in the NH winter over the past 50 years. **D. Karoly** showed evidence that both greenhouse gas increases and ozone depletion may have contributed to a strengthening of the tropospheric zonal circulation in the SH, and **D. Rind** presented analogous results for the NH. **J. Fyfe** showed that the SAM response to GHGs increases is sensitive to the ocean mixing parameterization used, due to its effect on the meridional gradient of surface warming. **N. Gillett** showed that the observed trend in SH surface circulation can be simulated in a high resolution GCM forced solely with stratospheric ozone depletion.

Some volcanic eruptions cause large increases in stratospheric sulphate aerosols, which heat the stratosphere and persist for 2-3 years. Observations and modelling evidence (**A. Robock, L. Oman**) suggest that large volcanic eruptions can induce positive NAM anomalies at Earth's surface, though the exact mechanism remains unclear. Some authors have argued that this effect comes about through changes in the strength of the stratospheric polar vortex, though other experiments appear to show a NAM-like response without such associated stratospheric changes (**A. Robock**). Likewise, changes in solar irradiance alter the thermal structure of the stratosphere, largely through induced changes in the stratospheric ozone distribution. **K. Coughlin** demonstrated a solar signal in geopotential observations that extends from Earth's surface to the middle stratosphere. The signal is latitude-independent and, hence, unrelated to annular modes. **J. Haigh** demonstrated that solar changes may induce changes in the strength and position of the subtropical jets and in this case the suggested mechanism was tropical. **L. Gray** suggested that the solar cycle may play a role in determining the strength of the connection between the QBO and the polar vortices (the so-called Holton-Tan relationship). Her results indicated that the strength of the Arctic polar vortex is affected by the winds in the upper equatorial stratosphere and, thus, that the phase of the QBO indirectly affects the surface NAM.

Summary

The evidence presented at this workshop suggests that the stratosphere plays an important role in the climate system on timescales from weeks to decades. In the seasons when stratosphere-troposphere coupling is strongest its role may be of comparable importance to that of the tropical oceans. The participants reached a consensus that stratospheric circulation anomalies influence the troposphere, but the mechanisms underlying this coupling are not yet fully understood. Improving our understanding of these mechanisms may help us to better predict the climate response to greenhouse gas and ozone changes, as well as improving seasonal forecasts.

Meeting Web page (abstracts and presentations): **http://www.atm.damtp.cam.ac.uk/shuckburgh/whistler/**

Report on ECMWF-SPARC Workshop on Modelling and Assimilation for Stratosphere and Tropopause

ECMWF, Reading, UK, 23-26 June 2003

Emmanouil K. Oikonomou, SPARC Office, France (eoikonomou@aerov.jussieu.fr)

The workshop jointly organized by ECMWF and SPARC consisted of talks on the current state of research about the stratosphere and the tropopause. There were 22 oral presentations. Three working groups were formed (Processes, Data Assimilation (DA), and Modelling) who then reported during a plenary session.

Presentations

The workshop opened with a summary by **A. Simmons** on the representation of the stratosphere in the ECMWF operations and their most recent Re-Analysis Scheme ERA-40. Overall the performance of the system is considered successful (e.g. sudden warming predictions, QBO); however, there are problems such as model and observation biases, handling of tides and performance difference between 3D and 4D-Var systems. **A. O'Neill** talked about the objectives of SPARC and DA requirements: long-term global data sets; 3-D velocity fields with reduced noise; parameterized mass fluxes; diabatic heating rates; ozone assimilation, aerosols and other tracers.

The first session focused on Radiative Transfer (RT) in the stratosphere, cross-Tropopause (TP) processes, Cirrus clouds and chemical forecast using CTMs. The current issues on representing stratospheric processes into modelling and DA include the momentum budget, Gravity Wave Drag (GWD), improvements in tropical winds, meridional circulation and mixing barriers, and the unbalanced flow component in the upper stratosphere and mesosphere (**T. Shepherd**). Over the tropics, recent inertial adjustments appear to be a real process suggesting that a lot of the upwelling may be resolved. However, outstanding problems remain: tropical winds; biases of models in polar temperatures; underestimation of GWD when parameterizing it in the presence of a zonal-mean sponge.

There have been recent developments with impact on the ECMWF RT stratospheric scheme, followed by comparisons of ozonesonde profiles with the ERA-40 fields and 10-day model profiles (**J-J. Morcrette**). There also exists future possibility for ECMWF to provide operational UV-B diagnostics once radiation becomes interactive with prognostic ozone. **H. Wernli** showed results on the cross-TP processes and quantification by using a Lagrangian approach and based upon ECMWF analyses combined with aircraft data from SPURT. TP folds are very important in the sub-tropics but less important in the extra-tropics. Significant differences were found between ERA-40 and ERA-15 near the TP and there was qualitative agreement between regions of maximal STE and storm tracks. **T. Peter** reported on results from the LITE project and emphasized the role of ultra thin tropical tropopause clouds, concluding that ECMWF analyses suggest maritime continent to be a major source for stratospheric air.

The way stratospheric chemistry and aerosols are understood and represented in DA CTMs remains a challenge. **D. Fonteyn** presented 4D-Var DA runs using non-operational MIPAS data with a constrained N_2O budget, which suggest that advection and tendencies are anti-correlated and the assimilation should constantly constrain the N_2O budget. Regarding which species to include into CTMs, the session concluded that complex CTMs may not work in short-time and the overall idea is to keep the schemes simple so that they can be controlled.

There were three talks that covered satellite observations in the UT/LS region including aerosols whose loading in 2002 was at the lowest. **L.W. Thomason** summarized the current state in gas/aerosol observational and retrieval techniques; these include Occultation coverage, Limb Emission (CLAES/HIRDLS) and Lidar observations and modelling. **B.J. Kerridge** reported on assimilated GOME Ozone data, which agree reasonably well when compared to SAGE-III, HALOE and MIPAS profiles using ECMWF winds. **A. Dudhia** presented an overview on the Infrared Limb Sounding instruments of MIPAS and HIRDLS; a Ray Tracing technique has been implemented to retrieve pressure and temperature with more of a problem being the transmittance calculations.

The session on DA comprised five talks, mainly on the ECMWF and UKMO DA systems. Approaches in chemical DA range from simple chemistry dynamics in GCMs to sophisticated photochemistry CTMs and coupled GCM/CTMs. The assimilation of satellite retrievals versus radiances in operational Numerical Weather Prediction (NWP) has proven to be less attractive, mainly because satellite retrievals retain characteristics of the *a priori* information, they constrain information from other observations, they have complicated error structures and the distribution retrievals may be significantly delayed compared to raw radiances. **T. McNally** presented an overview of the observing systems used at ECMWF, with HIRS and AMSUA proving to be the most reliable platforms for the stratosphere. **A. Dethof** gave a more in-depth analysis of the ECMWF DA scheme for ozone. **R. Swinbank** talked about assimilating stratospheric ozone and water vapour in the UKMO model; future plans include

the development of an Extended Global Assimilation System (DEGAS). A common conclusion is that the key limitations of all these DA satellite systems are their systematic errors and their vertical resolution. Furthermore, model errors are an important issue in chemical DA that can be considered as an unobserved variable requiring the knowledge of cross-error covariance (**R. Ménard**). Future challenges in DA focus on: understanding of systematic errors; tuning the error covariance specifically for the type of errors encountered in the stratosphere; making use of improved operational instruments along with synergistic use; coupling dynamics with chemistry in DA systems (e.g. GCM/CTM); and assimilating limb radiances, as for example currently developed by DARC from MIPAS data (**W. Lahoz**).

The final session was devoted to modelling. **V. Peuch** talked about developing UV index forecast in Météo-France. The results from CTM MOCAGE have been compared to MOZAIC data. The CTM approach (off-line/semi-online) can provide a flexible solution, e.g. for Chemical Weather Forecast (CWF), DA and climate chemistry. Another DA system is NASA's GEOS-4 with Limb-sounding temperatures from SABER effectively combined with TOVS and the inclusion of MIPAS ozone and SBUV (**S. Pawson**). The problems are mainly superfluous subtropical mixing, excessive cross-barrier transport and the fact that local assimilation seems to lead to noise.

Further results were presented from using meteorological analyses in the off-line CTM SLIMCAT and coupled chemistry-climate GCM (UKMO Unified Model) applied to study ozone depletion and past trends in mid-latitudes (**M. Chipperfield**). A study of NWP models showed that currently stratospheric forecasting at 6 days is comparable to 3-day forecast in the troposphere, with poorer results obtained when the polar vortex flow is rapidly changing (**G. Roff**). ECMWF have further developed a finite-element discretization technique for the vertical and they plan to increase the model vertical resolution; these changes are expected to improve the vertical stratospheric transport and reduce large model errors near the stratopause (**A. Untch**). Finally, reports on work in-progress included the NWP ICON project of the German Weather Service (DWD) and the MPI for Meteorology (**L. Bonaventura**) and issues in isentropic-coordinate and TP modelling (**J. Thuburn**).

Recommendations of the working groups

Processes (H. Wernli)

Six major issues were pinpointed: Ozone; Vertical resolution and upward extension; Global circulation with particular emphasis to the tape recorder effect; Cloud parameterization; Water vapour in the stratosphere; Data availability.

Prognostics of the ozone profile near the tropical tropopause remain problematic. Therefore, there is a need to validate against ozenesondes the ECMWF ozone fields and compare to the Fortuin and Langematz climatology. It was also suggested to revise the Cariolle-Déqué parameterization scheme implemented in the ECMWF ozone prognostics. The threshold of 195 K used for heterogeneous chemistry activation should be made altitude-dependent and a chlorine memory effect should also be included into the scheme. The results of the revised scheme can be then compared with the output from CTMs and MIPAS-like observations.

The group concluded that high vertical resolution has a large influence on the accuracy of CTMs. It was proposed that when the ECMWF model top exceeds 60 km the effect of non Equilibrium Ratiative processes might have to be included. The ECMWF RT model, which assumes Local Thermodynamic Equilibrium (LTE), can be validated through sensitivity studies and against models including non-LTE schemes. In addition, at about 85 km chemical heating might have to be taken into account. The tape recorder signal was found to be too fast in the ECMWF model coming from a too large mean vertical velocity at the equator, either due to variance in the vertical velocity, or from excessive numerical diffusion.

There is concern about the quality of the vertical transport in the ECMWF datasets. The production of accurate winds in the tropopause region represents a future aim, as well as to assess whether tracer simulation, such as N_2O, will improve the quality of the analyzed stratospheric winds. Also, any future parameterization upgrades should take into account the supersaturation of cirrus clouds. With respect to the water vapour in the stratosphere, MIPAS is moist compared to ECMWF but dry compared to HALOE. A systematic validation of the ECMWF moisture is needed against all available data sources. Finally, the group recognized the usefulness of archiving the diabatic 3D fields from ERA-40.

Data Assimilation (A. O'Neill)

There was an overall positive comment on the ECMWF system, with significant steps made towards improving the representation of the stratosphere, the existence of good analysis tools, an improved forecast performance, exploitation of novel datasets and interaction with data producers.

The issues for further attention include: calibrate and retune the stratospheric background error covariances; the Jb formulation; encourage the use of non-assimilated (i.e. independent) observations; deal with systematic errors within the analysis; capture an accurate representation of the Brewer-Dobson circulation and mixing barriers, with the suggestion for future inclusion of longer-term tracer species; impose additional constraints upon the DA system, such as balance and conservation. Recognized as particular weakness in the ECMWF system were the tides and the omission in the specification of explicit correlations among tracers and between the tracers and the dynamics in the error covariance.

The group emphasized the need for a robust system for meteorology and ozone DA, with AMSUA being identified as a particular example of a stable, well-calibrated instrument with excellent time continuity and important for the stratosphere. Other instruments also provide good quality measurements, such as ozone column from GOME/SBUV/ TOMS and ozone profiles from ENVISAT/AURA. ECMWF should continue to evaluate the need for limb-viewing data and aircraft observations (e.g. MOZAIC). Radiosondes and remotely sensed winds should provide more comprehensive time and location information and humidity sensors need to be improved, along with the Near Real Time (NRT) aspects of ozone sondes and ground based data. In addition, aerosol measurements are required to support the RT modelling, parameterization and chemistry/aerosol forecast. As a particular problem was seen the lack of organization and communication between the wide variety of research missions.

The group discussed the region and flow dependence of B matrix and it stressed the importance of choosing control variables and representations that facilitate the treatment of crucial regions, such as the UT/LS and shear zones, and the wider issue of STE. ECMWF should consider strategies for incorporating constituent modelling/ assimilation for both NWP and environmental monitoring. RT observational operations should keep

pace with the variety of measurements approaches (UV) and the new instrument developments.

OSEs/OSSEs (Observing System Experiment/Observing System Simulation Experiments) were suggested to assess remotely-sensed winds and humidity data in the UT/LS. The support for the ERA-40 project should continue and the 1990's should be used for validation of the Re-analysis. The group further suggested to explore the frequency and resolution of analyses and post-processed products (e.g. theta, fluxes) and their external availability to CTM users. The location of the upper boundary and its impacts to radiance assimilation and systematic errors were also discussed, along with the need to strenghten the assosciation between SPARC modelling and DA activity.

Modelling (J. Thuburn)

The group identified modelling issues related to dynamics and chemistry (ozone/CH_4/water vapour). The modelling issues regarding dynamics include: Mean meridional circulation and vertical transport; lateral dispersion; Model top, sponge layer and GWD; Inertial instability; Vertical resolution, advection and coordinate; and Mass conservation.

The ECMWF model vertical transport appears to be excessively fast in the stratosphere due to either: (a) excessive mean meridional circulation, in which case we need to examine whether the problem might be inherent in the free-running model or exacerbated by the DA, or (b) due to vertical advection errors, in which case a higher order advection scheme, or possibly an alternative model vertical coordinate, should be considered. NASA's experience also suggests excessive lateral dispersion when using analyzed winds for transport, but not when using winds from a free-running GCM.

In the issue of a model sponge layer, the group suggested: a sponge layer to be turned on from 0.1 hPa and a model lid placed at approximately 0.01 hPa; removal of the zonal-mean component of the sponge-layer; introduction of a momentum-conserving GWD scheme. It was also suggested to diagnose the presence of inertial adjustment in the ECMWF model and to explore the possibility of parameterizing this effect.

Vertical resolution is another important issue and several criteria were discussed for what might constitue it sufficient. Re-examination in the current DA schemes is also required if limb data are to be introduced. Regarding the vertical coordinate, the options of a hybrid isentropic and of a quasi-Lagragian were suggested to be considered, if the problems with vertical transport cannot be resolved by simpler measures. Nevertheless, there is experience suggesting that increments in GCM DA schemes can cause problems in the horizontal circulation. ECMWF is currently going ahead with their plan to move into a 91-level model expanding to 0.01 hPa.

With respect to ozone chemistry the group recommended: (i) to investigate the ozone prognostics in the current Cariolle scheme since there are clear discrepencies between the forecast ozone fields and the observations; in particular there is an under-estimated Antarctic ozone hole, a negative bias in the tropics and a positive bias in mid-latitudes; (ii) explore better ozone parameterizations since the current scheme is based on a 2D-model output, whereas 3D-CTMs seem to perform better; and (iii) coupling ozone to radiation scheme in the future. There was an overall agreement for inclusion of a long-lived tracer for dynamic diagnostics, such as CH_4, and the recommendation that possible extension of the model into the mesosphere may require inclusion of the H_2O chemical sink at high altitudes.

Aspects of Modelling and Assimilation for the Stratosphere at ECMWF

Antje Dethof, ECMWF, Reading, UK (Antje.Dethof@ecmwf.int)

Introduction

The ECMWF model is a global spectral model with a horizontal truncation of T511, corresponding to about 40 km grid spacing. In its current form the model has 60 levels in the vertical, 25 of which are above 100 hPa. The model top is at 0.1 hPa, corresponding to about 65 km. The model has a hybrid vertical coordinate, with terrain following coordinates in the lower troposphere and pressure coordinates in the stratosphere above about 70 hPa. The operational model uses a 4D variational analysis scheme to assimilate observations in 12 hourly intervals.

The main developments that led to a better representation of the stratosphere in the ECMWF model and analysis system took place in the last four years. In March 1999 the model top was raised from 10 hPa to 0.1 hPa, and the number of vertical model levels was increased from 31 to 50 [Untch *et al.,* 1999]. The additional levels were all added above 150 hPa. In October 1999 the vertical resolution was further increased to give the current 60 level version. This time most of the new levels were added in the boundary layer. The raising of the model top and the increased vertical resolution in the stratosphere meant that stratospheric processes could now be better represented in the ECMWF system and led to improved analyses and forecasts in the stratosphere. It also gave scope for further developments. A simple parameterization of stratospheric methane oxidation was included in the model [Simmons pers. comm. **http://ifsdoc.ecmwf.int/html/rd/cy26r1/ifs/documentation/PHYSICS/Cha1_Oveview.html)** to improve the stratospheric water vapour distribution. Ozone was added as a model variable and an ozone chemistry parameterization was included. Finally, ozone was included in the data assimilation system [Hólm *et al.,* 1999]. This 60 level version of the model was used in the ECMWF re-analysis ERA-40 project that covers the years from 1957 to 2002 [Simmons and Gibson, 2000].

Ozone model and analysis

Ozone is fully integrated into the ECMWF forecast model and analysis system as an additional 3D-model and analysis variable. The ECMWF ozone assimilation system allows the assimilation of ozone retrievals in the form of ozone layers in 3D-VAR or 4D-VAR.

Since April 2002, ozone layers from the SBUV/2 instrument on NOAA-16 and total column ozone retrievals from GOME on ERS-2 (provided by KNMI's Fast Delivery Service) have been assimilated in the operational ECMWF system. In the ERA-40 project, retrievals from TOMS and SBUV instruments on various satellites are assimilated in 3D-VAR with a horizontal truncation of T159 (about 125 km grid spacing) from December 1978 onwards. No ozone data is assimilated in ERA-40 during 1989 and 1990 for technical reasons.

Model

The ECMWF forecast model includes a prognostic equation for the ozone mass mixing ratio O_3[*kg/kg*]

$$\frac{dO_3}{dt} = Ro_3 \qquad (1)$$

where Ro_3 is a parameterization of sources and sinks of ozone. Without such a source/sink parameterization the ozone distribution would drift to unrealistic values in integrations longer than a few weeks.

The parameterization used in the ECMWF model is an updated version of Cariolle and Déqué (1986), which has been used in the ARPEGE climate model at Météo-France. This parameterization assumes that chemical changes in ozone can be described by a linear relaxation towards a photochemical equilibrium. It is mainly a stratospheric parameterization. The relaxation rates and the equilibrium values have been determined from a photochemical model, including a representation of the heterogeneous ozone hole chemistry. The updated version of the parameterization (with coefficients provided by P. Simon, Météo-France) is

$$Ro_3 = c_0 + c_1(O_3 - \bar{O}_3) + c_2(T - \bar{T}) + c_3(O_3^{\uparrow} - \bar{O}_3{\uparrow}) + c_4(Cl_{EQ})^2\, O_3 \qquad (2)$$

where

$$O_3^{\uparrow}(p) = -\int_p^o \frac{O_3(p')}{g}\, dp' \qquad (3)$$

Here c_i are the relaxation rates and $\bar{T}$, $\bar{O}_3$ and $\bar{O}_3{\uparrow}$ are photochemical equilibrium values, all functions of latitude, pressure and month. $O_3{\uparrow}$ denotes the ozone column above pressure p.

Cl_{EQ} is the equivalent chlorine content of the stratosphere for the actual year and is the only parameter that varies from year to year. For the ECMWF model it was necessary to replace the photochemical equilibrium values for ozone with an ozone climatology derived from observations [Fortuin and Langematz, 1995]. The heterogeneous term $c_4(Cl_{EQ})^2O_3$ is only turned on in daylight and below a threshold temperature of 195 K.

Analysis

In the ECMWF analysis system there is no separate ozone analysis, but ozone is analysed simultaneously with all the other analysis variables in the 3D-VAR or 4D-VAR system. Ozone is analysed univariately at present, which means that the analysis increments of ozone and other variables are assumed to be uncorrelated. The univariate treatment was chosen to prevent ozone sensitive observations from directly changing any variable other than ozone, while the assimilation of ozone data is being further developed and improved. For similar reasons, model ozone is not used directly in the radiation calculations of the forecast model, where the ozone climatology of Fortuin and Langematz (1995) is used instead. The only way ozone can affect the dynamics in 3D-VAR is through the use of the model ozone in the radiance observation operators. In the ECMWF model/analysis configuration this is a weak feedback, which should mostly improve the usage of radiance observations. In 4D-VAR ozone affects the dynamics through the adjoint integrations, even if the ozone analysis is univariate.

In the ECMWF assimilation system retrievals in the form of ozone layers or partial columns (unit kgm^{-2}) are assimilated, not ozone profile points. The main difficulty with the assimilation of retrieved ozone data, which are given as vertically integrated layers spanning several model levels (e.g. TOMS, GOME and SBUV retrievals), is how to distribute the analysis increments in the vertical. This distribution is controlled by the background error covariance matrix of the ECMWF assimilation system. The vertical covariances directly determine the weights with which the layer increment is spread in the vertical and, hence, the shape of the resulting analysis increment profile. The ozone background error covariances used in the ECMWF system were determined statistically from an ensemble of analysis experiments. The observations used in each analysis were perturbed randomly according to the observation error. Differences between the background fields valid at the same time, but from different experiments, are taken to be representative of the background error and give fields from which the background error statistics can be calculated [Anderson and Fisher, 2000].

Validation of the ECMWF ozone field

To validate the ECMWF ozone analysis, analysed ozone fields are compared with independent observations that were not used in the assimilation, concentrating on the total column ozone fields from ERA-40. **Figure 1** (p. III) shows a timeseries of monthly mean ERA-40 ozone values in Dobson Units (DU) and ground based total ozone from four stations for the whole ERA-40 period from 1957 to 2002. We see good agreement for those years when TOMS and SBUV data are assimilated (1979-1988; 1991-2002, though with some gaps in coverage). There are some biases, e.g. the minima are not low enough at Barrow and Bismarck and va-lues are slightly too low at Mauna Loa. Also the ozone hole is not quite deep enough at the South Pole in October, but the trend toward lower total ozone values at the South Pole during the 1980s is well captured.

For the pre-1979 period, when no ozone data were assimilated, ERA-40 total ozone is also reasonable during many of the years, but some larger biases can be seen. Bismarck and Barrow have a good annual cycle in the years prior to 1972 when no satellite data of any sort are assimilated in ERA-40. From 1973 to 1978 data from the Vertical Temperature Profiler Radiometer (VTPR) are assimilated into the ERA-40 system. Too high late-winter values are seen during those years when no other ozone data but VTPR data are assimilated. The same can be seen in 1989 and 1990, when no other ozone data but TOVS-1b data are assimilated. This suggests that the assimilation of these satellite data might upset the Brewer-Dobson circulation, possibly either through a forcing due to the strong convection excited in the tropical troposphere due to the spin-up problem or through a forcing caused by correcting biases in the upper stratosphere. The effect of this on ozone is to be masked when TOMS and SBUV data are assimilated. The timeseries for tropical station at Mauna Loa is very similar in the pre-1979 period to the later years.

The most noticeable difference between ERA-40 ozone and the ground based observations prior to 1979 is seen at the South Pole, where total ozone in ERA-40 is underestimated in many months. The equivalent chlorine loading, which determines the strength of the heterogeneous term in the chemistry parameterization (see Equation 2) is smaller during the earlier years of ERA-40 than in later years, but it is not zero. Comparisons with ozone sondes from Amundsen-Scott during the 1960s show that ERA-40 ozone

values are considerably lower than the sonde values below the ozone maximum of the profiles (not shown). ERA-40 temperatures (in these years prior to the assimilation of satellite radiance data) are about 30 K lower at these altitudes than the sonde temperatures at Amundsen-Scott during October, and considerably below the temperature threshold for PSC formation. At these temperatures the heterogeneous term in Equation 2 is active and some of the ozone is depleted in an 'ozone hole-like' manner in ERA-40 during these early years. During the rest of the year, the ozone maximum at the South Pole is located at higher altitude in ERA-40 than in the observations, and ozone values below the maximum are too low, resulting in a lower total column value. It is possible that the ozone climatology used in the ECMWF system is not appropriate for South Pole conditions during the early years.

During the later years of ERA-40, the PSC term in the ozone chemistry is not quite strong enough to produce a deep enough ozone hole if no ozone data are assimilated.

When ozone data are assimilated the total column ozone field is much improved. This is illustrated in **Figure 2** (p. IV), which shows the total ozone field in DU on 30 September 1990 from ERA-40 (top panel; no ozone observations were assimilated in 1989 and 1990), the total ozone field for the same day from an experiment, which uses the ERA-40 configuration and in which TOMS and SBUV ozone observations are assimilated (middle panel), and TOMS data (bottom panel).

The ECMWF total ozone field shows a bias relative to independent observations that varies depending on the time of year and the geographical location. Generally, the model overestimates total column ozone in the extratropics and underestimates it in the tropics. The positive bias is largest at high latitudes in the NH during winter and spring. There are signs that the Brewer-Dobson circulation in the ECMWF analyses is too strong, and the ozone bias might be a result of transport problems.

While the assimilation of total column ozone data clearly improves the ECMWF total ozone field, a bias between the model and the data can lead to problems in the vertical distribution of ozone in the analysis. Problems arise from having to distribute large total column analysis increments in the vertical. The way the analysis increments are distributed in the vertical is determined by the background error covariance matrix of the ECMWF analysis system. The covariances for ozone originally used in the ECMWF system (and used in ERA-40 from 1991 to October 1996) had anti-correlations between the stratosphere and the troposphere. In situations where the analysis increments were large, the increments were distributed in the vertical in such a way that they caused an almost complete depletion of ozone in the UT/LS and an overestimation of ozone in the lower troposphere [Dethof and Hólm, 2002]. When this problem was noticed, the ozone covariances were modified, and the anti-correlations between the stratosphere and the troposphere removed. The modified covariances are currently used in the operational system, and they were used in ERA-40 between October 1996 and August 2002, and also from the beginning of the ozone assimilation in December 1978 until 1989. With the new covariances the analysis increments are more confined in the vertical and there are no anti-correlations between the stratosphere and the troposphere, or between levels at and above the stratospheric ozone maximum. While this improves the profiles in the troposphere and lower stratosphere, the ozone maximum can be reduced too much in situations where the analysis increment is large and negative.

Work is under way to improve the vertical structure of the analysed ozone field. Several aspects have to be considered here. First, a better representation of the ozone background error covariances is needed. Alternative ways to represent ozone in the analysis (such as normalised quantities) will be explored. Secondly, the bias between the data and the model has to be removed. This problem is two-fold because both the data and the model can have biases. Work is required to understand the reason for the model bias and how to reduce it. Biases in the data will be corrected by implementing a bias correction scheme for ozone data, which makes use of independent ground based observations.

Stratospheric humidity

Accurate simulation of water vapour in the stratosphere is one of the most challenging issues for a general circulation model. The accurate representation of the low humidity entering the stratosphere in the tropics depends on several factors, including convection, condensation processes, the large scale circulation and radiative processes that determine the tropopause temperature. A good representation of water vapour in the stratosphere requires a realistic calculation of the upward transport in the tropics, mixing into the extra tropics and descent at high latitudes. Furthermore, a reasonable representation of the upper stratospheric moisture source due to methane oxidation and mixing across the extratropical troposphere is needed.

In the ECMWF analysis system no humidity data are assimilated in the stratosphere at present and there are no humidity increments in the stratosphere. The background humidity provides the initial stratospheric analysis for the next forecast, except in areas of supersaturation caused by a reduction of the temperatures by the analysis, where the supersaturation is removed. Thus, the stratospheric humidity largely evolves according to the model's dynamics and the parameterization of physical processes (for more information see Simmons *et al.,* 1999).

A new humidity analysis scheme is being developed at ECMWF [Hólm *et al.,* 2002]. A global humidity analysis is difficult because humidity values decrease by several orders of magnitude between the troposphere and the stratosphere. To carry out a tropospheric and stratospheric humidity analysis at the same time, a normalized control variable is required. In the troposphere, specific humidity and temperature are highly correlated and a relative humidity-based control variable is necessary. For the low relative humidities in the stratosphere, specific humidity and temperature background errors are not correlated, but transport processes are much more important for the humidity distribution. Here an analysis based on specific humidity as control variable is appropriate. Such a system is currently undergoing testing at ECMWF and will be implemented in the next model update.

Methane oxidation and photolysis in the mesosphere

The ECMWF model includes a simple parameterization of the moisture source by methane oxidation in the upper stratosphere [Simmons pers. comm.], as well as a sink representing the photolysis of water vapour in the mesosphere. Before this parameterization was included, humidity values in the upper tropical stratosphere and in much of the extratropical stratosphere were too low [Simmons *et al.,* 1999].

Methane is produced by natural and anthropogenic sources at the Earth's surface. It is well mixed in the troposphere and it is carried upwards in the tropical stratosphere. It decreases in relative density (due to oxidation) from tropospheric values of about 1.7 ppmv to values of around 0.2-0.4 ppmv around the stratopause. Mean stratospheric descent

at higher latitudes leads to relatively low values of methane in the extratropical middle and lower stratosphere.

There is observational evidence that over much of the stratosphere the quantity

$$2[CH_4] + [H_2O] \quad (4)$$

is relatively uniformly distributed. Based on values reported by Jones *et al.* (1986) and Bithell *et al.* (1994), a value of 6 ppmv was assumed for this sum in the original ECMWF implementation of the parameterization and for ERA-40. The operational ECMWF parameterization currently uses a value of 6.8 ppmv based on Randel *et al.* (1998) UARS climatology. The rate of increase in the volume mixing ratio of water vapour (in ppmv) due to methane oxidation is currently calculated in the ECMWF model as

$$k_1(6.8 - [H_2O]) \quad (5)$$

The rate k_1 is given by a simple analytical form that varies only with pressure.

The effect of photolysis of water vapour in the mesosphere is included in the parameterization as a simple sink term at heights above 60 km. In this case the full source/sink term becomes

$$k_1(6.8 - [H_2O]) - k_2[H_2O] \quad (6)$$

Like k_1, the rate k_2 is given by an analytical form that varies only with pressure.

Validation of the ECMWF stratospheric humidity

With this simple parameterization ERA-40 has a reasonable stratospheric humidity distribution, but shows a dry bias compared to observations. **Figure 3** (p. V) shows the zonal mean stratospheric water vapour distribution from ERA-40 compared to the UARS climatology for the years 1989-1995. ERA-40 values are about 10-15 % drier than UARS in the upper stratosphere and lower meso-sphere, except near the winter stratopause where the model lacks the resolution to represent correctly the descent of drier air from the mesosphere. It was these generally drier upper stratospheric and lower mesospheric values that led to the operational increase in the equilibrium values from 6 to 6.8 ppmv used in the parameterization of methane oxidation.

In the lower stratosphere there is a too rapid upward progression of the annual cycle of drying and moistening in the tropics in ERA-40 (and in ECMWF's operational analyses). This upward progression in data assimilation cycles is considerably faster than in free-running model simulations, indicative again of a too strong Brewer-Dobson circulation in the assimilating model.

Outlook

It is planned to further increase the vertical resolution of the ECMWF model from 60 to 91 levels in 2004. The tropopause region will benefit most from the resolution increase, with a doubling in resolution near 100 hPa (from about 1 km to 0.5 km), but almost everywhere in the model domain the vertical resolution will be increased. The model top will be raised from 0.1 hPa to 0.01 hPa (about 80 km). **Figure 4** (p. V) shows the level distribution for the current 60-level model and the future 91-level version. The increase in vertical resolution is laying the foundation for improvements in modelling and assimilation around the tropopause and in the upper stratosphere. Here the current model has deficiencies, and it is hoped that a higher vertical resolution will lead to a better vertical tracer transport in the stratosphere and improved stratosphere-troposphere exchange.

The representation of the stratosphere in the ECMWF system will be further improved by the implementation of the new humidity analysis in the ECMWF system. This will enable us to assimilate humidity data in the stratosphere and should lead to a better stratospheric humidity field in the ECMWF analyses.

Further improvements are planned for the ozone assimilation. With its relatively simple ozone chemistry parameterization the ECMWF model manages to reproduce a realistic ozone field. However, there are some biases compared to independent observations and the very low ozone values observed in the Antarctic ozone hole are not reproduced well. The assimilation of ozone data leads to a good total column ozone field in the ECMWF analysis that agrees well with observations. Additional work is required to improve the vertical distribution of ozone in the analyses. This work includes developping a bias correction scheme for ozone data, and an improved formulation of background error covariances or control variable for ozone.

Preparations are under way to make use of new satellite data that give more information about ozone and water vapour in the stratosphere. The prime candidates for this are data from various instruments onboard ESA's ENVISAT. Retrievals from MIPAS and GOMOS give ozone and water vapour profile information in the stratosphere and mesosphere, and have a better vertical resolution than the ozone data currently used at ECMWF. These retrievals together with total column ozone from SCIAMACHY are currently monitored at ECMWF and their quality is being assessed. It is planned to assimilate these data in the near future, provided the data quality is good and the data products are stable.

Acknowledgements

A. Dethof would like to thank **A. Simmons, E. Hólm** and **A. Untch** for their helpful comments and contributions to this article.

References

Anderson, E. and Fisher, M., 2001, Developments in 4D-Var and Kalman Filtering, *ECMWF Tech. Memo.,* **347**.

Bithell, M. *et al.,* 1994, On the synoptic interpretation of HALOE measurements using PV analyses. *J. Atmos. Sci.,* **51,** 2942-2956.

Cariolle, D. and Déqué, M., 1986, Southern hemisphere medium-scale waves and total ozone disturbances is a spectral general circulation model. *J. Geophys. Res.,* **91,** 10825-10846.

Dethof, A. and Hólm, E., 2002, Ozone in ERA-40: 1991-1996. *ECMWF Tech. Memo.,* **377.**

Fortuin, J.P.F. and Langematz, U., 1995, An update of the global ozone climatology and on concurrent ozone an temperature trends. *SPIE Proceedings Series,* **2311,** "Atmospheric Sensing and Modeling", 207-216.

Hólm, E., *et al.,* 2002, Assimilation and modelling of the hydrological cycle: ECMWF's Status and Plan. *ECMWF Tech. Memo.,* **383.**

Hólm, E., *et al.,* 1999, Multivariate ozone assimilation in 4D data assimilation. SODA *Workshop on Chemical Data Assimilation Proceedings.*

Jones, R.L., *et al.,* 1986, The water vapour budget of the stratosphere studies using LIMS and SAMS satellite data. *Quart. J. Roy. Meteor. Soc.,* **112,** 1127-1143.

Randel, W. *et al.,* 1998, Seasonal cycles and QBO variations in stratospheric CH_4 and H_2O observed in UARS HALOE data. *J. Atmos. Sci.,* **55,** 163-185.

Simmons A.J., and Gibson, J.K., 2000, The *ERA-40 project plan. Era-40 Project Report Series 1.*

Simmons A.J., *et al.,* 1999, Stratospheric water vapour and tropical tropopause temperatures in ECMWF analyses and multi-year simulations. *Quart. J. Roy. Meteor. Soc.*, **125,** 353-386.

Untch, A., *et al.,* 1999, Increased stratospheric resolution in the ECMWF forecasting system. *SODA Workshop on Chemical Data Assimilation Proceedings.*

EuroSPICE: The European Project on Stratospheric Processes and their Influence on Climate and the Environment - Description and brief Highlights

John Austin (john.austin@metoffice.com) and **Neal Butchart,** U.K. Meteorological Office (UKMO), UK
C. Claud and **C. Cagnazzo,** Laboratoire de Météorologie Dynamique (LMD), France
A. Hauchecorne and **J. Hampson,** Service d'Aéronomie (CNRS-SA), France
J. Kaurola, J. Damski and **L. Tholix,** Finnish Meteorological Institute (FMI), Finland
U. Langematz, P. Mieth, K. Nissen and **L. Grenfell,** Freie Universität Berlin (FUB), Germany
W. Lahoz and **S. Hare,** University of Reading (UR), UK
P. Canziani, University of Buenos Aires (UBA), Argentina

1. Introduction

EuroSPICE was composed to bring together observations and a full range of 3D-dimensional models to improve our understanding of the impacts on the atmosphere of changes in the concentrations of the greenhouse gases (GHGs) and halogens. Europe is strong in these activities and funding under the European Framework 5 umbrella has proved to be a particularly useful way of stimulating collaboration between the research groups, which consisted of the UKMO, LMD, CNRS-SA, FMI, FUB, UR and UBA. Addressing the issue of the impact of the stratosphere on climate was from the beginning a long-term aim of EuroSPICE, and assuming that contract negotiations are successful, this will be continued in the European Framework 6 project SCOUT. EuroSPICE has just a few more months to run and this would seem to be an apposite time to summarise its preliminary results, and we welcome informal discussions on the material.

The work was designed to cover the recent past (1980 to 2000), for which good data coverage exists, and the near future (2000 to 2020) to address issues, such as the recovery of stratospheric ozone. The work concentrated on trends in temperature, ozone and surface UV. The major data sources were utilised for this purpose with, where possible, a detailed statistical model employed to determine trends. Model simulations were based around transient climate model simulations, with and without coupled chemistry, supported by 3D-mechanistic and chemical transport models. To provide consistency between the model simulations, the sea surface temperatures (SST) were specified from observations and the concentrations of halogens and the well-mixed greenhouse gases (WMGHGs) were taken from WMO [1999, Chapter 12] and IPCC [1992, Scenario IS92a], respectively. Finally, with the model results now available, the impact of the stratosphere on the troposphere is beginning to be investigated, initially using some basic tropospheric parameters.

2. Past trends

(a) Temperature

The cooling trend in the stratosphere and warming trend in the troposphere is by now an established feature of the global atmosphere [see e.g. Shine *et al.,* 2003]. This is reproduced by all the models of EuroSPICE. **Figure 1** shows the trends determined for transient model simulations. All the models used the same evolution in the concentrations of GHGs and halogens. The UKMO and FUB models are full climate models and used coupled chemistry. The Reading model is a climate model, the Unified Model (UM) is the same version as used by the UK Met. Office, but it doesn't have coupled chemistry. Instead, the ozone trends are specified from the observations determined by Langematz (2000). The CNRS-SA model is a mechanistic model with a lower boundary near the tropopause. Although there are many similarities between these model temperature simulations, differences arise from the different ozone trends as shown in Section 2b.

Figure 1. Annual mean temperature trend for 1980 to 1999 in K/decade simulated by the different models of EuroSPICE. The contour interval is 0.5 K/decade; regions where the trend is significantly different from zero are shaded for the 95 % (light blue) and 99 % (dark blue) confidence levels.

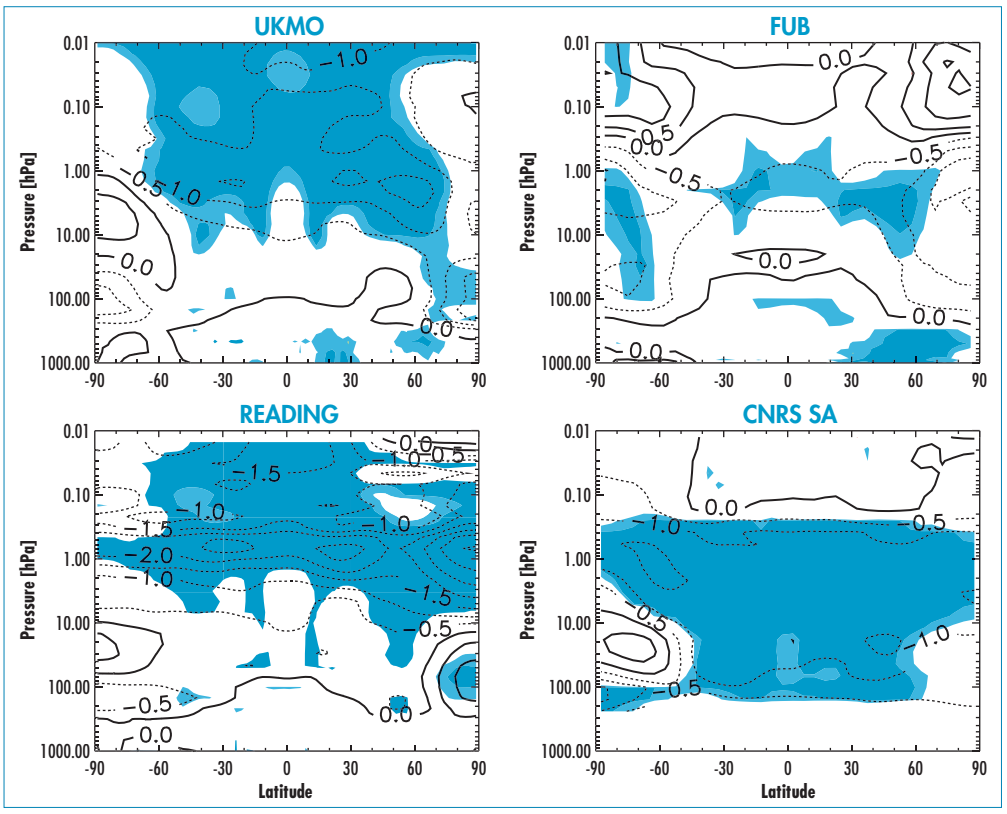

The above model trends have been computed using a simple linear trend model without additional parameters. During EuroSPICE a more detailed statistical analysis has been undertaken of observations from the SSU and MSU satellite data using the AMOUNTS statistical model [Hauchecorne *et al.*, 1991]. Results are shown for the near-global average in **Figure 2**, together with a sample of the model results shown in Figure 1. Also shown in Figure 2 are the NH temperature trends computed from the FUB analyses using the AMOUNTS model. These results are compared with an additional simulation of the UM in which the GHGs concentrations increase as in the observations but with no trend in ozone, indicated by the broken line in Figure 2. The two UM simulations are significantly different in the upper stratosphere and lower stratosphere (LS), confirming the role of ozone decreases in contributing to the temperature trends in those regions. With the observed ozone trends, the model agrees reasonably with observations through much of the pressure range, except possibly in the LS. These results are very similar to those obtained by Shine *et al.* (2003) who further suggested that the absence of water vapour trends in the models may be one of the reasons for the remaining discrepancies with observations, particularly in the LS.

Figure 2. Near global average temperature trends from observations and model results. Data for both model and observations are averaged between 70°N and 70°S because of the limited domain of the SSU data. The results of the Unified Model (UM) are the mean for an ensemble of five members. The thick solid line indicates the mean trend calculated by the UM with the ozone trends specified. The 95 % confidence interval is given by the thin solid lines.

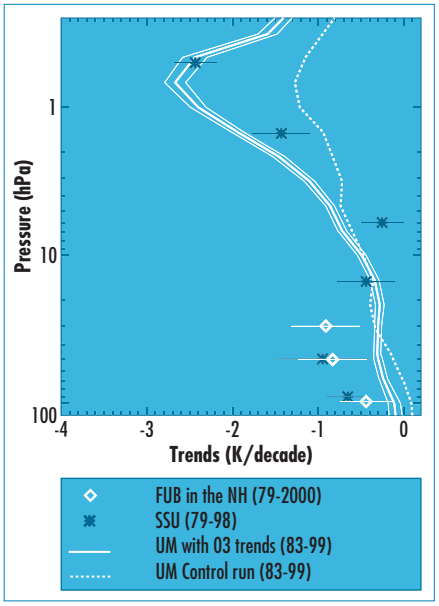

Figure 3. Top panel: Annually averaged temperature trend from the SSU/MSU data. The light and dark shading indicates where the trend is significantly different from zero at the 90 % and 95 % levels, respectively. Bottom panel: The QBO component of the temperature signal observed by SSU/MSU instruments. The units are K per QBO cycle assuming a 7 month phase lag. The statistical significance of the signal is indicated for the 90 % and 95 % as light and dark blue, respectively.

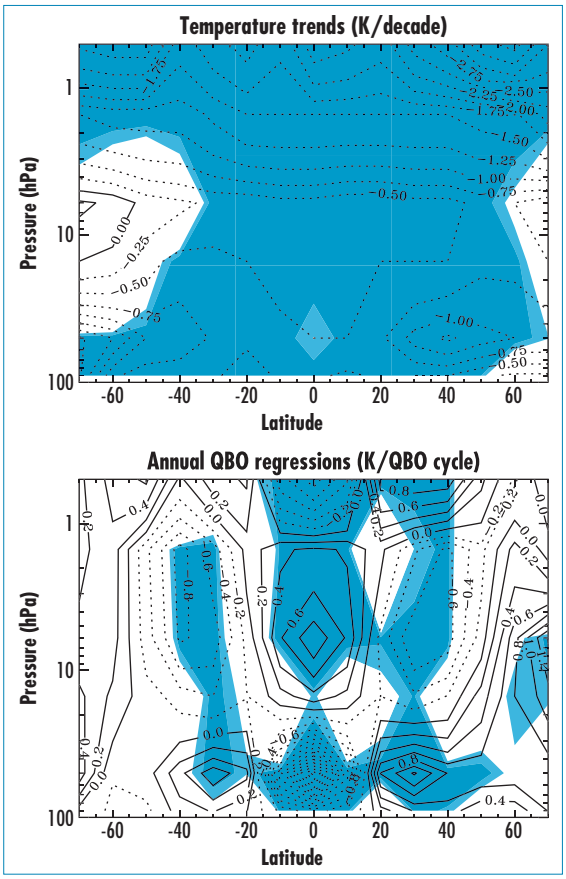

By using the AMOUNTS model, it was possible to investigate the temperature data to separate the various processes affecting variability and to provide, ultimately, a more accurate determination of the underlying trends. The observations were regressed against aerosol, El-Nino Southern Oscillation, Arctic Oscillation, solar variability and the Quasi-Biennial Oscillation (QBO) terms, as well as seasonable terms and the secular trend. As an example, we show in **Figure 3** the secular trend and the impact of the QBO on temperature determined from the SSU/MSU data and assuming a phase delay of 7 months. A significant signal is present in the lower and middle stratosphere with opposite phase signals at middle latitudes. The fact that the signal is quite large, comparable with the decadal trend (top panel), implies the need for careful analysis of the model results in the tropics particularly for models such as the UM (used by UKMO and UR), which has a naturally occurring QBO. Without detailed analysis, the significance of the model trends could be lowered by the large interannual variability in the tropics, which might otherwise be interpreted as noise by the statistical trend calculation.

(b) Ozone

Figure 4 shows the past ozone trends computed by the models of EuroSPICE. An explanation of some of the differences in the model temperature trends is apparent in the large differences in modelled ozone. The models generally fit into two general types: one with large ozone losses in the upper stratosphere (UKMO and FMI) and one with small increases in this region (FUB and CNRS-SA). The first two models also indicate large ozone losses in the polar LS in both hemispheres, consistent with the development of the Antarctic ozone hole and northern spring depletion. These are the very regions affected by halogen chemistry and they are being further investigated by the two models showing ozone increases. The observations from SAGE (**Figure 5**) show the high ozone losses expected from the halogen chemistry. At 3 hPa the ozone trends equate to typically 6% per decade with peak values exceeding 8% per decade. The Antarctic ozone hole is clearly visible in the annual mean. Note also the slight increase in ozone at some levels up to 10 hPa over the equator, which is reproduced in the UKMO and FMI models, although it is not statistically significant.

(c) Surface ultraviolet

One of the main aims of EuroSPICE is to clearly establish the relationship between the parameters affecting surface Ultraviolet. While it is clear that ozone trends have been a contributing factor, in principle, aerosol and cloud changes may also have played a role in regions where the UV trend is small. For EuroSPICE we have adopted a simplified way of using climate model output to provide an estimate of the cloud-corrected UV. We have also determined surface UV trends from TOMS, as well as measurements from ground-based instruments over high latitudes in Europe. **Figure 6** (p. 18) compares the UV trends from TOMS with those from the UKMO model. Good agreement between model and observations is generally seen, but

Highlights from the Joint SPARC-IGAC Workshop on Climate-Chemistry Interactions

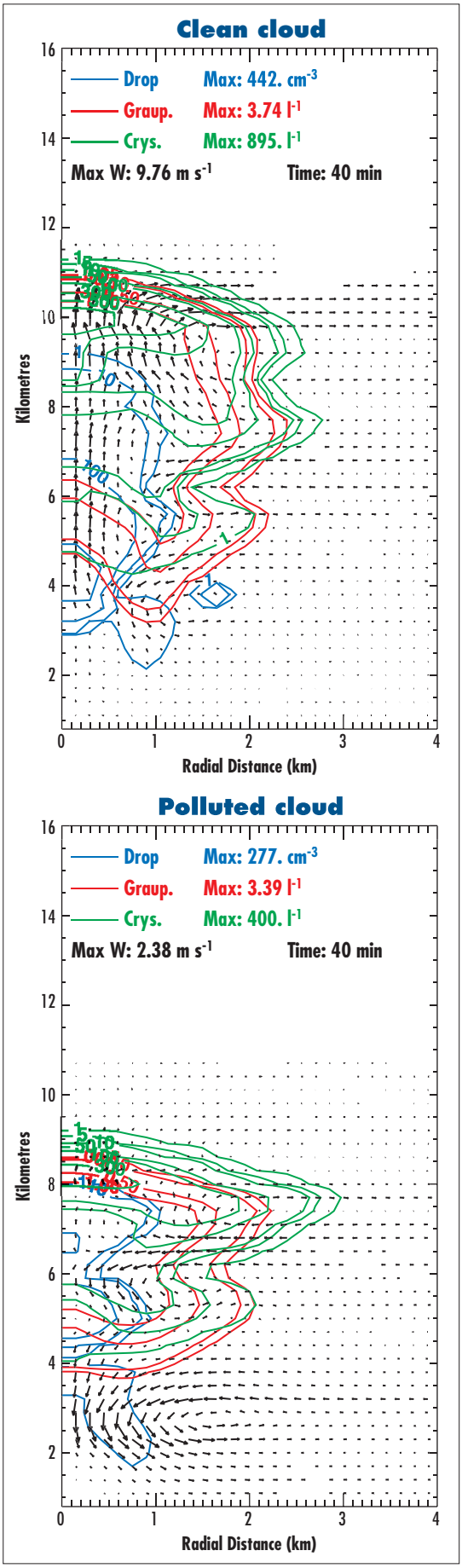

◀ **Figure 4**
The influence of anthropogenic aerosols on cloud properties as computed in a microphysical model shows a significant sensitivity to aerosol loading. Such variations form part of the basis for the current major emphasis on understanding the influence of aerosols on clouds and, thus, on radiation. [From K. Carslaw, Y. Yin]

▼ **Figure 6**
The integrated column abundances of NO_2 for the same geographical region and same time from two satellites with differing horizontal resolutions. The lower resolution GOME satellite yields smaller peak column abundances than the higher resolution SCIAMACHY satellite. Since the net ozone production is non-linearly dependent on NO_x amounts, these two column abundances would lead to different ozone production rates. These pictures emphasize the need for high resolution atmospheric data and modelling in climate studies. [From J.P. Burrows]

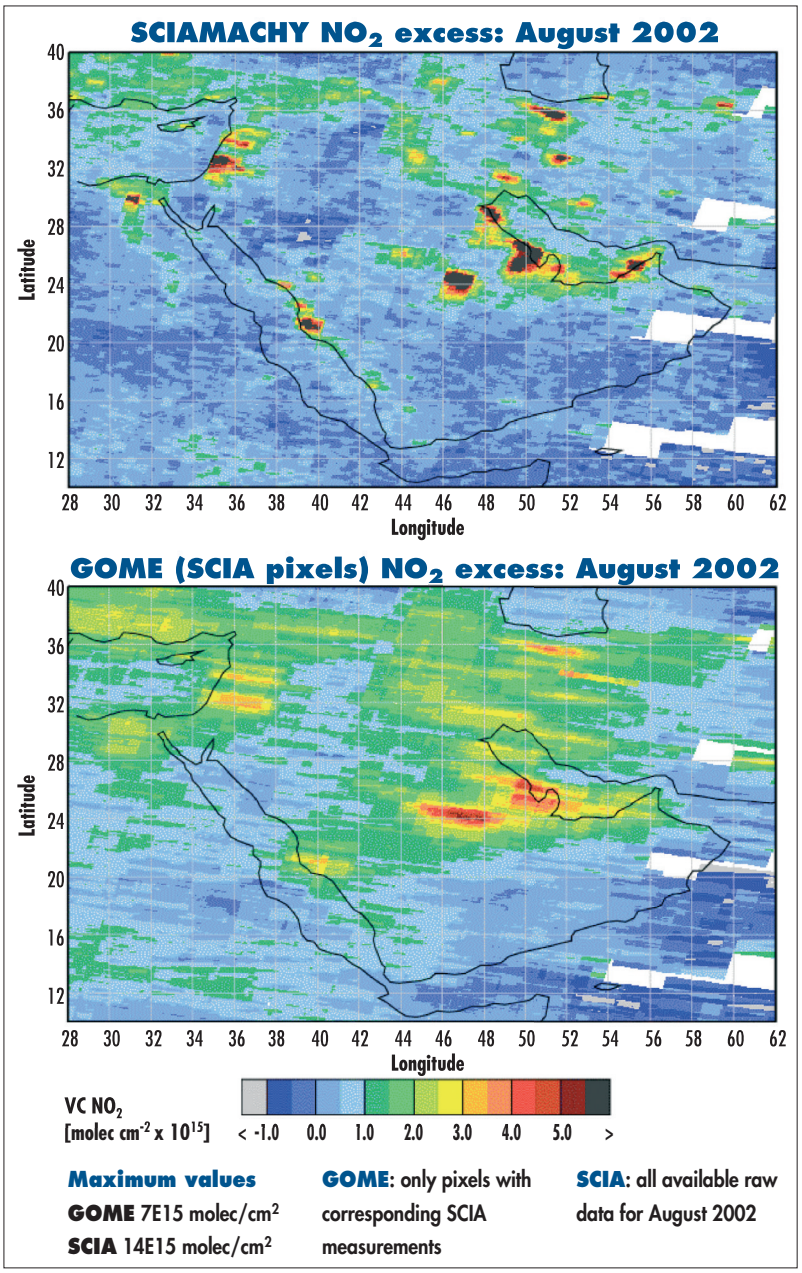

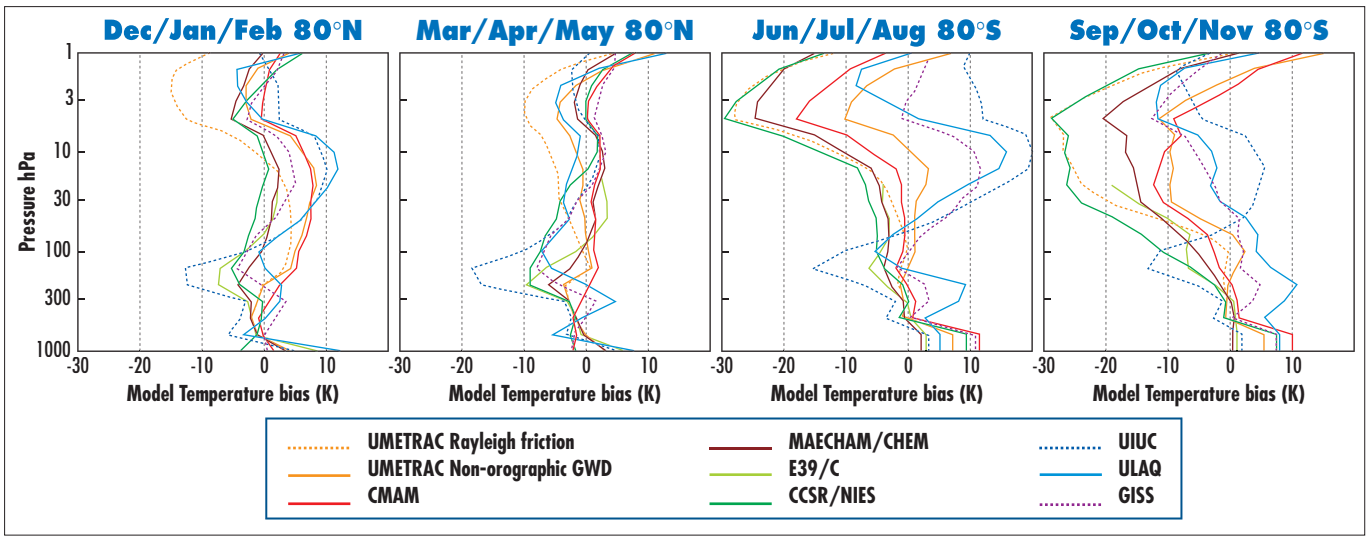

▲ Figure 7
Calculated vertical profiles of temperatures from different climate models. The large differences in calculated temperatures lead to differing abundances of species and ozone changes. [From J. Austin *et al.*]

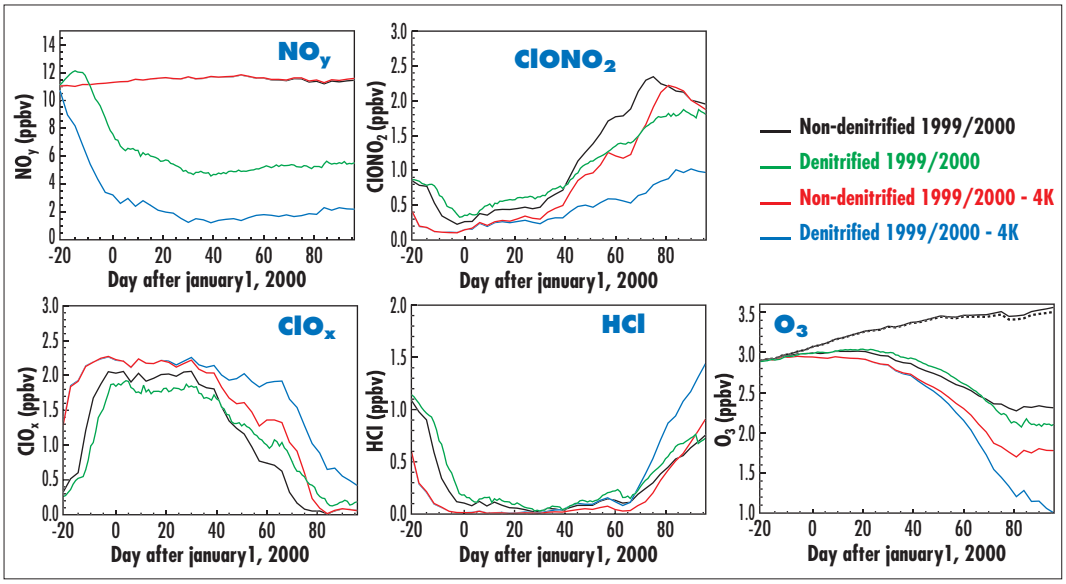

▶ Figure 8
Evolution of different chemical species (noted in the panels) in the Arctic LS calculated with a 3D-model and using different assumptions of the extent of denitrification produced for various temperatures. [From S. Davies, University of Leeds].

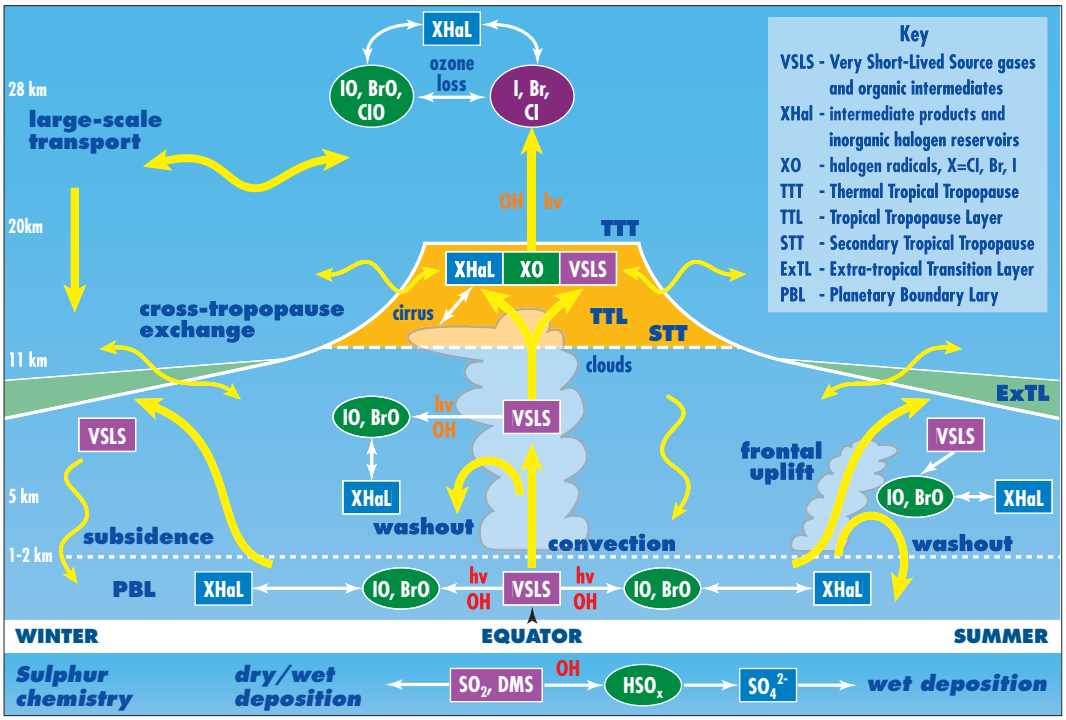

▶ Figure 9
A schematic representation of the chemical and transport processes that influence stratosphere-trosposphere interactions. In particular, these processes have a significant influence on the TTL region. [From P. Haynes, R. A. Cox, and K. Law]

Report on the SPARC Workshop on the Role of the Stratosphere in Tropospheric Climate

Participants at the «Role of the stratosphere in troposphere climate» workshop, in Whistler, BC, Canada.

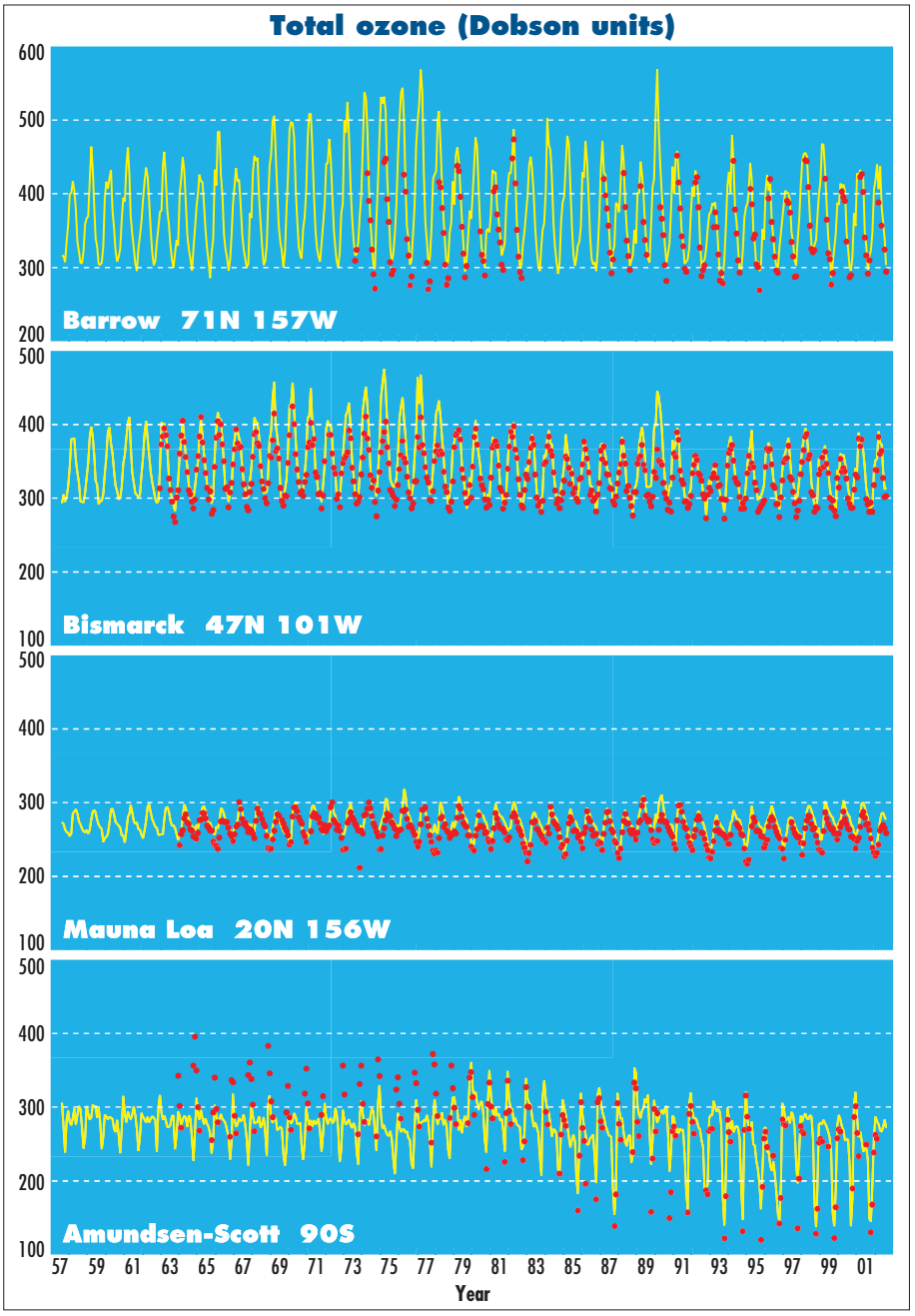

Aspects of Modelling and Assimilation for the Stratosphere at ECMWF

III

◀ Figure 1
Timeseries of monthly mean total ozone in DU from independent ground based observations (red dots) and ERA-40 (yellow curve) for the stations Barrow, Bismarck, Mauna Loa, and Amundsen-Scott. [Figure provided by A. Simmons, following similar calculations by P. Simon].

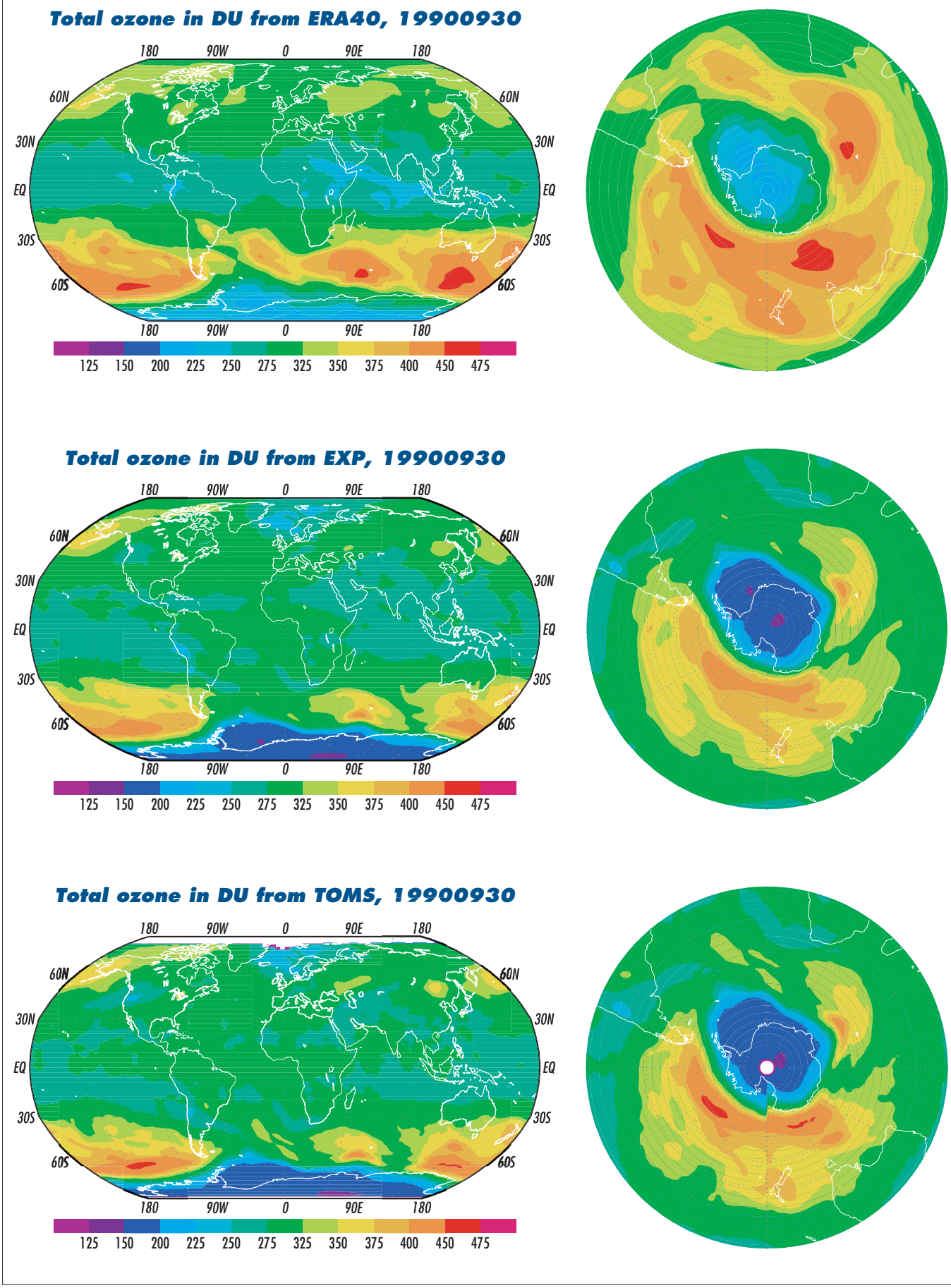

▲ Figure 2
Total column ozone in DU on 30 September 1990: from the ERA-40 production in which no ozone observations are assimilated at this time (top), from an experiment which uses the ERA-40 configuration and in which TOMS total column ozone and SBUV ozone layers are assimilated (middle), and from gridded daily TOMS data (bottom).

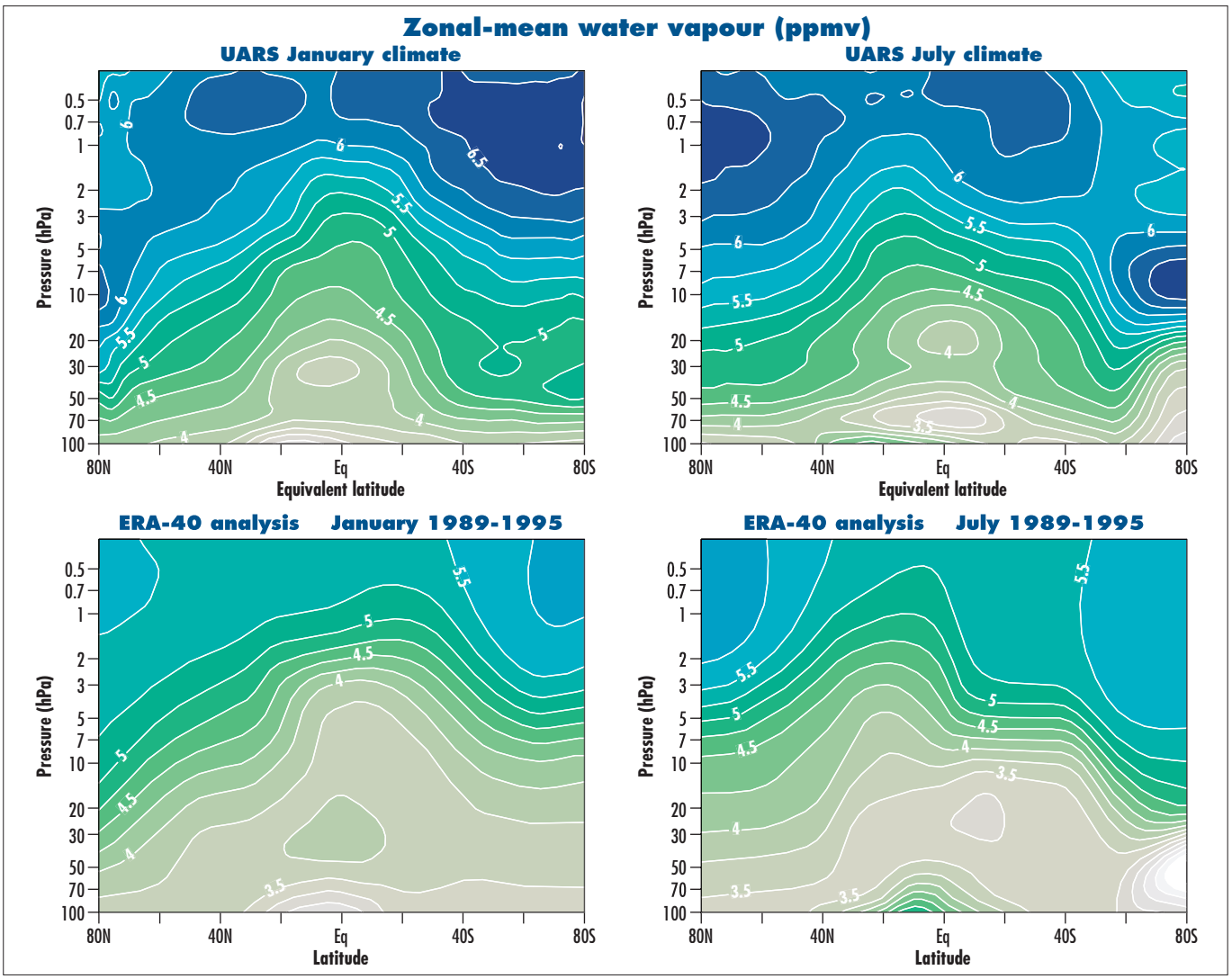

▲ Figure 3
Upper: Monthly-mean distribution of the mixing ratio of water vapour (ppmv) as a function of pressure and potential vorticity (expressed as equivalent latitude), based on UARS (HALOE, supplemented by MLS) data analyses by Randel et al. (1998). Lower: Monthly-mean distribution of the mixing ratio of water vapour (ppmv) as a function of pressure and latitude derived from ERA-40 analysis for the years 1989-1995. January (left-hand panels) and July (right-hand panels). [Figure provided by A. Simmons]

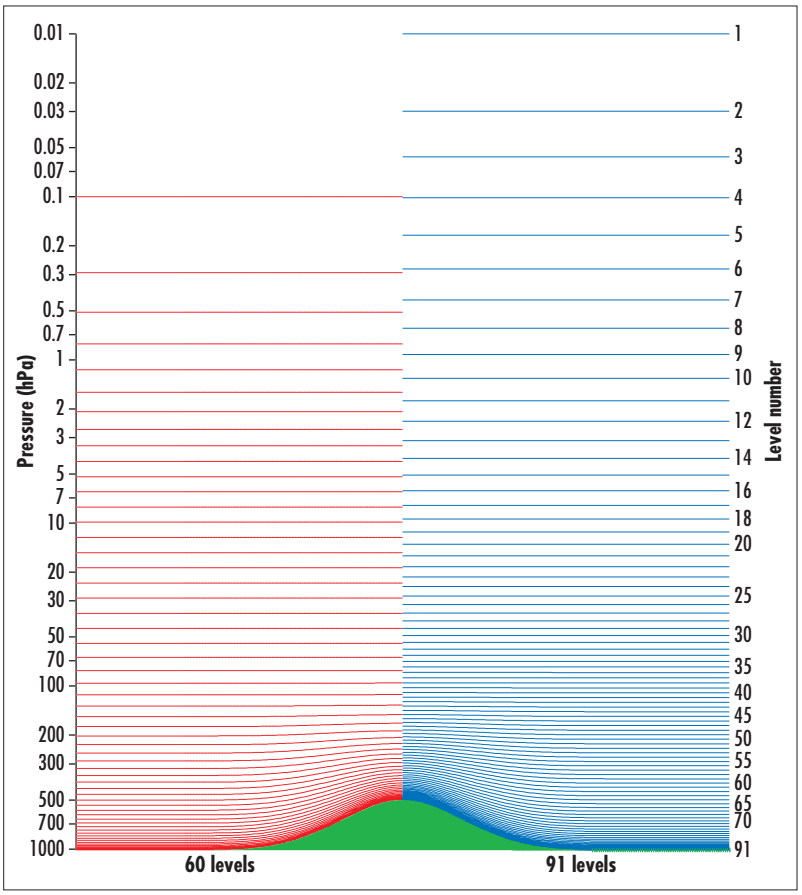

◀ Figure 4
Distribution of the full-model levels, at which wind, temperature, humidity and ozone are represented, for the current 60-level (left) and the future 91-level (right) vertical resolution. [Figure provided by A.Untch].

V

EuroSPICE: The European Project on Stratospheric Processes and their Influence on Climate and the Environment - Description and brief Highlights

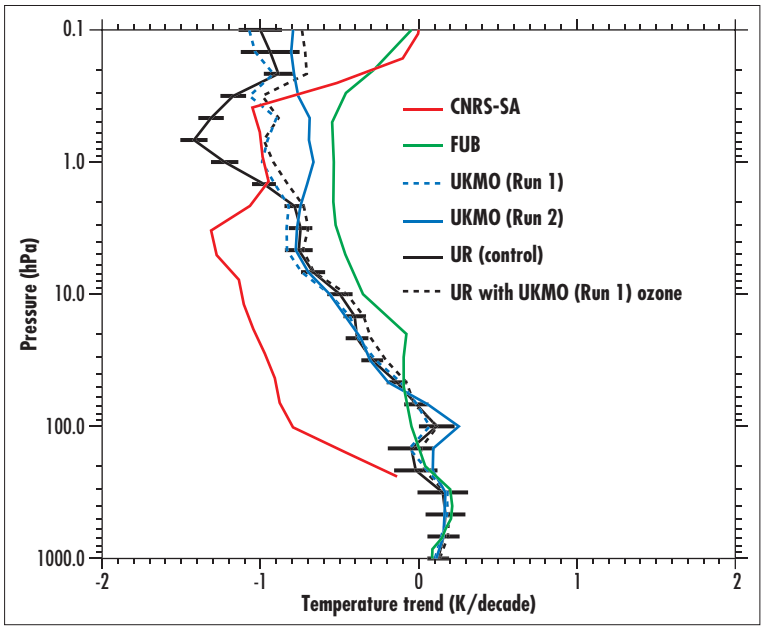

◀ Figure 7
Simulated globally and annually averaged temperature trends in the models for the period 2000-2019 as a function of pressure. The UR results are shown as a control run with fixed ozone (black line) and a run (black broken line) with ozone from Run 1 of the UKMO simulation. The error bars in the control run indicate the 95 % confidence intervals. For clarity, the uncertainties are not included in the other model simulations but are of similar magnitude.

UV Index Forecasting Practices around the World

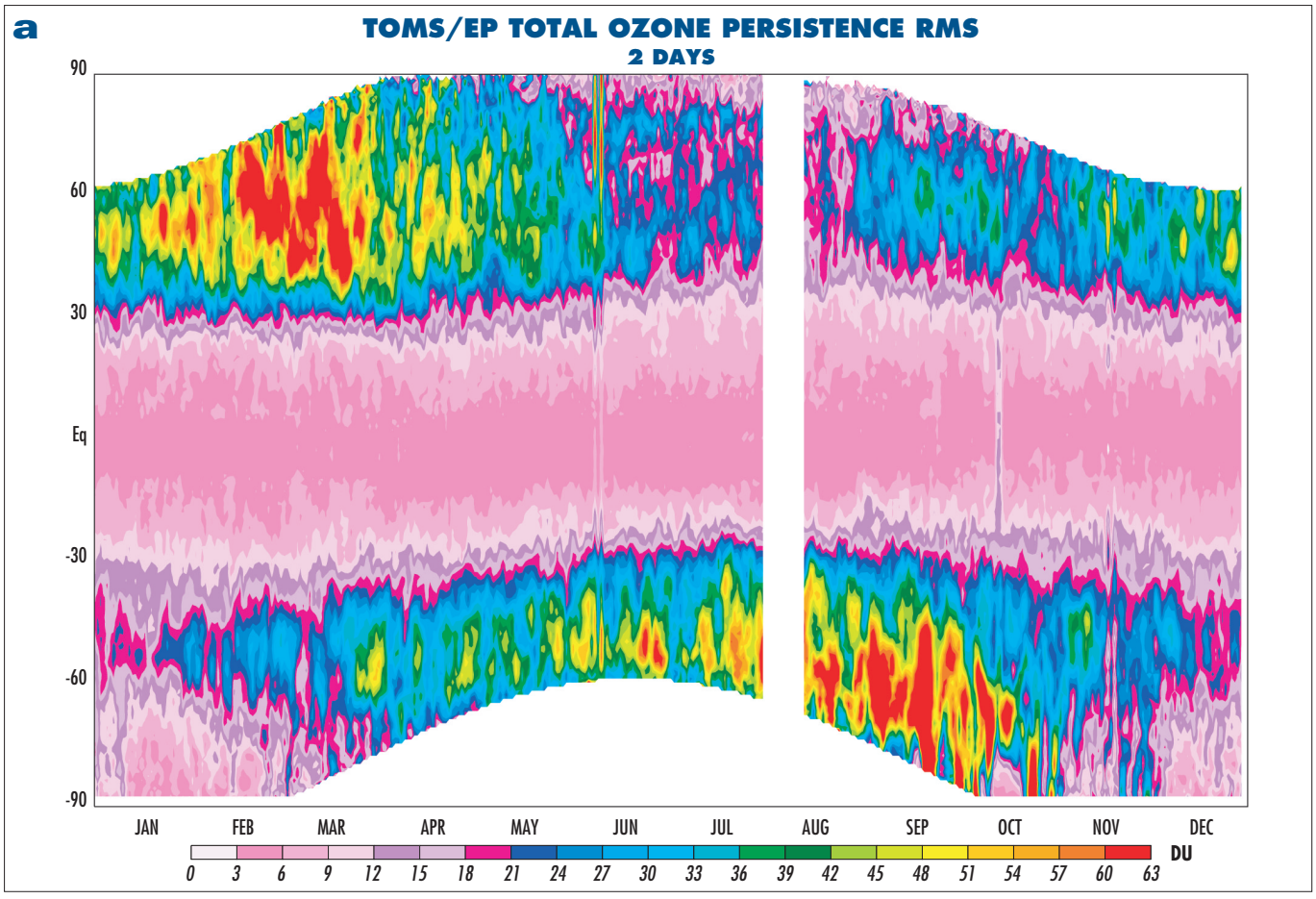

▲ Figure 3a
Daily zonal mean RMS errors (DU) obtained by persisting the TOMS total ozone over a 2-day period for the year 2002.

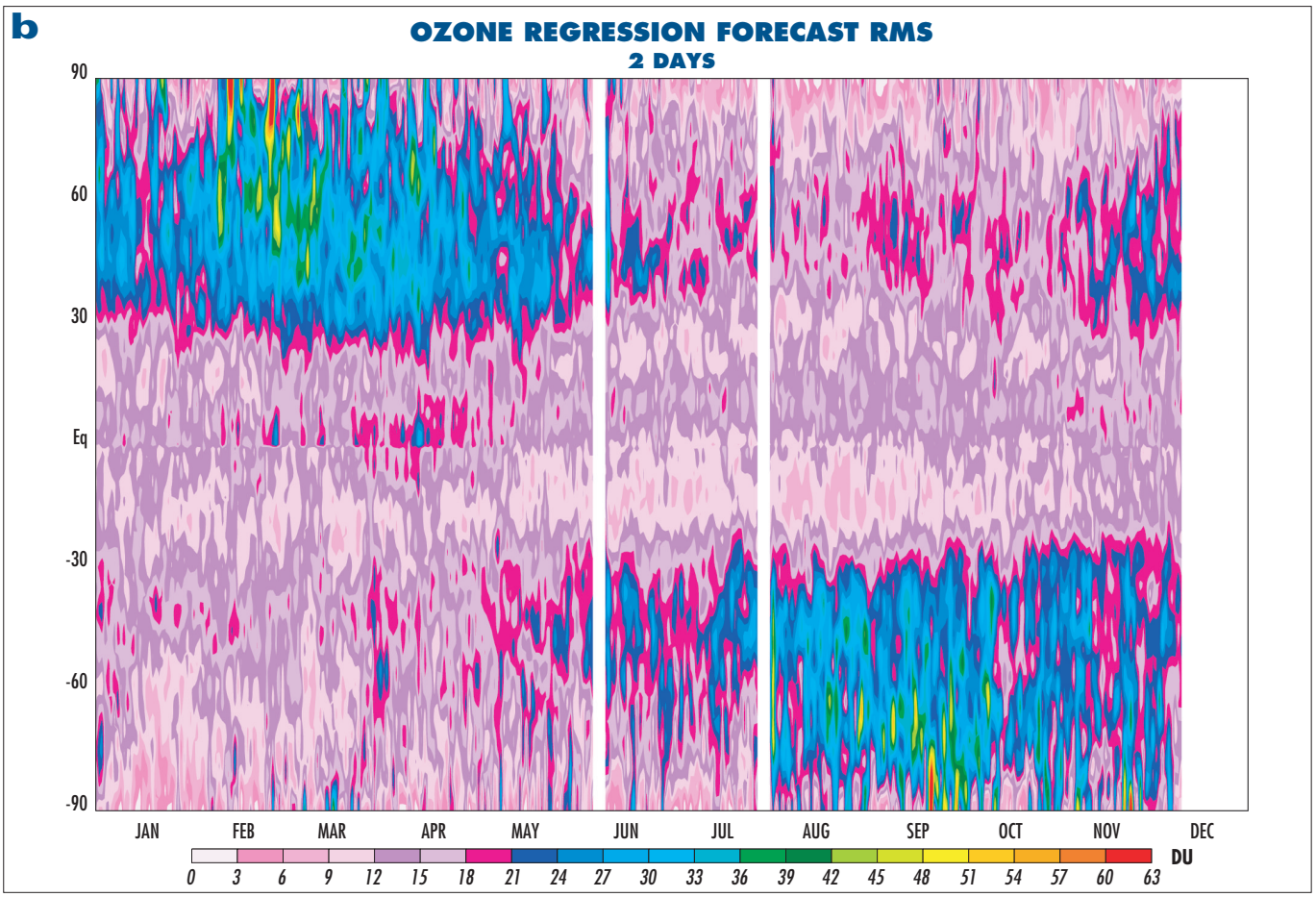

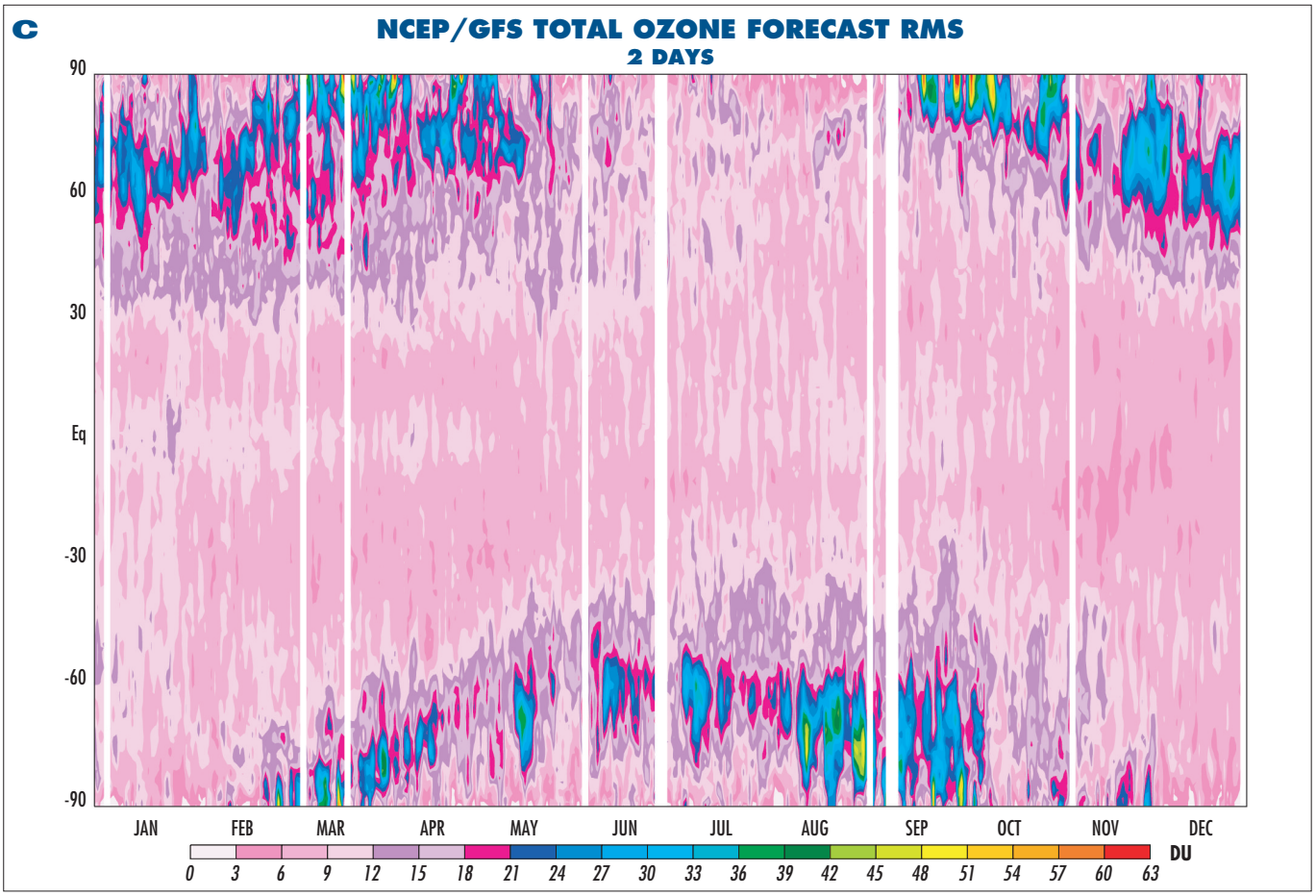

▲ **Figure 3**
b) Daily zonal mean RMS errors (DU) obtained by using a regression method previously used at NCEP to produce a 2-day forecast of ozone.
c) Daily zonal mean RMS errors (DU) obtained using the 2-day ozone forecasts from the NCEP/GFS model.

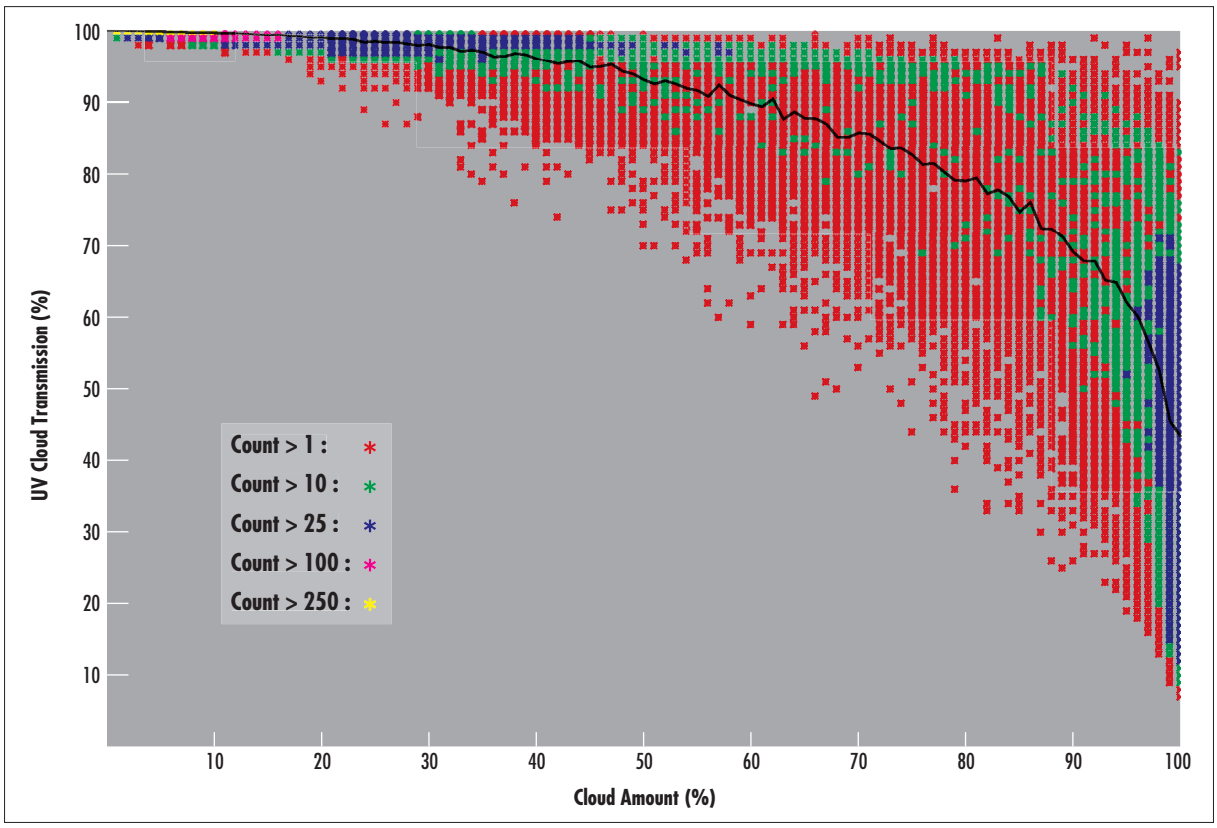

▲ **Figure 4**
Scatter plot of the ratio of UV band «cloudy sky» and UV band «clear sky» with total cloud amount for each NCEP/GFS model grid point for a single day in the NH mid latitudes (30°– 60°N). The different colour symbols denote the frequency of occurrence. The line is the mean ratio for each cloud amount percent.

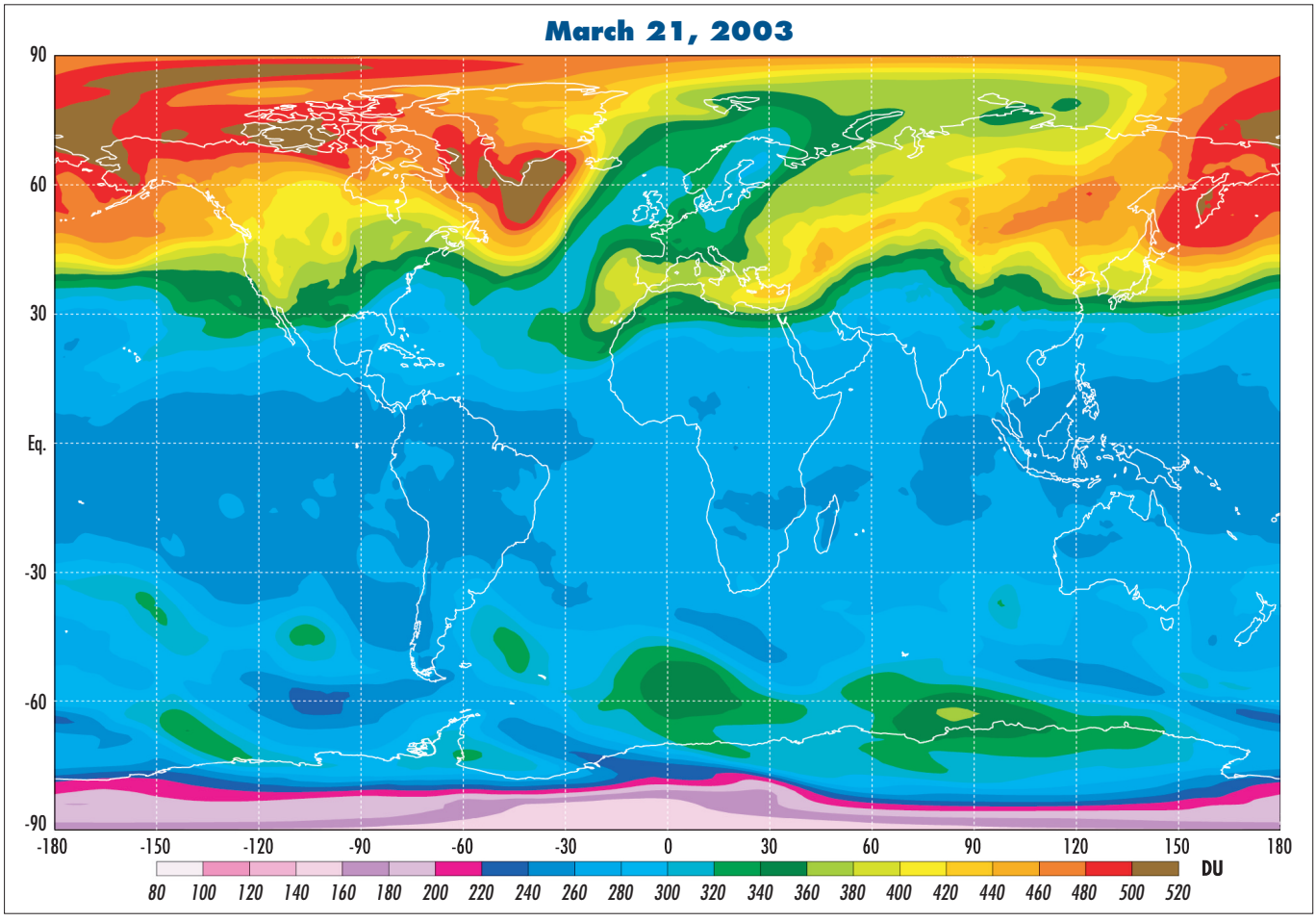

▲ **Figure 5a**
2-day total ozone (DU) forecast field generated by the NCEP/GFS model valid for 00Z on March 21, 2003.

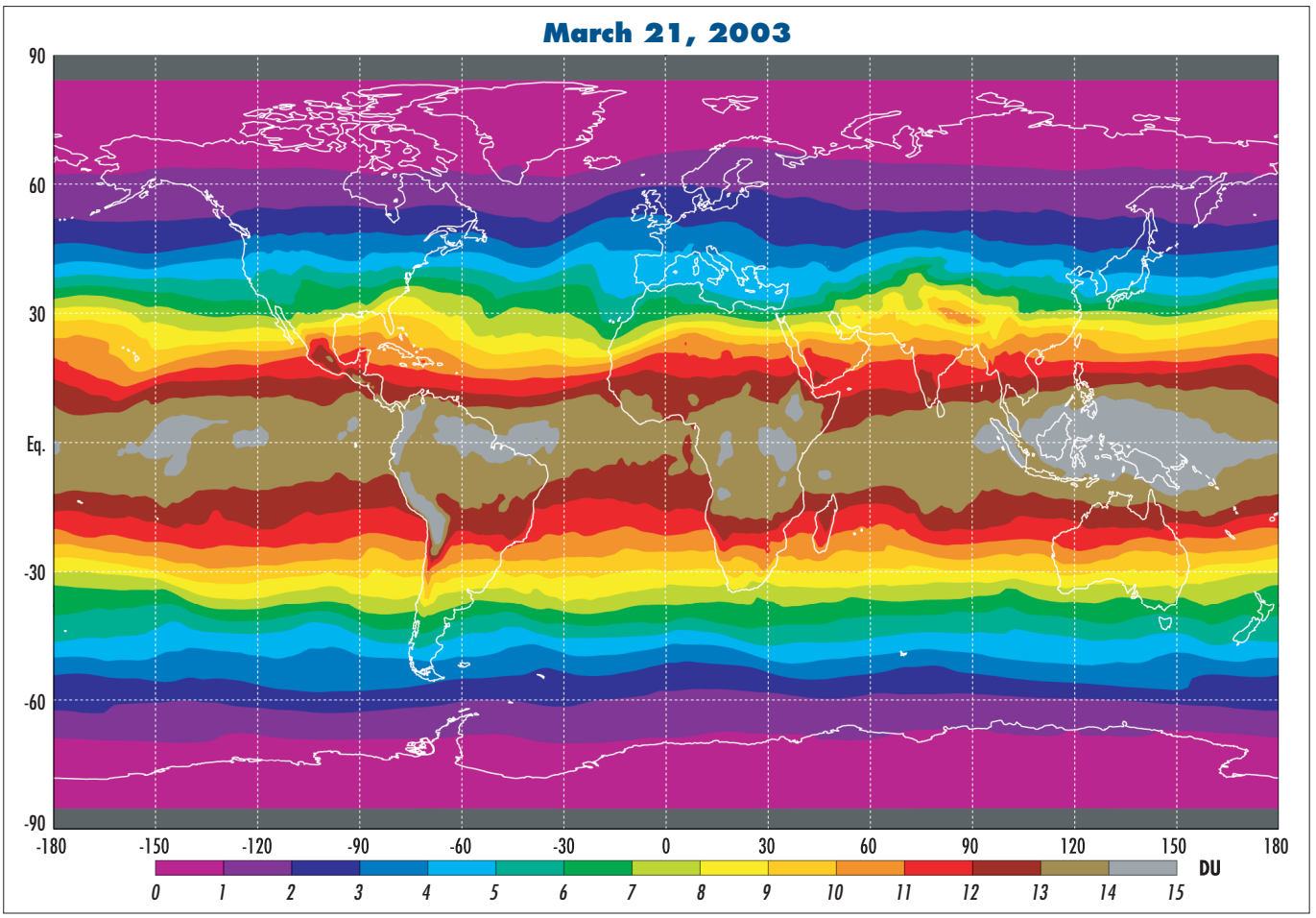

▲ **Figure 5b**
2-day clear sky UV Index forecast field valid for solar noon at all longitudes on March 21, 2003. Noontime UV Index values were generated from the total ozone forecast fields like that shown in Figure 5a but for all hours of March 21, 2003.

The SAGE III/Meteor Mission One Year in Operation

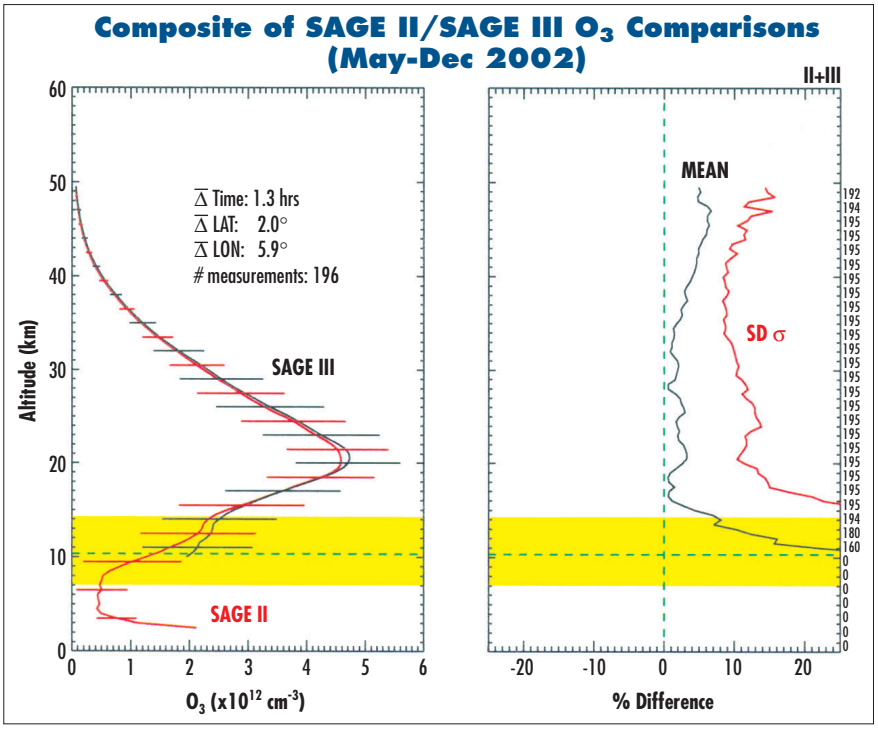

◀ **Figure 1**
The mean difference and standard deviation of composite comparisons between coincident SAGE III and SAGE II ozone profiles during the time period of May to December 2002 are shown. Coincidence is defined as measurements made within 4° latitude, 12° longitude, and 12 hours. For these coincidences, the mean time difference is 1.3 hours, mean latitude difference is 2°, and the mean longitude difference is 5.9°. The number of coincidences at a given altitude is given on the right hand side of the right panel. The mean is defined as SAGE III-SAGE II / the average of SAGE III + SAGE II. The yellow shading in each panel indicates the range of tropopause heights for the comparisons and the horizontal dashed green line is the mean tropopause level. Note that the two instruments agree within 3% from 15 to 40 km.

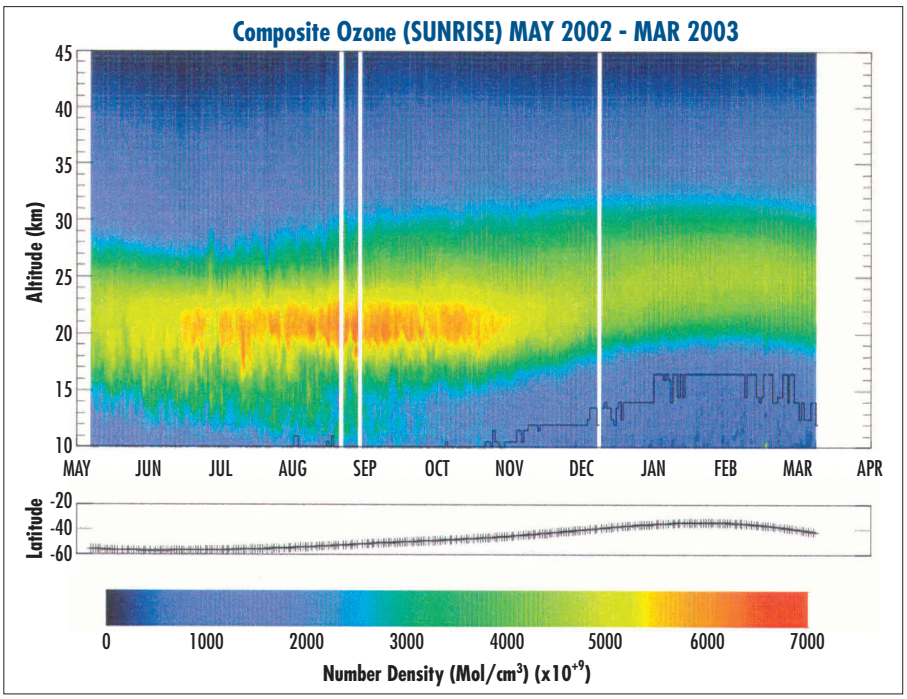

Figure 2
The SAGE III sunrise time-history of ozone density profiles from May 2002 through February 2003 in the Southern Hemisphere is shown. The measurement latitudes and tropopause heights (thin black line) at the measurement location are also shown.

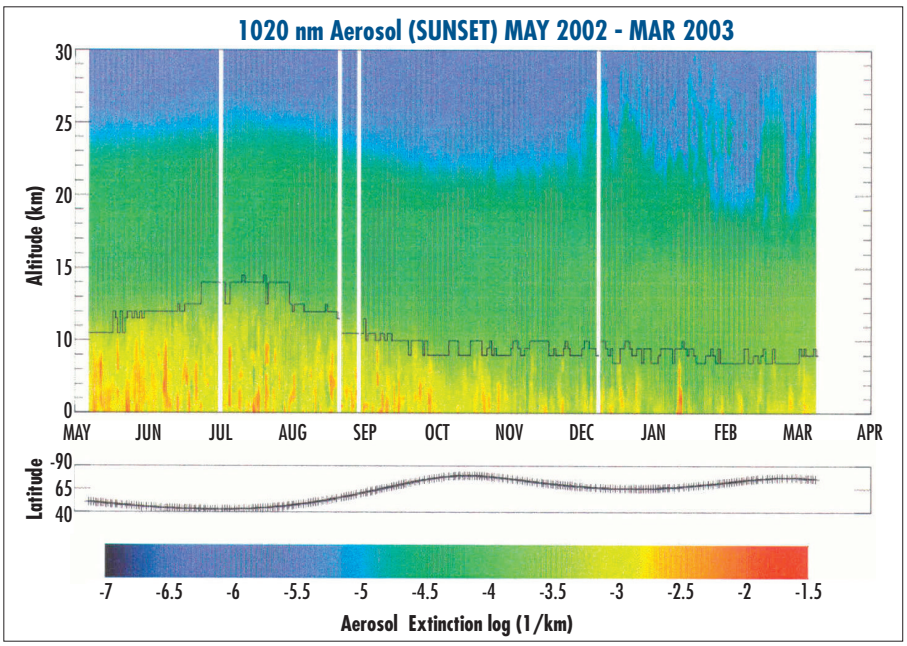

Figure 3
The SAGE III sunset time-history of aerosol extinction profiles at 1020 nm wavelength from May 2003 through February 2003 in the Northern Hemisphere is shown. The latitude and tropopause height for each measurement are also shown.

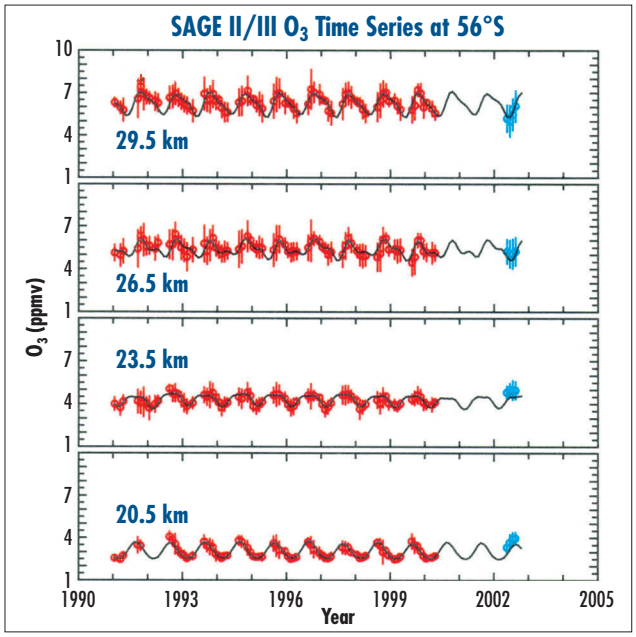

Figure 4
Time-series of SAGE II (red circles) and SAGE III (blue circles) monthly zonal averages centered near 56°S is plotted for a number of altitudes. The black line is the model fit of SAGE II ozone data between October 1984 and June 2000, and extended to August 2002. It is clear that the SAGE III data follow the natural seasonal cycle (climatology) and «fill in» monthly gaps of the SAGE II time series. The SAGE II model climatology consists of a mean, linear trend, seasonal, quasi-biennial oscillation, and Solar cycle terms.

Start of ILAS-II Operation for the Observation of Stratospheric Constituents

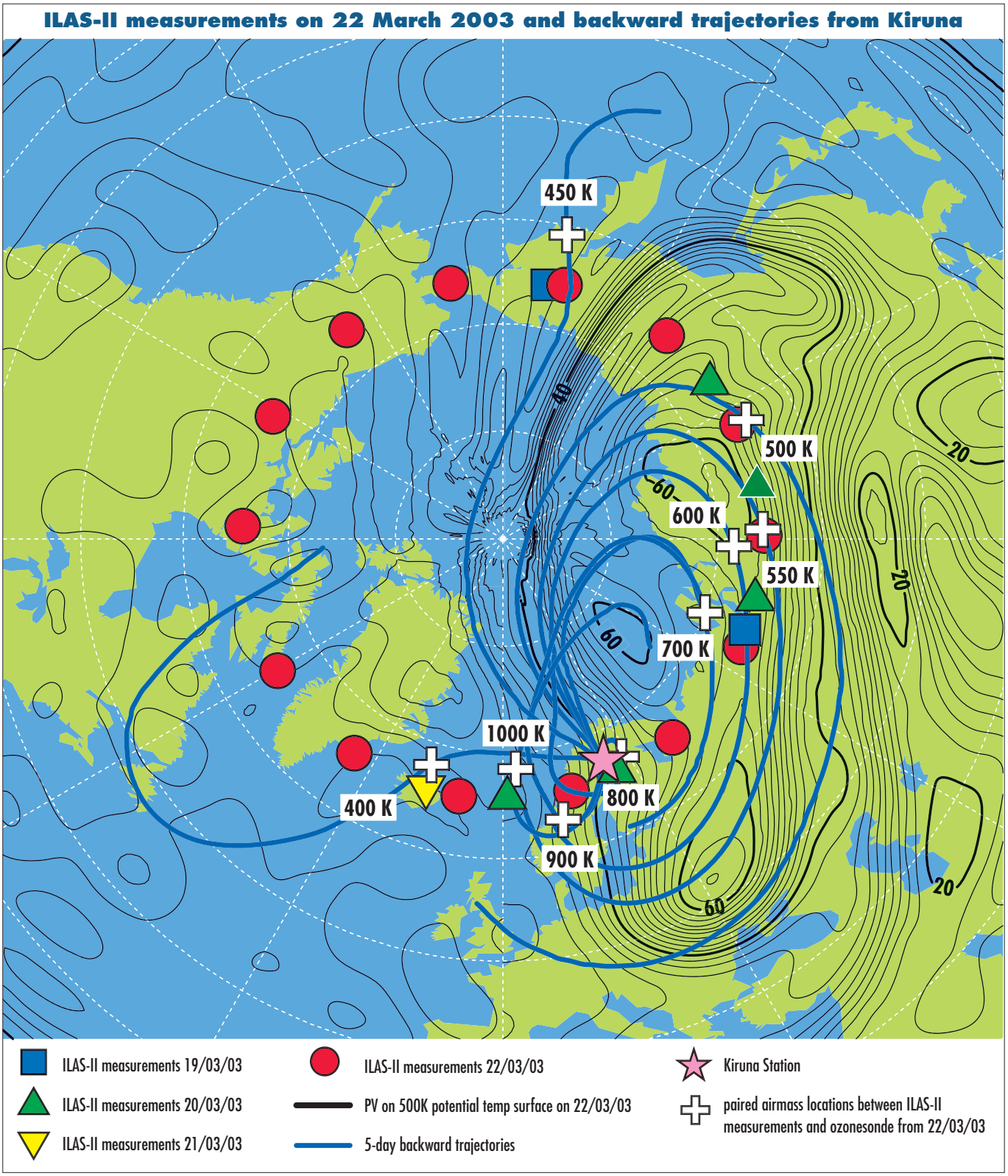

▲ Figure 1

Map of potential vorticity (black contours) at 500 K potential temperature surface on 22 March, 2003. The 14 red circles show the measurement points of ILAS-II on that day. The pink star represents the location of Esrange station, Kiruna (68°N, 21°E), Sweden, where an ozonesonde sounding was made on 22 March, 2003. Blue curves correspond to 5-day backward trajectories for the ozonesonde measurement (the 400, 450, 500, 550, 600, 700, 800, 900, and 1000 K isentropic surfaces shown here). Blue squares, the green triangles and the reverse yellow triangle correspond to the measurement points of ILAS-II on 19, 20, and 21 March, 2003, respectively, which were then hunted by the backward trajectories. The white crosses along each trajectory are the location of the air mass paired with the ozonesonde measurements.

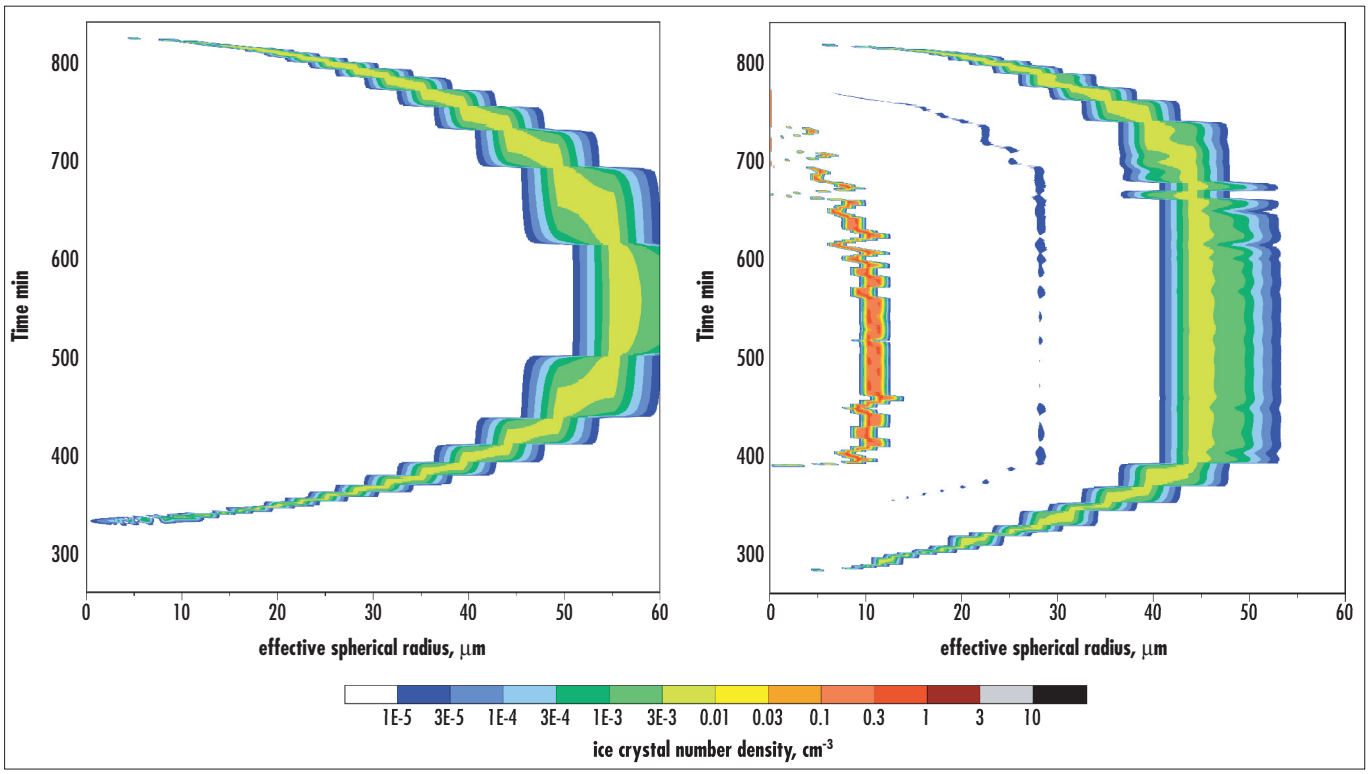

▲ **Figure 1**

Temporal evolution of ice crystal size distributions in a synoptic wave with a peak amplitude of 5 cm s^{-1} (left) and with superimposed small-scale temperature fluctuations consistent with INCA observations (right). The aerosol consists of 400 cm^{-3} liquid supercooled droplets and 0.01 cm^{-3} IN, the former (latter) freezing at ~150% (130%) relative humidity over ice. The marked differences between the size spectra are brought about by the combined action of gravity waves and the presence of a few efficient IN. [Figure provided by B. Kärcher].

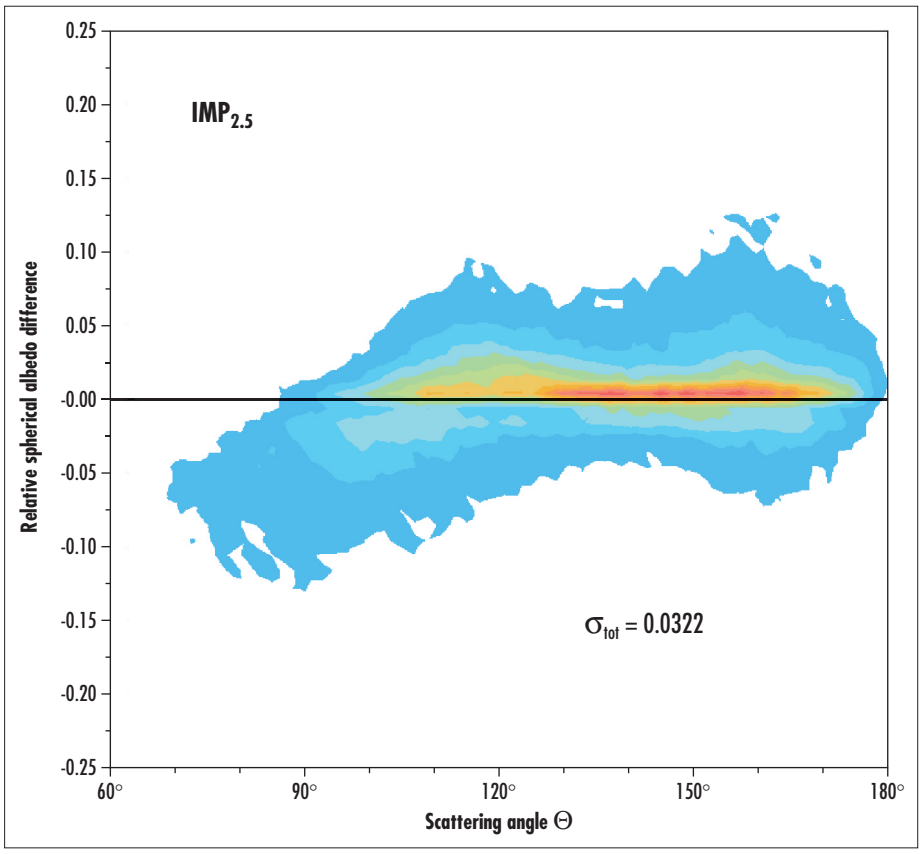

◀ **Figure 2**

Relative spherical albedo difference for cirrus clouds. Polazired radiances are measured with POLDER and model calculations are performed for a cloud consisting of rough hexagons with an aspect ratio of 2.5. [from Knap *et al.*, 2003].

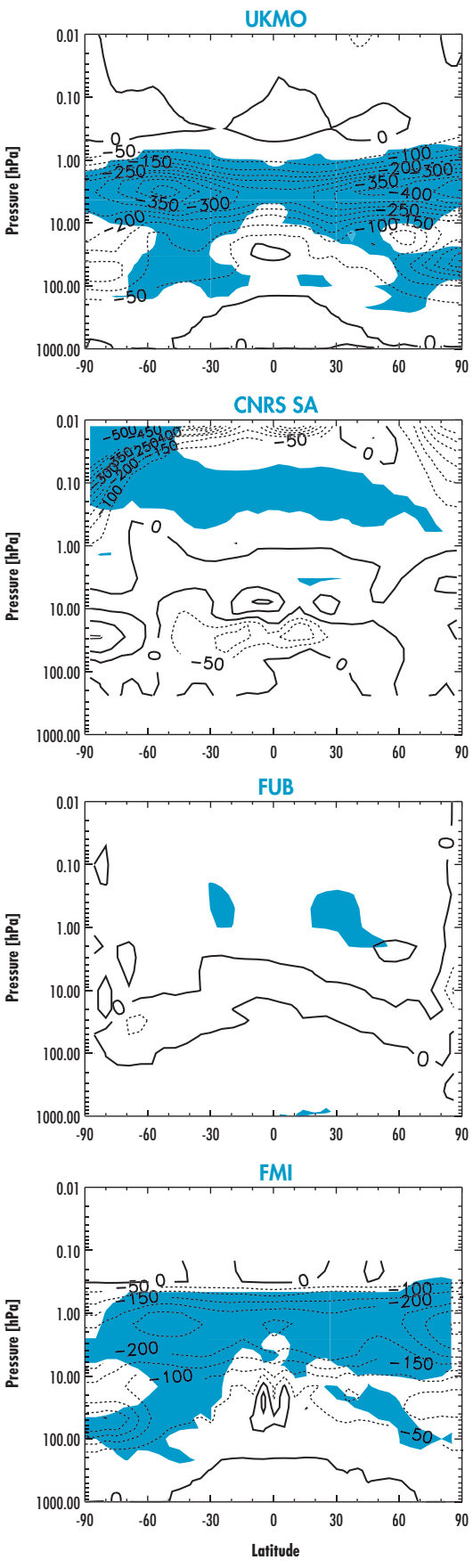

Figure 4. Annual mean ozone trend for 1980 to 1999 in ppbv/decade simulated by the different models of EuroSPICE. The contour interval is 50 ppbv/decade; regions where the trend is significantly different from zero are shaded for the 95 % (light blue) and 99 % (dark blue) confidence levels.

although the trends at high latitudes are substantial, the large interannual variability increases the uncertainty in the trends. Further analysis of the results indicates that the cloud trend is small. Hence, the cloud-corrected UV levels are dominated by ozone amounts, albeit with the cloud variation increasing the variability and uncertainty in the computed UV trends.

3. Future trends

(a) Temperature

The future temperature trends calculated by the models of EuroSPICE are shown in **Figure 7** (p. VI). Comparisons are shown with the UR control run (solid black line with 95% confidence intervals), which assumes constant ozone and projected increases in the concentrations of the WMGHGs. The UR results indicated by the black broken line were calculated using the same underlying climate model but with ozone computed from the first of two runs of the UKMO model. All the UKMO results shown earlier in this article were from Run 2, and they are also shown here for comparison with Run 1.

All the models are generally very close, except for the CNRS SA model which has much higher temperature trends in the lower and middle stratosphere. This model is a mechanistic model with wave amplitudes supplied at the lower boundary, whereas the other models are complete climate models with the same SSTs specified.

(b) Ozone

Figure 8 illustrates the future ozone trends calculated by the models. All the models have a small but statistically significant ozone recovery in at least part of the upper stratosphere, in the region most influenced by halogen chemistry. In the LS, the overall trends are much lower and not statistically significant, suggesting the need for longer integrations before ozone recovery can generally be predicted.

(c) Surface ultraviolet

The small future changes in ozone indicated in Figure 8 and in the total ozone results (not shown) suggest that the future surface UV trends will also be small. This is confirmed in **Figure 9** (p. 19) which shows the predicted UV trends for just one of the EuroSPICE models. While in the SH the decrease in UV is not statistically significant during the spring (not shown), in the northern spring the model predicts a significant decrease of about 10% in high latitude UV.

4. Tropospheric impacts

The impact of the stratosphere on the troposphere is one of the major themes of EuroSPICE, but has not so far received full attention because the model simulations have only recently been completed. All the climate model simulations of EuroSPICE show tropospheric

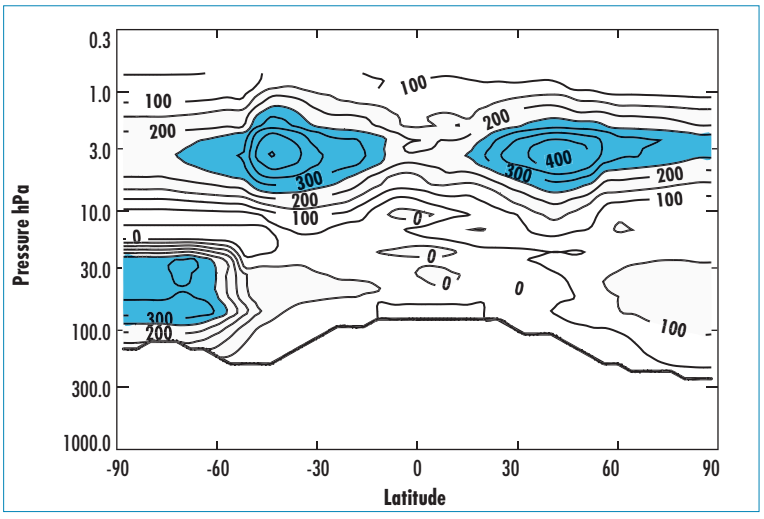

Figure 5. Observed annual average stratospheric ozone trend over the period 1979 to 1997 as a function of latitude and pressure. Data were obtained from Randel and Wu (1999) and the approximate position of the tropopause is indicated by the thick line. Ozone decreases exceeding 250 ppbv per decade are indicated by the shading.

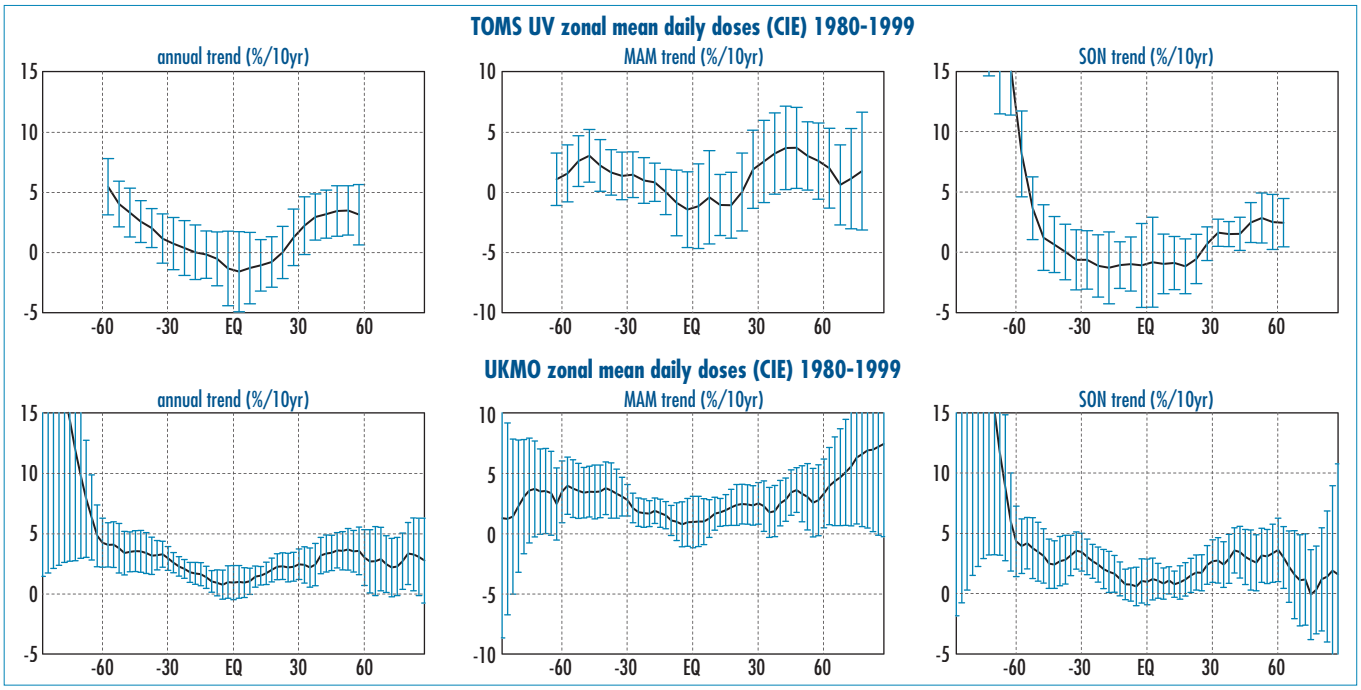

Figure 6. Zonal mean UV trends (% per decade) for TOMS data (top panels) and UKMO model data (bottom panels) during different seasons (annual, March to May, and Sept. to Nov.). The error bars represent the 95 % confidence range computed using the Student t-test.

warming due to increases in the GHGs concentrations. The uncertainty in the trend, though, arises from the large inter-annual variability in the troposphere, so that it is difficult to detect a difference in this trend despite a range of stratospheric changes. Other factors which have been examined are cloud cover, precipitation amounts and storm track numbers or intensities with a similarly null result. **Figure 10** shows the trend in the tropopause pressure over the full 40 years of a control run with the UM. Most latitudes show a statistically significant decrease in tropopause pressure and in mid-latitude the trend is about –1 hPa/decade, similar to that observed (e.g. Santer *et al.*, 2003). However, so far no significant differences have been detected, suggesting that stratospheric ozone trends have not contributed significantly to tropopause height changes.

5. Conclusion

With just a few more months to run, EuroSPICE is nearing its completion. The main highlights so far have been a thorough analysis of temperature data and the completion of simulations with a range of 3-D models from mechanistic to fully coupled chemistry-climate models. Comparisons with observations of ozone and surface UV have also underpinned the project.

Most models captured the broad characteristics of the observed stratospheric temperature trends due to CO_2 increase. Differences existed particularly where models were unable to simulate past ozone trends. Those model trends which agreed with observed ozone trends also generally agreed with past UV trends. For the first time, cloud-corrected UV was computed from the climate model simulations. It emerged, however, that cloud trends were very small and did not affect overall UV trends.

Future simulations indicated only a small recovery in

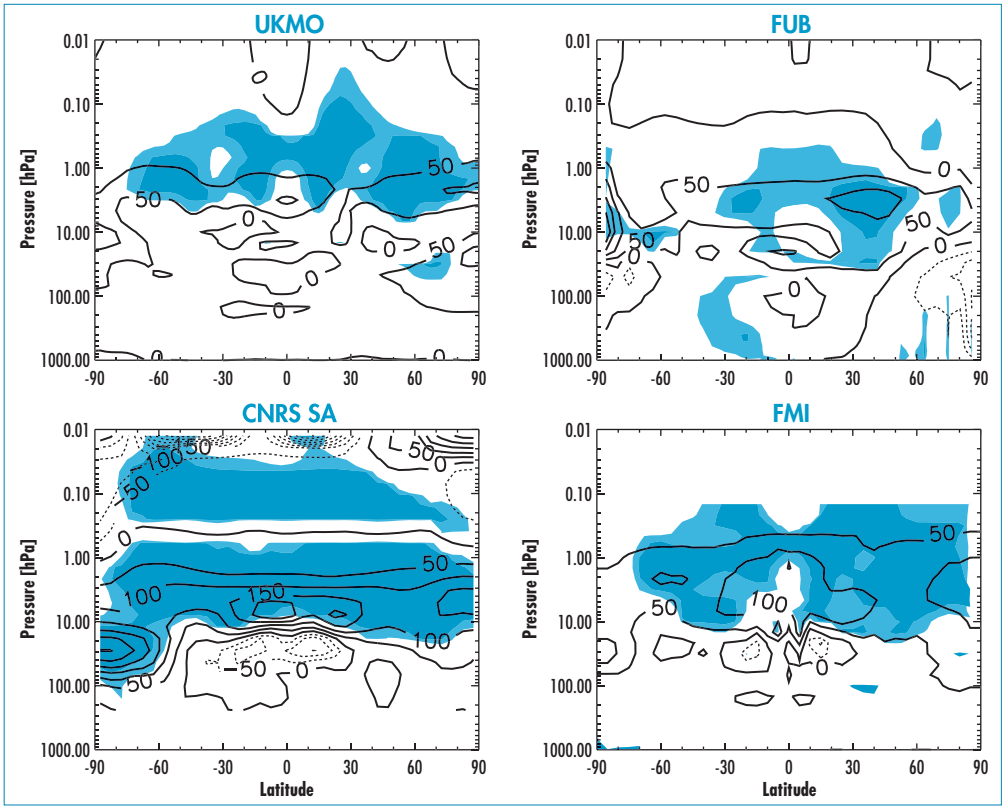

Figure 8. Annually averaged future ozone trends (ppbv/decade) simulated by the models as a function of latitude and pressure. Shading denote the regions where the trend is significantly different from zero at the 95 % (light blue) and 99 % confidence levels (dark blue).

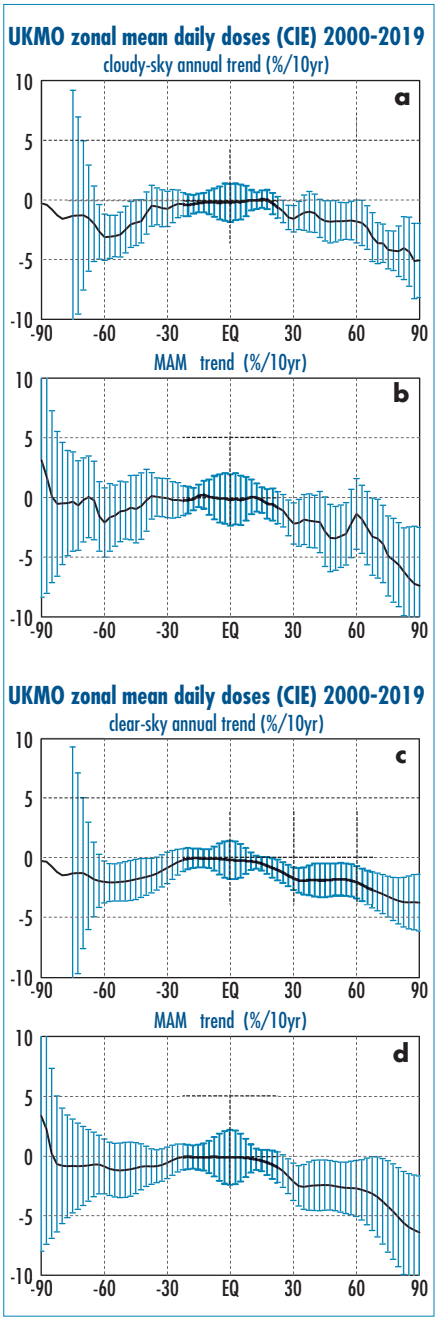

Figure 9. Zonal mean UV trends (% per decade) for UKMO cloudy sky data (a, b) and clear sky data (c, d) for the annual average and the March-May season. The error bars represent the 95 % confidence range computed using the Student t-test.

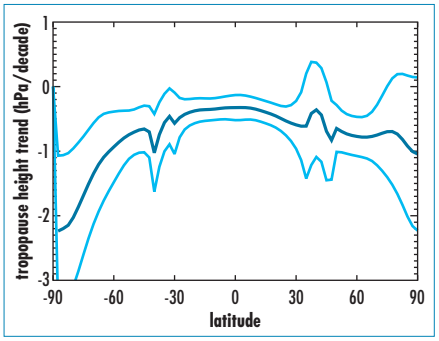

Figure 10. Trend in annual mean, zonal mean tropopause pressure in the 1980-2019 control run. The central line shows the trend with 95% confidence intervals delimited to either side.

stratospheric ozone by 2020 and, hence, only a slight decrease in future surface UV on this timeframe. Nonetheless, for those models which reproduced the past trends, the future temperature trends were also reduced, particularly in the upper stratosphere, indicating the importance of ozone trends on the temperature.

Although some tropospheric impacts have been investigated, the diagnostics examined so far have not revealed a significant impact of stratospheric change on the troposphere. This may have been related to the model set up, in which SSTs and the concentrations of the WMGHGs were specified. One of the ways that stratosphere-troposphere interaction might be important is through changes in the Brewer-Dobson circulation [e.g. Butchart and Scaife, 2001]. This could have the effect of changing the concentrations of the halogens and the WMGHGs in the atmosphere with consequences for the climate model radiative heating rates.

In the future, further analysis of the model results will take place, to investigate some of the remaining details. There would also likely be opportunities, under European Framework 6, for further model comparisons to take place with the results already obtained. Simulations are also becoming available from countries outside Europe, as illustrated in WMO (2003, Chapter 3) and Austin *et al.* (2003), which point to a need for broader international collaboration in chemistry-climate coupling. This process is indeed well under way, with for example the workshop on `Process-orientated validation of coupled chemistry-climate models' to be held in Garmisch-Partenkirchen in November 2003.

References

Austin, J. *et al.,* Uncertainties and assessments of chemistry-climate models of the stratosphere, *Atmos. Chem. Phys.,* **3,** 1-27, 2003.

Butchart, N., and Scaife, A.A., Removal of chlorofluorocarbons by increased mass exchange between the stratosphere and troposphere in a changing climate, *Nature,* **410,** 799-802, 2001.

Hauchecorne, A. *et al.,* Climatology and trends of the mid- atmospheric temperature (33-87 km) as seen by Rayleigh lidar over the south of France, *J. Geophys. Res.,* **96,** 15297-15309, 1991.

IPCC, Intergovernmental Panel on Climate Change, Climate change: the supplementary report to the IPCC scientific assessment, ed. J.T. Houghton, B.A. Callander, and S.K. Varney, Cambridge University Press, Cambridge, UK, 1992.

Langematz, U., An estimate of the impact of observed ozone losses on stratospheric temperatures, *Geophys. Res. Lett.,* **27,** 2077-2080, 2000.

Randel, W.J. and Wu, F., A stratospheric ozone data set for global modeling studies. *Geophys. Res. Lett., 26,* 3089-3092, 1999.

Santer, B.D. *et al.,* Behaviour of tropopause height and atmospheric temperature in models, reanalyses and observations. Part I: decadal changes, *J. Geophys. Res., In press,* 2003.

Shine, K.P. *et al.,* A comparison of model-predicted trends in stratospheric temperatures, *Q. J. R. Meteorol. Soc.,* **129,** 1565-1588, 2003.

WMO, Scientific Assessment of Ozone depletion: 1998, WMO Gobal Ozone Research and Monitoring Project, Report No. 44, Geneva, Switzerland, 1999.

WMO, Scientific Assessment of Ozone depletion: 2002, WMO Gobal Ozone Research and Monitoring Project, Report No. 47, Geneva, Switzerland, 2003.

Announcement

We announce the departure of **Yuri Koshelkov** from the position of project scientist at the SPARC office. We all express our gratitude to Yuri for his hard work, creative contribution and devotion to the SPARC activities and the editing of the SPARC Newsletter during the last ten years. Yuri will be greatly missed by all of us but he will keep in touch from Russia

We would also like to welcome **Emmanouil K. Oikonomou** who has recently joined the SPARC Office replacing Yuri. Emmanouil has a PhD in Oceanography from Southampton University, UK and he has been involved in several European research projects. He has previously worked as a lecturer with UK Open University in Atmospheric and Computational Fluid Dynamics, followed by a 2-year PostDoc at Reading University UK working on Water Vapour and Ozone from ERA-40 and MOZAIC aircraft data. Emmanouil's position is supported by an ESA Post-Doctoral Fellowship.

UV Index Forecasting Practices around the World

Craig S. Long, NOAA/NCEP, Camp Springs (MD), USA (Craig.Long@noaa.gov)

Introduction

The forecasting of ultraviolet (UV) radiation at the surface is really the result of separate forecasts of stratospheric ozone, clouds, and eventually aerosols. It was in 1992 when Canada began issuing the first forecasts of UV radiation and actually created the term "UV Index". Shortly thereafter, many more countries began to issue next day forecasts using simple forecasting techniques. Over the years as the radiative transfer models have become more accurate and the understanding of how other physical conditions like clouds, aerosols, surface albedo and elevation affect UV radiation, the forecast errors of the UV Index have diminished. This article will discuss the latest methods meteorological services are using to forecast the UV Index.

Background

In the summer of 1994 a new international atmospheric parameter was created: the Ultraviolet Index. Until then there were almost as many variations of the UV Index as there were countries giving out this information. The WMO "Meeting of Experts" [WMO, 1994, and WMO, 1997] not only defined what the UV Index was, but also created standards for its forecasting. In 2001 the World Health Organization (WHO) hosted a meeting to further standardize the health messages, exposure categories, and presentation issues dealing with the UV Index [WHO, 2001]. Currently, a few countries have adopted these new standards. Several more are making plans to switch over to these new standards in 2004.

UV Index was defined to be the scaled integral of spectral irradiances between 290 and 400 nm weighted by the CIE erythemal action spectrum [McKinlay and Diffey, 1987]. **Figure 1** shows a typical spectrum of irradiances in the 290 to 400 nm range along with the CIE weighting function. Note that the variability of the irradiances is fairly small in the UV-A (320-400 nm) part of the spectrum, whereas in the UV-B (280-320 nm) part there are several orders of magnitude changes in the irradiances. Ozone in the stratosphere absorbs all of the incoming UV-C (λ<280 nm), some of the shorter UV-B wavelengths, and virtually none of the UV-A wavelengths. As ozone amounts increase (decrease), less (more) UV-B radiation penetrates the ozone layer and reaches the surface.

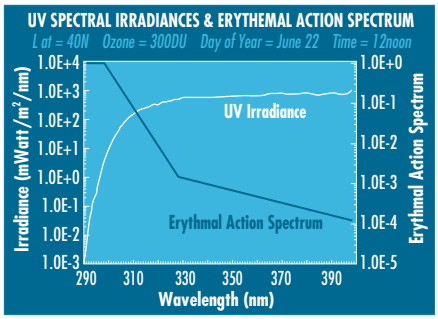

Figure 1. Spectral irradiances (white line) derived from an RTM in the UV-B and UV-A wavelengths for clear sky conditions at 40°N, 300 DU of total ozone, on June 22 at solar noon, at sea level with albedo of 5 %. The CIE (erythemal) action spectrum (blue line) has greatest weight at the shortest wavelengths.

The CIE action spectrum seeks to replicate the average human skin response to UV irradiances. The human skin has evolved to be most sensitive to that part of the UV spectrum, which has the greatest variability due to ozone changes and lesser sensitivity to the part of the UV spectrum that varies the least with ozone changes. The weighted irradiances are shown in **Figure 2**. Note that the greatest contribution occurs near 310 nm for the described conditions. The peak will vary between a range of

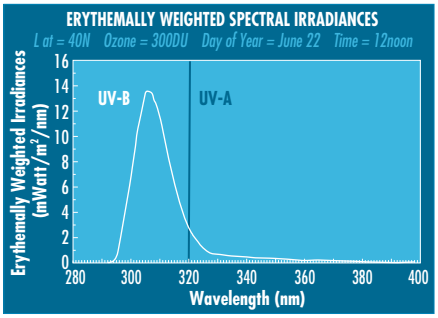

Figure 2. Spectral irradiances from Figure 1 weighted by the CIE action spectrum. Integrating these weighted irradiances provides an erythemal dose rate (W/m²). The UV Index is determined by scaling the dose rate by 40.

305 and 310 nm for different ozone and solar zenith angle (SZA) conditions. As total ozone decreases (increases) and the SZA decreases (increases), the peak will move to shorter (longer) wavelengths.

Integrating these weighted irradiances results in an erythemal dose rate given in units of Watts/m^2. The UV Index is then determined by scaling the erythemal dose rate expressed in W/m^2 by 40 W/m^2 resulting in a unitless value that can range from zero at nighttime or in polar night to greater than 15 on top of high mountains in the tropics at solar noon. The greater (lesser) the UV Index, the shorter (longer) the period of time before skin damage will occur. Just how long the time of exposure can be depends upon how much melanin is in your skin and other genetic factors.

Physical Factors affecting UV Radiation Forecasting

Radiative Transfer Models determine the Clear-Sky UV radiation

Several physical factors determine how much UV radiation passes through the atmosphere and reaches the surface. These include extraterrestrial solar radiation, total ozone amount, clouds, aerosols, surface elevation and albedo. Most countries use a radiative transfer model (RTM) to determine the clear-sky UV Index inputting some or all of the above parameters (except clouds). Koepke *et al.* (1998) discuss most of the RTMs used today as part of the European COoperation in the field of Scientific and Technical research (COST-713) action on "UV-B forecasting" (**http://www.lamma. rete. toscana.it/ uvweb/index.html**). In this paper three groups of models are identified: multiple scattering spectral models, fast spectral models and empirical models. In lieu of utilizing the spectral models, empirical relationships can be determined from observed ozone and observed surface UV radiation. For example, Canada utilizes its network of Brewer spectral radiometers to measure the total ozone and UV radiation. Then, by using forecast fields from their numerical weather prediction (NWP) model, the next day's ozone and surface UV amounts are empirically derived. Some countries that have one or multiple Brewers have chosen this way of performing their UV forecasting. The limiting factor with this technique is that the empirical relations have to be tuned to the Brewers used.

Total Ozone Source and Forecasting Techniques

Instead of using ground-based measurements of total ozone, satellite-derived total ozone amounts can be used with the RTMs to determine the UV radiation at the surface. There are four instrument sources of total ozone currently used by the different meteorological services. These are the NASA/Total Ozone Mapping Spectrometer (TOMS), NOAA/Solar Backscatter UltraViolet Instrument (SBUV/2), the ESA/Global Ozone Measurement Experiment (GOME), and the NOAA/TIROS Operational Vertical Sounder (TOVS). The choice of the instrument used will affect the surface UV results by about 5 %. The first three are UV backscattering instruments. The TOVS algorithm uses the 9.7 µm ozone window in the infrared. Comparisons of the TOMS and GOME with surface observations from the Dobson network have shown that the TOMS data are consistently positively biased by about 2 %, whereas the GOME data are negatively biased by about 2 %. The GOME data also show a seasonal variation of this bias. The SBUV/2 has been shown to be positively biased against Dobson observations by 2 %. Comparisons of TOVS and SBUV/2 have consistently shown the TOVS to have a low bias of 2 to 3 % in the tropics and a large positive bias of 3 to 6 % in the winter hemisphere middle latitudes.

There are three techniques for making a forecast of total ozone: persistence of the present ozone amounts, utilizing regression statistics between ozone and other meteorological parameters, such as geopotential height, temperature, and/or potential vorticity, and lastly assimilation of the ozone data into a NWP model. **Figures 3a, 3b,** and **3c** (p. VI, VII) show the RMS error for over a year's worth of data utilizing the above three methods. All forecasts are validated against their own "truth". The figures show that the persistence has the greatest RMS errors. The regression method shows reduced RMS errors, and the assimilated ozone shows the smallest RMS errors.

Aerosols

The other inputs into the RTM to determine the clear-sky UV Index are determined for the geographic location and day of the year. Next to ozone the most variable parameter influencing the clear-sky UV Index is aerosol content. Aerosols either scatter or absorb UV radiation. The aerosols in the troposphere can be characterized by their optical depth (AOD) and their Single Scattering Albedo (SSA), which is the ratio of the scattered to the total extinction (total extinction = scattered + absorbed). AOD can vary from 0.1 in very clear air to 1.5 in very turbid air. SSA can range from 0.7 to 1.0. As the AOD increases, more UV radiation is scattered and the smaller the SSA becomes, the more UV radiation is absorbed. The AOD and SSA do vary with wavelength. Medium to large AOD can be detected by satellite over the ocean, but is difficult over land due to the variable emissivities of different ground cover and geographic features. Standard AOD, SSA, and aerosol profiles have been developed for different times of the year and source regions (continental, desert, maritime). These standard aerosol parameters are the best that can be done currently until AOD and aerosol profile information can be determined over land by satellite. Then just like ozone it can be assimilated in a NWP scheme to provide forecasts.

Elevation

The elevation (or the pressure) of the surface dictates through how much of the atmosphere the direct beam is scattered. The greater the depth of the atmosphere the UV radiation has to be scattered, the lesser the amount reaches the surface. Given the surface elevation, the RTM will determine how much more radiation reaches the surface. Generally, UV radiation will increase by about 8 % per kilometre. The RTMs do indicate that the rate per kilometre decreases over the second and third kilometre of elevation gain. Some studies have shown much larger rates of up to 18 % between valley and peak observations. These results did not account for the change in aerosol loading in the atmosphere, which significantly contributes to decreased amounts of UV radiation especially in mountain valleys.

Surface Albedo

The albedo of the earth's surface is nearly black in the UV-B part of the spectrum with values typically between 3 and 5 %. Thus, a very small component of the UV radiation is reflected upwards. Even water has a relatively low albedo of 10 %. Sand is brighter at 30 %. But snow is the most reflective surface. A pure fresh snow surface uninterrupted for several miles can have an albedo of 80 %. However, such situations are rare in the mid-latitudes. More frequently, the surface is not flat and has vegetation that extends upward beyond the snow surface. These all reduce the albedo to more like 50 % for fresh snow. As snow ages or melts its reflective qualities decrease to a value more like 30 %. Due to snow's higher albedo, UV conditions on the ski slopes can approach summer conditions.

Extraterrestrial Radiation

The RTMs use the irradiances at the top of the atmosphere as detected by the Atlas 3 or the SUSIM instruments. Both are within good agreement of each other. The RTMs will also determine from the day of year what the earth - sun distance ratio is, so that the extraterrestrial solar radiation is adjusted to be greater in January than in July. Along with the day of year, the time of day, the latitude and the longitude the RTM can determine the SZA. The greater the SZA, the greater the path length through the atmosphere, and the greater the amount of absorption by ozone and scattering by aerosol.

RTMs can be computationally expensive if need to run for more than just a few locations. In practice, the meteorological services that make forecasts on grids develop Look Up Tables (LUT) based upon different scenarios of ozone amounts, aerosol content, SZA, and snow/no snow albedos. These LUTs are computationally much faster than running the RTM for each grid point. The errors associated with LUTs tend to be smaller than 5 %.

Cloud Effects

The UV Index value that the RTM or empirical method determines is the maximum amount of UV radiation to be expected under "clear sky" conditions. Since the earth is covered 50-60% of the time with clouds, appropriate cloud modification factors (CMF) have been developed by several campaigns noting the attenuation of observed UV radiation in the presence of clouds and using a RTM to determine what the clear sky condition would have been. One of the recommendations coming from the COST-713 action are the CMFs to be used based upon the cloud fraction and the level (low, mid or high) of the clouds. **Table 1** shows these recommendations. The table gives mean conditions for

Table 1. COST-713 suggested cloud modification factors for various cloud amounts and cloud levels.

CMF Suggested Based upon Cloud Level and Cloud Amount					
Cloud Level	Cloud Amount	0 - 2 Octas	3 - 4 Octas	5 - 6 Octas	7 - 8 Octas
	Low (<3 km)	1.0	0.8	0.5	0.2
	Middle (3-7 km)	1.0	1.0	0.8	0.5
	High (>7 km)	1.0	1.0	1.0	0.9

cloud level and amount. As cloud amount increases, the optical qualities of the clouds can vary dramatically, thus making the RMS error of these recommendations increase.

Cloud parameters coming out of a NWP model usually give the low, mid and high cloud fractions. Information about their optical depths is rarely output. But within the NWP model the shortwave radiation code takes into account the optical properties of clouds as they are parameterized within the model. The Global Forecasting System at NCEP determines the surface flux in discrete bands within the UV-B part of the spectrum with and without the clouds determined by the model. The ratio of the two provides the attenuation in the UV-B wavelengths due to clouds. **Figure 4** (p. VIII) shows the scatter plot of cloud fraction versus attenuation for one day's set of NWP model grid points. The mean value is very similar to that suggested by COST-713 and that observed by other campaigns. The more outstanding feature is the large range of values at higher cloud fractions. Validation of these attenuation values needs to be performed. The timing of the clouds is equally important as the amount of attenuation. With model forecasts being output at a low frequency of every 6 or 3 hours, mean conditions are usually assumed over that period of time. A better cloud output frequency would be every 1 hour. Higher frequencies are limited by the frequency of the radiation package being called within the NWP model and the storage available for the greater amounts of output.

Many countries do not have the budget or computer facilities to determine a UV Index forecast. For Europe's benefit, another action coming out of the COST-713 was that the Deutscher Wetterdienst (DWD) would produce gridded ozone forecasts and UV Index values primarily over Europe. The DWD also produces global gridded fields as well.

The University of Vienna produces a global clear sky UV Index forecast. These maps are posted on their web page. The U.S. National Weather Service NCEP and Australian Bureau of Meteorology (BOM) also generate global forecast grids of ozone and clear sky UV Index values. **Figures 5** (p. VIII, IX) shows the NCEP/GFS ozone forecast field valid for March 21, 2003 and the resulting clear sky UVI forecast. The NCEP ozone forecast grids are available via anonymous ftp at **ftpprd.ncep.noaa.gov/pub/cpc/ long/avn_ozone.**

Inquiry results

Table 2 lists the current thirty countries whose weather service or other agency provides some form of a UV Index forecast. These include almost all the countries of Europe, the U.S., Canada, Taiwan and Israel in the NH. Australia, New Zealand, Brazil, Argentina, Chile and South Africa are the only countries from the SH to produce UV Index forecasts. Notable exceptions are mainland China, India, and Russia. There are also several other cities or countries that report observed UV Index values. All weather services follow the WMO standard of producing a 1-day forecast for solar noon either for the entire country or for selected cities. A few weather services provide multi-day forecasts. About half of the weather services provide just a clear sky forecast while the rest do incorporate cloud conditions into their forecasts. Some weather services also provide the expected UV Indices at other hours of the day. All but the three that use empirical relationships use a RTM actively or LUT based upon RTM results. As expected, weather services of countries where snow would be a factor incorporate it into their forecasts. Only one weather service (South Africa) uses persisting ozone amounts due to its tropical location. All the other weather services use ozone forecasts from model assimilations or statistical regressions. Those making statistical regressions most commonly use TOMS, a few use GOME, and one uses TOVS ozone data. Those using the ozone forecasts from NCEP will be using the assimilated SBUV/2 data. The BOM assimilates TOVS ozone data, the KNMI assimilates GOME ozone data, and the DWD assimilates both GOME and SBUV/2 ozone data. At least three European weather services make use of

Table 2. Current UV Index web pages.

Country - Region	UV Index Forecast Web Page	Comment
Argentina	http://www.conae.gov.ar/iuv/iuv.html	Spanish
	http://www.meteofa.mil.ar/http://www.meteofa.mil.ar/	Spanish
Australia	http://www.bom.gov.au/weather/national/charts/UV.shtml	
Austria	http://i115srv.vu-wien.ac.at/uv/uv_online.htm	
Belgium	http://www.meteo.be/ozon/uv/uv-index.php	
Brazil	http://www.master.iag.usp.br/ind.php?inic=00&prod=indiceuv	Portuguese
Canada	http://www.msc-smc.ec.gc.ca/education/uvindex/index_e.html	
Catalonia	http://www.meteocat.com/marcs/marcos_previsio/marcs_uvi.ht	Spanish
Chile	http://www.meteochile.cl/	Spanish
Czech Republic	http://www.chmi.cz/meteo/ozon/o3uvb-e.html	
Denmark	http://www.dmi.dk/vejr/index_sol.html	Danish
Finland	http://www.fmi.fi/research_atmosphere/atmosphere_10.html	
France	http://www.infosoleil.com/previsions.php	French
Germany	http://www.dwd.de/en/wir/Geschaeftsfelder/Medizin/uvi/index.	
Greece	http://lap.physics.auth.gr/uvindex/	Greek
Israel	http://www.ims.gov.il/en2.htm#1	
Italy	http://www.lamma.rete.toscana.it/previ/eng/ruva.html	
New Zealand	http://www.niwa.cri.nz/services/uvozone/	
Netherlands	http://www.temis.nl/uvradiation/index.html	
Norway	http://www.luftkvalitet.info/index.cfm?fa=uv.main	Norwegian
Poland	http://www.imgw.pl/wl/internet/uv/uv.html	Polish
Portugal	http://www.meteo.pt/uv/uvindex.htm	
Slovakia	http://www.shmu.sk/ozon/ozon.cgi?predpoved	Slovak
Slovenia	http://www.rzs-hm.si/zanimivosti/UV.html	Slovenian
South Africa	http://www.weathersa.co.za/uv/Hourlyuvbmain.html	
Spain	http://infomet.am.ub.es/uv_i_ozo/	Spanish
Sweden	http://www.smhi.se/en/index.htm	
Switzerland	http://www.uv-index.ch/de/home.php	German/ French
Taiwan	http://www.epa.gov.tw/monitoring/1-1/uv.htm	Chinese
United Kingdom	http://www.metoffice.com/weather/uv/	
United States	http://www.cpc.ncep.noaa.gov/products/stratosphere/uv_index/	
Country - Region	**UV Observations Web Page**	**Comment**
Hong Kong	http://www.hko.gov.hk/wxinfo/uvindex/english/euvtoday.htm	
Luxemburg	http://meteo.lcd.lu/	
Macau	http://www.smg.gov.mo/te_newuvidx.php	
Mexico City	http://sima.com.mx/t1msn_valle_de_mexico/uv-index.asp	

the DWD ozone and UV Index forecast fields. Four weather services use NCEP ozone forecast fields.

The Future of UV Index Forecasts

As stated in the beginning of this article, UV forecasting is the combination of ozone, cloud and aerosol forecasting. Improvements in these three fields will improve tomorrow's UV forecast, as well as extend the range of reliable forecasts out to several days. Reliable ozone forecasts can be received right now from a number of the world's leading forecast centres. Clouds affect other products besides the UV Index, so weather services that run NWP models will constantly be trying to improve their cloud schemes. The future of aerosol forecasts is dependent upon the ability to detect aerosols over land via satellite and determine its vertical distribution. Once available, aerosol parameters can be assimilated into NWP models and forecasted.

Changes will be forthcoming in the health aspects of the UV Index. A fact sheet [WHO, 2002] about these new standards is now available on-line. It is the WHO's wish that all countries which issue a UV Index forecast adopt these new health related standards.

Conclusions

To date approximately 30 countries are producing UV Index forecasts. There are notable exceptions making up a substantial fraction of the world's population. The models and needed information for making more accurate UV Index forecast have dramatically improved over the past ten years. Ozone forecasting techniques have improved greatly with the assimilation of ozone into NWP models. Cloud forecasting is more difficult as NWP models must forecast the levels, amounts and timing of the clouds. A better product may be for the model to output the total cloud attenuation in the UV part of the shortwave radiation. Aerosols are still parameterized from surface observations and climatologies, as satellite aerosol observations over land are still sometime away. Albedo and elevation effects have been studied sufficiently to provide good parameterizations in RTMs. Alternatively, empirical relationships based upon surface observations of ozone and UV amounts provide good results for specific geographical domains.

Validation of the UV Index forecasts was not discussed in this article. It is a vital subject that provides direct feedback to all the components of UV forecasting. To do the subject justice would require another complete article.

References

Koepke, P., and 23 co-authors, 1998, Comparison of models used for UV Index calculations, Photchem. *Photobio.,* **67,** pp 657-662.

McKinley, A.F. and B.L. Diffey, 1987, A reference action spectrum for ultraviolet induced erythema in human skin, *CIE Journal,* pp 17-22,.

WHO, 2002, Global Solar UV Index, A practical guide. Fact Sheet 271, http://www.who.int/mediacentre/factsheet/who271/en/index.html

WMO, 1997, Report on the WMO-WHO meeting of experts on standardization of UV Indices and their dissemination to the public, WMO GAW No 127.

WMO, 1994, Report on the WMO meeting of experts on UV-B measurements, data quality and standardization of UV Indices, WMO GAW No 95.

The SAGE III/Meteor Mission – One Year in Operation

Patrick McCormick, (PAT.MCCORMICK@hamptonu.edu) and **J. Anderson,** Hampton University, Hampton (VA), USA

W.P. Chu, C.R. Trepte, L.W. Thomason, J.M. Zawodny , NASA LARC, Hampton (VA), USA

Introduction

The Stratospheric Aerosol and Gas Experiment (SAGE III) instrument is a fourth-generation satellite instrument designed to provide long-term measurements of ozone, aerosol, water vapour, and other gases in the atmosphere. It was launched on-board the Russian spacecraft Meteor-3M from the Russian launch site Baikonur Cosmodrome in Kazakhstan on December 10, 2001. A Ukrainian built Zenit-2 rocket was used to place the spacecraft into a sun-synchronous orbit with an inclination of 99.64°, and an ascending node crossing time of 9 am. and an orbital height of 1018 km. The SAGE III mission is part of NASA EOS program [McCormick, 1991], and is a collaborative mission between NASA and the Russian Aviation and Space Agency (RASA).

The SAGE III science team* was selected in 1990 to aid in all scientific aspects of the mission. It was composed of scientists from different U.S. government agencies (NASA, NOAA, and DOD) and researchers from various US universities (Harvard, Columbia, Georgia Tech, North Carolina State, and Wyoming), and non-U.S. institutions (University of Lille in France, Russian Institute of Atmospheric Physics, and the Russian Central Aerological Observatory). A Solar Occultation Satellite Science Team (SOSST), soon to be announced by NASA, will continue validation and perform studies using the data from SAGE III, as well as other occultation data sets, e.g. SAGE II.

The Meteor-3M satellite

The Meteor-3M is a 3-axis stabilized spacecraft and is an advanced version of the Meteor series designed and built by the Electromechanics Research Institute (NIIEM) located in Istra, Russia. This series of spacecraft has been the main platform for Russian space-flight instruments serving meteorological, environmental and natural resource research purposes. Earlier versions of the Meteor series spacecraft were developed by the All-Union Electromechanics Research Institute (VNIIEM) in Moscow, Russia. Meteors have been in operation for over 20 years and have a well-proven design with a high degree of reliability. The Meteor-3M spacecraft is equipped with advanced components, such as GPS/GLONASS receiver, a refined attitude control system and an L-band transmitter with expected lifetime of over three years.

*The SAGE III Science Team (1990-2002)

M. P. McCormick, C. Brogniez, A.A. Chernikov, W.P. Chu, D.M. Cunnold, J. DeLuisi, P.A. Durkee, N.P. Elansky, B.M. Herman, P.V. Hobbs, G.S. Kent, J. Lenoble, A.J. Miller, V.A. Mohnen, V. Ramaswamy, D.H. Rind, P.B. Russell, V.K. Saxena, E.P. Shettle, L.W. Thomason, C.R. Trepte, G. Vali, S.C. Wofsy, and J.M. Zawodny.

Description of the SAGE III instrument

The SAGE III instrument is designed similar to the SAGE I and SAGE II instruments, with the exception of using an advanced detector package consisting of a two dimensional CCD array detector plus a near-IR photodiode. The new detector design enhances the measurement capability to provide atmospheric spectral coverage from 280 nm to 1040 nm, with a spectral resolution of about 1.2 nm, plus a channel at 1550 nm for separating aerosols and clouds and for measuring larger aerosols.

The SAGE III instrument consists of three subsystems. The first subsystem is the scan head that consists of the scan mirror mounted on an azimuth drive that can rotate over 360°. The scan mirror scans in elevation so that it can point to the Earth's limb when the instrument is in orbit. The second subsystem is the imaging optics consisting of a telescope and azimuth target acquisition detectors. The telescope is an f/4 Dall-Kirkham configuration with a one-half arc minute vertical by five arc-minute horizontal slit in the focal plane that serves as the science aperture and as the entrance slit to the grating spectrometer. The whole telescope assembly including the scan mirror can rotate together in azimuth to eliminate the problem of image rotation during azimuth rotation. The third subsystem of the SAGE III sensor is the spectrometer detector package. The spectrometer consists of a holographic grating in a Rowland configuration operating in both zeroth and first orders. The first order dispersion is imaged on the 800 x 10 element CCD, which is backside thinned to enhance UV response. The zeroth order reflection from the grating is used with a photodiode together with a spectral bandpass filter centered at 1550 nm.

Measurement technique

The SAGE III instrument is designed to perform the well-proven technique of Solar occultation for monitoring the different atmospheric species that scatter and/or exhibit spectral absorption characteristics in the near UV, visible and near IR [Chu and McCormick, 1979; McCormick *et al.,* 1979]. The instrument was also designed and built to perform Lunar occultation measurements. The capability of Lunar measurements arises from the use of the CCD detector, which can provide high sensitivity with variable signal integration time. Since SAGE III is capable of measuring the moon's brightness (about 600,000 times less bright than the sun), it possesses the ability to make measurements of limb scattering on the bright side of each orbit. Limited limb scattering measurements are being made but are being treated as research products since the instrument was not optimized for such measurements.

For Solar occultation measurements, the operation of the SAGE III instrument in orbit is similar to the operation of the previous SAGE instruments. Before a Solar occultation event, the telescope and scan head are first slewed to the azimuth position where the sun will appear. As soon as the sun appears in the instrument's field-of-view, the scan mirror begins to scan in elevation to acquire the Solar image. The 0.5 arc-minute science aperture in the vertical direction provides approximately a one-half kilometer vertical resolution in the atmosphere. Measurements are obtained by repeatedly scanning up and down over the Solar disk at the Earth's limb over a height region from the ground to about 300 km altitude as the sun rises or sets from the satellite perspective. Radiometric data are sampled at a rate of 64 samples per second. Due to the limitation on the data downlink from the spacecraft, the instrument can only sample 85 spectral channels of data from the CCD instead of the total available 800 pixels. These 85 spectral channels are selected to provide optimum information for the retrieval of ozone in the stratosphere, mesosphere and down into the troposphere, plus information on aerosol, NO_2, water vapour, and the oxygen A-band used for the retrieval of temperature and pressure.

Lunar occultation measurements are being performed by the SAGE III instrument when the brightness of the moon is 40 % or greater of a full moon. Lunar measurements are sampled at 10 samples per second due to the needed long integration time for the weaker signal. The spectral coverage for the Lunar measurement can, therefore, be increased to 340 spectral channels over the CCD. The limb scattering measurements are considered to be a research mode for SAGE III and are just now beginning to be conducted. Early limb scattering results are of high quality and showing success, especially for ozone profile measurements.

Retrieval algorithm and data processing

The algorithm used to process the SAGE III measurements is similar to the SAGE II algorithm [Chu, *et al.,* 1989]. A complete description of the SAGE III retrieval algorithm is available in the SAGE III Algorithm Theoretical Base Document: Solar and Lunar Algorithm, which is available from the NASA Earth Observing System Project Science Office Web Site (**http://eospso.gsfc.nasa.gov**).

The algorithm consists of two main modules. The first module performs calibration of the measured radiance over the 280 to 1040, and 1550 nm spectral channels, and converts the measurements into slant-path transmission profiles of the atmosphere. This procedure involves both geometric calibration and radiometric calibration. The geometric calibration is to precisely locate each measured data point through a detailed spacecraft and Solar ephemeris calculation, including atmospheric refraction. The position information consists of slant-path tangent height, the latitude and longitude of the ground location for the tangent point, and the angular position of the viewing direction on the Solar disk. The radiance calibration is done simply by rationing the measurements within the atmosphere to the exoatmospheric Solar limb profiles. The second module performs the retrieval from the transmission data into species profile data. The multi-wavelength slant-path transmission profiles are first separated into transmission profiles for individual species, such as ozone, nitrogen dioxide, water vapour and oxygen across their absorption bands, and aerosol attenuation at select wavelengths. The slant-path transmission profile for aerosol, ozone and nitrogen dioxide is then inverted into vertical concentration profiles using an onion-peeling procedure. For water vapour and oxygen, a non linear least-squares retrieval method is used to retrieve water vapour concentration and temperature profiles.

Data production software for routine processing of the SAGE III measurements has been implemented at the NASA Langley Research Center, SAGE III Science Computing Facility (SCF). Both level 1 and level 2 data from the SAGE III measurements are currently being produced, archived and available from the NASA Atmospheric Sciences Data Center at Langley. The level 1 data products consist of the multi-wavelength atmospheric slant-path transmission data from the Solar occultation measurements. The level 2 data products from the Solar measurements consist of O_3 profiles from cloud-top to 85 km, aerosol extinction profiles at nine wavelengths from cloud-top to about 40 km, pressure and temperature profiles from cloud-top to 85 km, H_2O profiles from cloud-top to 50 km, and NO_2 profiles from 10 to

50 km. For Lunar measurements, the level 2 data products consist of O_3 profiles from 10 km to 50 km, NO_2 profiles from 15 to 45 km, NO_3 profiles from 20 to 55 km, and OClO profiles, under perturbed atmospheric conditions, from 15 to 25 km.

Post launch status and early results

After the launch of SAGE III on December 10, 2001, the instrument was powered up and put on standby for outgassing. Two major spacecraft problems occurred during this period. The primary spacecraft transmitter failed on January 1, 2002. Fortunately, a back-up L-band transmitter worked well when turned-on. The second was the failure of the GPS/GLONASS receiver. Since accurate spacecraft ephemeris data are necessary for the operation of the instrument and processing of the data, another means had to be found to provide the needed ephemeris data. Fortunately, a newly designed retro-reflector built by the Russians for ground-based laser tracking is aboard the spacecraft. The SAGE III team was given permission by RASA to allow the International U.S. Laser Ranging System (ILRS) to track the Meteor-3M spacecraft. With the availability of the laser tracking data, accurate spacecraft ephemeris information is easily being calculated.

With the two major problems solved, and with a sufficient time allowed for outgassing, the instrument was turned on February 27, 2002, and Solar occultation measurements were made. By early March 2002, the SAGE III instrument was acquiring all the available Solar measurements. Similarly, routine Lunar measurements began on March 4, 2002. The first attempt at acquiring limb scattering data with the SAGE III/Meteor instrument was performed on June 30, 2002. Currently, limb scattering measurements have only been taken on an occasional basis and the data are considered to be for research studies only.

The first public release of the SAGE III dataset is available through the website **http://eosweb.larc.nasa.gov/PRODOCS/sage3/table_sage3.html.** The SAGE III aerosol, ozone, and nitrogen dioxide dataset can also be accessed through the SAGE III website at **http://www-sage3.larc.nasa.gov/data/login_form.php.** The second public release of the data should be available in the summer of 2003. **Figures 1-4** (p. IX-X) illustrate the type of data products that are being produced by the SAGE III instrument.

Work is underway to validate the existing products and to refine the algorithms to produce new products. One major emphasis of the SOSST will be to validate the publicly released SAGE III data with comparisons to other instruments and model outputs.

Summary

After some initial problems, SAGE III is working well and producing high quality data. After an initial validation, the O_3, NO_2, and aerosol data are being routinely archived and are publicly available at NASA's Atmospheric Sciences Data Center at the Langley Research Center. The SAGE III Ozone Loss and Validation Experiment (SOLVE-2), sponsored by NASA's Office of Earth Sciences, was held from December 2002 through February 2003, as an intensive field campaign staged out of Kiruna, Sweden. It involved coordinated balloon launches, ground-based measurements and aircraft deployments. It was coordinated with not only SAGE III overflights but with a number of international satellite experiments and thereby provided validation data for ILAS-II on ADEOS-II and SCIAMACHY, GOMOS, and MIPAS on ENVISAT. These data and other validation data will become available over the near future and used to further validate and improve the SAGE III data products. It is expected that the remainder of the SAGE III Solar and all of the Lunar data will become publicly available during the summer of 2003.

References

Chu, W.P. and M.P. McCormick, Inversion of stratospheric aerosol and gaseous constituents from Spacecraft Solar extinction data in the 0.38-1.0 micrometer wavelength region. *Appl. Opt.,* **18,** 1404-1413, 1979.

Chu, W.P., et al., SAGE II inversion algorithm. *J. Geophys. Res.,* **94,** 8339-8351, 1989.

McCormick, M. P., SAGE III capabilities and global change, AIAA-91-0051, 29th Aerospace Sciences Meeting, Jan. 7-10, 1991, Reno, Nevada.

McCormick, M. P., *et al.,* Satellite studies of the stratospheric aerosol. *Bull. Am. Meteorol. Soc.,* **60,** 1038-1046, 1979.

Start of ILAS-II Operation for the Observation of Stratospheric Constituents

Hirokazu Kobayashi, NIES, Ibaraki, Japan (satmng@nies.go.jp)
Takafumi Sugita, NIES, Ibaraki, Japan (tsugita@nies.go.jp)
Yukio Terao, NIES, Ibaraki, Japan (terao.yukio@nies.go.jp)

Introduction

The ILAS-II sensor (Improved Limb Atmospheric Spectrometer- II) aboard the sun synchronous, polar orbiting satellite ADEOS-II (Advanced Earth Observing Satellite-II) launched by the H-IIA rocket system on December 14, 2002 and has started operation. ILAS II is the successor of ILAS (Sasano, SPARC Newsletter, N°10, 1998). Both ILAS and ILAS-II sensors are solar occultation instruments developed by the Ministry for the Environment of Japan (MOE), and designed to observe vertical profiles of various trace gas constituents including ozone (O_3), nitric acid (HNO_3), nitrogen dioxide (NO_2), nitrous oxide (N_2O), methane (CH_4) and water vapour (H_2O), profiles of atmospheric temperature and pressure, as well as profiles of aerosols and polar stratospheric clouds (PSCs) (Hayashida, SPARC Newsletter N°19, 2002). The MOE ozone observational programme is expected to clarify the trends of the ozone layer and other stratospheric properties by obtaining long-term stratospheric ozone data from the ILAS and ILAS-II missions. ILAS-II has similar characteristics and design as the former ILAS sensor but with various advanced features. For example, ILAS had two observational channels (one

infrared and one visible), whereas ILAS-II has four: two of those are the same as in ILAS-I, whereas the two new channels are a mid-infrared channel for obtaining precise information on aerosol/PSC characteristics, and another channel to retrieve the profile of $ClONO_2$, which is regarded as a reservoir of ClO_x. **Table 1** shows the spectral coverage of each channel and its planned observation parameters. In order to improve the tangent height resolution, on the focal plane of the fore telescope ILAS-II has a narrower optical slit corresponding to 1 km vertical IFOV (Instantaneous Field of View) compared to that of ILAS whose slit corresponded to 2 km vertical IFOV.

Due to the orbital parameters of ADEOS-II (now named Midori-II) solar occultation occurs at high-latitudes in both hemispheres, making it possible for ILAS-II to take measurements from 57° to 73°N and from 64° to 90°S and with about 14 observation points in both hemispheres. These parameters are the same as those of ILAS, except that the recurrent period of ILAS-II is 4 days and that of ILAS was 41 days; hence, the longitudinal distance in observation points of ILAS-II between the adjacent nominal orbits is about 240 km at 70° latitude, compared to about 23 km in the case of ILAS. Although ILAS instrument operated only between the beginning of November 1996 till the end of June 1997 when the ADEOS satellite suddenly failed, a large amount of measurements has been acquired that enabled NIES to improve the data retrieval algorithms (currently using version 6.00). We are going to continue the ILAS/ILAS-II data distribution program and also maintain the correlative measurement database (CMDB), which contains and manages ILAS/ILAS-II validation experimental data.

Channel	Wave number range	Target parameters
Ch. 1	850 - 1,610 cm^{-1}	O_3, HNO_3, NO_2, N_2O, CH_4, H_2O, aerosol
Ch. 2	1,754 - 3,333 cm^{-1}	O_3, N_2O, CH_4, H_2O, aerosol, CO_2 (for pressure measurement)
Ch. 3	778 - 782 cm^{-1}	$ClONO_2$
Ch. 4	12,755 - 13,280 cm^{-1}	temperature, pressure, aerosol

Table 1. The spectral coverage and planned observation parameters for each channel of the ILAS-II.

Preliminary operation results

The initial checkout (ICO) exclusively for ILAS-II was implemented over four consecutive days from January 20, 2003. Various satellite functions were running according to schedule, and both the output of the spectrometers and the performance of the solar-tracking sensor were confirmed to be functioning satisfactorily. Some of the data measured by ILAS-II during the ICO were processed and analysed at NIES and vertical profiles of ozone and other atmospheric trace species were retrieved; these results were announced at a press release. However, during ICO and a later checkout on 08/02/2003 it was found that the sun-edge sensor (SES) was not performing as expected. Despite various attempts to adjust the relevant sensor parameters, the normal functions of the SES could not be recovered. Starting on February 12, 2003, the Early Turn-On (ETO) was implemented for a total of four days. Even though ILAS-II had already been confirmed to be fully capable of fulfilling its primary mission to measure the stratospheric chemical species, we still need to investigate the cause of the SES non-conformance after the ICO period. By using an engineering model (EM) it was clarified that the slit of the FOV, which concurrently serves as a mirror to project light onto the SES, was deformed due to heating by solar radiation, thereby causing partial attenuation of the amount of light conveyed to the SES. To counter this problem, it was decided to incorporate into the operational system some other tangent height determination methods that do not use the SES; it was also decided to start analysing ILAS-II data at the System Total 1 on March 19, 2003, at which point the entire satellite was operational, and to end on March 22, 2003; also the System Total 2 was to begin on April 2, 2003, and the routine operations were to begin in due course. Clarification of the SES behaviour and assessment of its impact on the data will be continuously investigated, and recently we found that the partial data from SES can still be useful for defining the tangent heights.

The ILAS-II data validation

The validation conducted by the ILAS-II project consists of the core experiments, as well as cooperative experiments conducted by various scientists group worldwide. The core experiment plan is composed of the Kiruna balloon campaigns, in cooperation with CNES (France) and with the validation principal investigators, and the ozone/aerosol sonde observations program in Antarctica based on the Syowa station. We plan to validate each target parameter of ILAS-II that is defined as a standard product, and to publish papers on the validation analysis. Unfortunately, the Kiruna campaign planned on April 2003 has been postponed; however, we expect the balloon experiments to be carried out during this winter season. The sensor validation is being conducted by using ozone/aerosol sonde and data from other satellite sensors, such as POAM-III, SAGE-III, and sensors aboard Odin and ENVISAT. Preliminary validation for the ozone profiles was performed using the ozone sondes from the Kiruna and Syowa stations in February and March 2003. A 'Lagrangian' trajectory hunting method has been applied that makes matching data pairs by pursuing the air mass in which ILAS-II and/or sonde observations were carried out. **Figure 1** (p. XI) shows an example of these hunted matching data sets, on a potential vorticity map at the 500 K potential temperature surface. For the ILAS-II measurements made between March 19 and 21, 2003, the blue

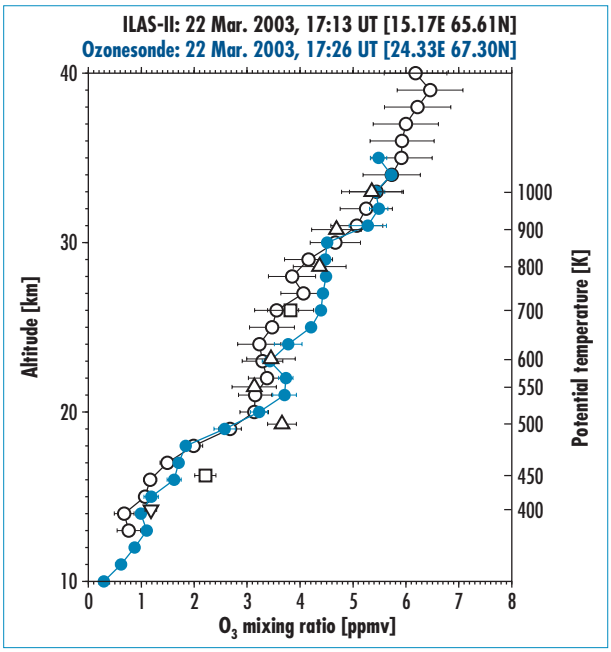

Figure 2. Vertical profiles of ozone mixing ratios measured by ILAS-II (black open circles) and ozonesonde (blue open circles) on 22 March, 2003. The ozonesonde profile was averaged using 1 km altitude grid. Several ozone mixing ratios measured by ILAS-II on 19, 20, or 21 March, which were then hunted by the trajectories shown in Figure 1, are also shown as black open squares, a triangle, and a reverse triangle, respectively.

curves indicate the 5-day isentropic backward trajectories for several theta levels, ending over Kiruna where an ozone sounding was performed at 15 UT on March 22, 2003. **Figure 2** shows vertical profiles of ozone mixing ratios obtained by ILAS-II and the ozonesonde on March 22, 2003. These two measurements coincided closely with respect to both time and location, allowing a 'traditional' approach of validation analysis. The ozone values hunted by the trajectories using the 'Lagrangian' approach are also shown in Figure 2. The co-located ILAS-II ozone profile and the hunted ILAS-II ozone values on several theta levels were also in good agreement with the ozonesonde profile.

For further details, please visit:
http:// www-ilas2.nies.go.jp/en/

Report on the Cirrus Symposium De Bilt, The Netherlands, 2 February, 2003

Organizers: B. Bregman (bregman@knmi.nl) and **P. Stammes** (stammes@knmi.nl)

Ice clouds play an important role in the radiation budget, chemical processing and the ozone budget. They are, however, poorly represented in large-scale Chemistry-Transport Models (CTMs) and Chemistry-Climate Models (CCMs), since the formation and physical properties are not well understood. This caveat formed the reason for the symposium at KNMI, De Bilt, Netherlands, February, 2003.

B. Kärcher outlined a parameterization scheme for homogeneous freezing of ice clouds. In many cases the time scale of depositional growth of nucleated ice crystals is fast compared to that of the freezing event; the number of crystals formed is rather insensitive to details of the freezing aerosol size distribution and number, but increases rapidly with updraft speed and decreases with temperature. Subvisible cirrus clouds (SVCs) preferentially form at low temperatures (<215 K) and small updraft velocities (< few cms^{-1}). A limited number (<0.1 cm^{-3}) of effective heterogeneous Ice Nuclei (IN) can control the formation and properties of SVCs.

The data from the INterhemispheric differences in Cirrus properties from Anthropogenic emissions (INCA) campaign provide compelling evidence for both homogeneous and heterogeneous freezing and for prevalence of mesoscale variability in vertical velocities driven by ubiquitous gravity waves (GW). These findings render the parameterization of cirrus in large-scale models more difficult (**Figure 1** (p. XII)), because global information about small-scale temperature fluctuations in GW and the distribution and properties of IN is not yet available.

Recently the ECWMF and ECHAM model vertical winds were compared to the INCA observations (**Figure 2** (p. XII)). The models significantly underestimate the mean velocities and variability. As a result, the ice cloud number densities were underestimated. In the ECHAM model, the results are improved by superimposing a 'turbulent kinetic energy' (TKE) parameter on the vertical velocities, but still remain unsatisfactory.

P. Siebesma discussed the representation of ice clouds in the ECWMF model. The occurrence frequency of high thin ice clouds was compared with observations from the NOAA satellite [Jakob, 2003]. The comparison reveals an underestimation by the ECMWF model in middle and high latitudes and an overestimation in the ITCZ. The reason is in the relatively crude treatment of microphysical processes of cirrus. In addition, the major source and sink terms for liquid and ice water are an order of magnitude larger than the mean state. One can argue whether process-oriented or statistical approaches should be used in large-scale models.

D. Donovan presented ice particle size retrievals from radar and lidar observations of cirrus at the ARM SGP site. The effective radius depends on the physical shapes of particles. Different shapes were considered and complex polycrystals seemed to give the best agreement [Donovan *et al.,* 2002]. Generally the size distribution was bi-modal, with a peak at around 10 micron and a broad tail with radii of 100-200 microns. The size spectrum strongly depends on both temperature and ice water content (IWC), and the bi-modal distribution appeared at and above IWC of 0.011 g m^{-3}.

W. Knap discussed a comparison between global multi-angle (polarized) radiance measurements made by the POLDER satellite instrument and model calculations of the angular-dependent radiation field over ice clouds [Labonnote *et al.,* 2001; Knap *et al.,* 2003], see Figure 2. For this comparison, model clouds consisting of different ice particles are used: hexagonal crystals with smooth/rough surfaces and with/without air bubble inclusions, and the ISCPP polycrystal. It is found that the POLDER measurements are adequately simulated using smooth hexagons with air bubble inclusions or rough hexagons without inclusions. Slightly less favourable results are obtained for the polycrystal. Clear disagreement between model and measurements is obtained for the pristine hexagon.

In conclusion, cirrus observations show that both homogeneous and heterogeneous freezing are important, a bi-modal size distribution explains the ARM radar/LIDAR observations, and an optical ice crystal model with imperfect or air-bubble hexagons seems to give best agreement with POLDER satellite observations.

Current representation of cirrus and SVCs in assimilation and climate models shows significant discrepancies with observations, due to crude assumptions in the physical formation and loss processes of ice clouds. More work on mesoscale dynamical variability and heterogeneous freezing is required.

Different parameterization approaches may be needed *via* physical process modelling, statistical model PDFs and detailed cloud-resolving models.

References

Donovan, D.P., and A.C.A.P. van Lammeren, First ice cloud effective particle size parameterization based on combined lidar and radar data, *GRL,* **29,** 10.1029/2001GL013731, 2002.

Jakob, C., PhD Thesis, 2003.

Kärcher, B. and Lohmann, U., A parameterization of cirrus cloud formation: Homogeneous freezing including the effects of aerosol size, *J. Geophys. Res.,* **107**, 4698, 2002.

Kärcher, B., and Ström, J., The roles of dynamical variability and aerosols in cirrus cloud formation, *Atmos. Chem. Phys.,* **3,** in press,823-838, 2003.

Knap, W. H., *et al.,* 2003. Modelling light scattering in ice clouds using various ice crystal models: validation with POLDER and ATSR-2 measurements (in preparation).

Labonnote, C. *et al.,* Polarized light scattering by inhomogeneous hexagonal monocrystals. Validation with ADEOS-POLDER measurements, *J. Geophys. Res.,* **106,** 12139-12153, 2001.

Reports on the EGS-AGU-EUG Joint Assembly

Nice, France, 06-11 April 2003

AS1 Session: Open session on the lower, middle, and upper atmosphere

Convener: **M. Juckes** (M.N.Juckes@rl.ac.uk)

The session contained 21 oral and 28 posters presentations.

There were six presentations on GCMs, looking at the effects of ozone trends on climate variability (**C. Cagnazzo**); the response to volcanic forcing (**M. Caian** and **J. Haigh**); the impact of increasing stratospheric water vapour (**I. MacKenzie** and **R. Harwood**); stochastic gravity wave (GW) parameterisation (**C. Piani**); the beneficial impact of including interannual SST variability on the variability in the northern polar stratosphere (**P. Braesicke** and **J. Pyle**); and the increase in frequency of stratospheric warmings in a 4 times CO_2 experiment (**J. Kettleborough**).

There were three presentations on various aspects of stratospheric sudden warmings. **K. Kodera** described the Antarctic warming in September 2002 and the associated tropical response: cooling and reduced ascent in the stratosphere, enhanced ascent and a southwards shift of the Hadley cell in the troposphere; **V. Sivakumar** described Rayleigh lidar observations of the low latitude signal during NH events, and **K. Mimura** analysed dynamical feedback mechanisms.

Six presentations dealt with recent satellite measurements. **W. Chu** *et al.* described the first year of the SAGE III results (**http://www-sage3.larc.nasa.gov/data/**); Comparisons between HALOE temperatures and rocketsonde data showed agreement up to an altitude of 80 km (**F. Schmidlin**), SAGE II and SAGE III agree to within 7 % in the stratosphere (**P. Wang**), whereas SAGE II and GOMOS compare well on ozone and NO_2 (**G. Taha**). SAGE III limb scattering measurements may also provide ozone retrievals later in the year (**D. Rault**). In addition, a wide range of data is available from infrared sounders on EOS Aqua (**J Qin, http://daac.gsfc.nasa.gov/data/dataset/AIRS/**).

Six presentations dealt with advances based on laboratory measurements: a low cost handheld LED instrument measuring column water vapour for use in schools (**S. Limaye**); possible absorption of atomic oxygen and iron by noctilucent clouds (**B. Murray** and **J. Plane**); retrieving aerosol from 1064 nm lidar (**M. Adam**) measurements of peroxy radicals using catalytic amplification (**Z. Fleming**); a ground-based SAGE III calibration instrument (**B. Wenny**); and laser-induced fluorescence for measurement of NO_2 and RO_2s (**J. Matsumoto**).

Twenty-one presentations analysed various processes: trends in the mesospheric temperature and mesopause "length of summer" (**D. Offerman**); a climatology of equatorial waves in the lower stratosphere (**J. Tindall**); Kelvin waves in total ozone (**R. Timmermans**); the forcing of the mesospheric tides by tropospheric solar forcing (mainly), convective heating and planetary waves (**N. Grieger**); the net equatorwards meridional mass flux in the winter, mid-latitude lowermost stratosphere (**M. Juckes**); noctilucent clouds and GW structures (**P. Dalin** *et al.*); spatially coherent modes in the NCEP reanalysis (**P. Ribera**); classification of air masses using total ozone and 450 K isentropic gradients of PV (**M. Andrade**); lightning discharge statistics from New Mexico and from the Iberian Peninsula (**M. Vazquez-Prada**); a clear power law structure in atmospheric dynamical fields analysed with respect to zonal wavenumber (**A. Will**); the use of different forms of potential vorticity to identify the polar vortex (**R. Mueller** and **G. Guenther**); dynamically induced decadal changes in planetary scale total ozone anomalies (**D. Peters**); ionosonde spread-F data (**Daley** and **Wahi**); geomagnetic storms and mesospheric ice particle concentration (**V. Burabash**); and vertical GW momentum flux from CRISTA temperature profiles (**M. Ern**).

Ozonesondes data were the subject of five presentations looking at: the passage of the ITCZ over Paramaribo, Surinam (**J. Fortuin** and **H. Kelder**); the ozone QBO during the SHADOZ experiment (**J. Logan**); ozone lamination, tropopause height, and the passage of the subtropical jet over Ankara (**C. Kahya** and **D. Demirhan**); and long-term ozone changes over Poland (**Z. Litynska**).

There were four talks using simplified or analytic models, showing: substantial long wave momentum fluxes in a highly idealised linear model of GW generated by tropospheric convective events (**J. Holton** and **M. Alexander**); that a minus 3 power law is a consequence of a localised spectral power distribution in the Lagrangian framework (**C. Hines**); that there is a coupled inertial-barotropic instability mode, which may explain the 2-day wave at the summer mesopause (**H. Schroeder** and **G. Schmitz**); and describing analytical solutions for GW in the terrestial and solar atmospheres (**O. Savina**).

Chemical transport models showed that: improved representation of extended UV photolysis affects upper stratospheric and mesospheric ozone (**T. Reddman**); the stratospheric circulation in ERA-15 is more realistic than ERA-40 (**R. Ruhnke**); and CRISTA ozone, nitric acid and CFC-11 agrees well with ROSE model results (**V. Kuell**).

AS8.01 Session: Aerosols and cirrus clouds near the tropopause

Convenors: **B. Kärcher** (bernd.kaercher@dlr.de), **Th. Peter, C. Timmreck**

This session consisted of two sub-sessions focusing on aerosols and cirrus clouds followed by a poster session with more than 25 presentations. Initially, talks were given on a satellite perspective of particles in the UTLS region, including presentations about the physical processes involved in the formation of new aerosol particles and ice crystals, descriptions of *in situ* and lidar observations, and modelling studies. In addition, the cirrus sub-session ended with a talk on current and future *in situ* measurement capabilities.

H. Clark described thin cirrus observations in the TTL made with the CLAES instrument. Cirrus was found to be most prevalent over land and warm oceanic areas, whereas some variability seen in cirrus data was correlated with intraseasonal variations of water vapour. **E. Jensen** gave an overview of physical processes and mechanisms that control the formation and maintenance of thin, laminar cirrus near the tropical tropopause. These clouds can be formed *in situ* by cooling and subsequent freezing of suitable aerosol particles, or they can be residuals from anvils in the outflow of deep convective clouds. Model results stressed the importance of laminar cirrus for dehydration of air entering the stratosphere. **L. Moyer** showed *in situ* water vapour and relative humidity data taken within the TTL during summer in the presence of significant convective activity. Surprisingly, high supersaturations over ice were found

within cloud, thus, raising the question about the mechanism responsible for the maintenance of supersaturation in the presence of cirrus cloud particles in cirrus anvils. These results were contrasted with data taken in clear, unsaturated air. **S. Ismail** showed a collection of thin cirrus and water vapour data taken during the airborne Lidar Atmospheric Sensing Experiment used in conjunction with temperature and moisture data to characterize spatial cloud structure, cloud top height, optical depth, aerosol scattering, extinction-to-backscatter ratio, and relationships between cirrus clouds and water vapour fields. **F. Immler** discussed data taken with the Mobile Aerosol Raman Lidar at midlatitudes and in the tropics during the INCA project. The differences found in depolarization and colour index of midlatitude cirrus suggest differences in microphysical properties of the ice crystals. The fraction of subvisible clouds detected was significantly higher in the tropics. In general, tropical cirrus differed from midlatitude cirrus in terms of horizontal extent and lifetime. **U. Lohmann** reported about first simulations of cirrus clouds with the ECHAM model coupled to a novel freezing parameterization. The potential of volcanic aerosol emissions to alter cirrus occurrence and properties were discussed. Under the working assumption that both background and volcanic aerosol particles freeze homogeneously, no systematic trend was found on cloud microphysical or optical cirrus properties in the case of the Mt. Pinatubo eruption. **S. Dean** highlighted investigations of orographic cirrus in the UKMO Unified Model and compared model output to climatological cloud amounts available from ISCCP. Without special care, the global model lacks cirrus cloud in the lee of orography as seen on the satellite data, in particular at midlatitudes. The importance of including a prognostic ice variable in the model was stressed, and thoughts about a parameterization of orographic cirrus were discussed. **S. Borrmann** reviewed *in situ* measurements of thin and subvisible cirrus clouds. The few existing interstitial aerosol and ice crystal size distributions were discussed along with developments concerning the role of cirrus in heterogeneous chemistry. **A. Heymsfield** investigated the microphysics of a cirrus layer at the tropical tropopause with observations taken during the CRYSTAL-FACE experiment. As convective cells were absent, the cloud likely formed *in situ.* Size distribution measurements revealed the growth of crystals downward from the cloud top to base, whereas saturation over ice decreased from top to base, showing strong supersaturation in the formation zone near saturation conditions lower down. **J. Whiteway** presented results from the EMERALD-2 campaign conducted from Darwin to study cirrus outflow from intense tropical convection. *In situ* and remote sensing data taken from two aircrafts showed variations in the dynamical setting, ice crystal properties, water vapour, and ozone within and around convective outflow.

R. Grainger reported on the status of new retrieval algorithms (PARTS project), which determine aerosol effective radius, surface area, and particle volume from SAGE II spectral measurements, and aerosol optical depth from the ATSR/2 instrument. Initial maps showing the evolution of the aerosol in the UTLS region have also been presented. An aerosol history will be constructed with the help of the new retrievals and additional surface-based and *in situ* measurements. **M. Hermann** reported on aerosol particle measurements taken from commercial aircraft (CARIBIC project). Sulfur was found to be most abundant in northern midlatitude samples, exhibiting a strong latitudinal concentration gradient and a maximum during summer. Deep convection and photochemical activity was responsible for new particle formation in tropical regions. The measurements indicate that the main processes regulating the formation of small aerosol particles must act on spatial scales of ~10 km. **I. Ford** discussed a burst of aerosol particle formation in the upper tropospheric outflow of a huge midlatitude storm cloud observed during the SUCCESS experiment. The outflow regions of mesoscale convective systems were estimated to contribute significantly to the global aerosol budget. The observations are consistent with an analytical model for the nucleation burst, assuming that the particles are formed from binary homogeneous nucleation of sulfuric acid and water vapour. **D. Stevenson** investigated the behaviour of volcanic aerosol particles near the tropopause with the help of a global CCM. The model study focused on the processes following the Laki eruption in 1783/1784, which added 122 Tg of sulfur dioxide just above the tropopause over Iceland. It was concluded from the simulated aerosol production, transport and removal processes associated with this eruption that long-lived aerosol perturbations require sulfur dioxide to be injected to mid-stratospheric levels of 20-25 km altitude and producing new particles there; alternatively, the eruption must continue over an extended time period.

AS8.025 Session: Processes controlling the Chemical Composition of the UTLS.

Conveners: **B. Bregman** (bregman@knmi.nl), **K. Law,** and **H. Rogers.**

The session (30 posters and 16 oral presentations) covered kinetic laboratory work, analysis of air-borne tracer data, and chemical modelling.

N. Butskovskaya investigated the reaction OH + CH_3CHO at 298 K and found the predominant channel: $CH_3CO + H_2O$. **T. Bartels-Rauch** studied the interaction of acetone on ice and found a negligible effect. **L. Koch** showed that the reaction of CH_3S + CO is not important for the formation of OCS. **M. Blitz** reported reduced acetone photolysis rates due to temperature dependent absorption cross sections and lower quantum yields. Chlorine activation on cirrus ice particles was investigated by **M. Fernandez;** they found a significant suppression of the reaction HCl + $ClNO_3$ when the gas phase HNO_3 concentrations are larger than HCl. **D. Johnson** showed that radical propagation from the decomposition of butoxyl radicals decreases with decreasing temperature. **T. Shepherd** presented a model study on the HNO_3 uptake on aerosols and ice particles. **N. Hill** and **A. Horn** investigated interactions of organic species with ice and showed that acetone and methanol together with HNO_3 led to some ice surface modifications. Tropical ozone and NO_2 profiles were studied by **F. Borchi**, who showed that the relative contribution from transport and chemistry significantly depends on altitude. **N. Huret** investigated the influence of proton precipitation as a source for NO_x (=NO+NO_2) in the tropical LS. Space-borne total column and vertical profiles from NO_2 and NO_3 were used by **J. Shillito** to study night-time chemistry. A 3D-CTM was used by **M. Kanakidou** to investigate the importance of convection on oxygenated hydrocarbons in the UT and the impact on the HO_x (=HO_2+OH) budget. **B. Morel** showed the relative importance of large and small-scale planetary waves on meridional mixing at the edge of the tropical stratosphere. **V. Sivakumar** studied the subtropical tropopause structure; J. Baray and **T. Portafaix** focused on the relation between the southern subtropical barrier and ECMWF PV. **M. Sprenger** *et al.* used ECMWF analysis to estimate the global tropopause fold frequencies. Airborne *in situ* CO measurements were used by **P. Hoor** to investigate cross-tropopause transport, whilst **A. Zahn** used the CARIBIC O_3-CO

relationship. **M. Krebsbach** by using the SPURT aircraft data, examined dehydration in the extra-tropical lowermost stratosphere. **S. Assonov** explored isotopic observations of CO_2 during CARIBIC to characterize the lowermost stratosphere. O_3 and N_2O ERS-2 data were used by **B. Legras** and **J. Lefèvre** to study turbulent diffusion at the edge of and within the Arctic polar vortex. **G. Günther** used the CLaMS model and SPURT trace gas data to estimate cross-tropopause fluxes and to characterise the air mass origin in the tropopause region. **D. Brunner** investigated turbulent decay times of tropospheric filaments in the lowermost stratosphere from aircraft data. **M. Hegglin** investigated the impact of convective transport and small-scale turbulence on NO_y by using the SPURT observations.

J. Crowley presented new temperature dependent rates of the reaction of acetaldehyde with OH and its importance for the HO_x budget in the UT. **F. Pope** discussed new formaldehyde photolysis data. **T. Gierczak** presented results from the photolysis and thermal decomposition of pernitric acid, which seemed slower than the latest recommendations; FIR photolysis study is ongoing. Smaller quantum yields than previously measured were found by **D. Heard** for the photolysis of acetone (> 310 nm and low temperatures), resulting in a 2 times longer chemical lifetime and a factor of two less HO_x production in the upper troposphere. **E. Meijer** presented results from the 3D-CTM TM3 of the HO_x production by NMHC in the UT. **H. Fischer** gave a report on the SPURT campaigns, and addressed the depth and the seasonal cycle of the midlatitude tropopause mixing layer; there was evidence that the mixing layer follows the local tropopause. MOZAIC observations were presented by **J.-P. Cammas**, focusing on the CO – O_3 relation in the UTLS. **G. Vaughan** discussed dynamical mechanisms responsible for transport and mixing of air masses between troposphere and stratosphere. Breaking Rossby waves can generate inertia gravity waves, which then lead to layering and mixing of air masses. Other mechanisms were shear-induced turbulence and convection in post-cold frontal air masses. **J. Whiteway** showed very high-resolution turbulence measurements from the Egrett aircraft on flights over the Welsh mountains. **L. Pan** discussed a method for characterizing the extra-tropical tropopause using the thermal definition in order to look for thermal breaks in the tropopause, using aircraft data from SONEX, STRAT and POLARIS. **H. Scheeren** studied acetone and VOC data from STREAM campaigns; high concentrations of acetone and VOCs were found in the LS in summer (up to 2.5 ppbv acetone), but much lower in winter, with the VOC load being between 0.5 - 2.5 ppbC. **H. Feldman** presented water vapour from the assimilation model ROSE, which is nested with the high resolution EURAD model; the results suggest low biases of water vapour at 215 hPa compared to ECMWF data. **J.-P. Pommereau** presented tropical observations from long-duration balloon as part of the HIBISCUS project. Very large variability was found in the NO_x distribution near the tropical tropopause, whilst the variability in ozone was very small. **D. Fahey** stated that HCl would be a very useful tracer of STE on the basis of the correlation of HCl with O_3. **F. Borchi** compared tropical NO_x fields calculated by the 3D CTM REPROBUS with observations from the HIBISCUS project. **M. Hitchmann** discussed a connection between the Asian summer monsoon and the Australian High to explain the 'croissant-shape' area with high ozone columns found in the southern midlatitudes; different potential transport pathways were discussed. Finally **R. Salawitch** described the Tropical Chemistry-Climate Coupling experiment (TC^4); a campaign is planned for 2004-2005 over Darwin or Guam.

AS.9 Session: Chemical Data Assimilation

Conveners: **H. Eskes** (eskes@knmi.nl), **B. Khattatov, W. Lahoz**.

There were 6 oral presentations:

D. Lary showed how data assimilation and related data analysis techniques can be used to improve our knowledge of atmospheric chemistry. Kalman filter analyses of ATMOS and UARS observations were presented. The representativeness error, information content, skill score and data heterogeneity were also discussed. Based on the assimilation, information on ranking the species can be derived: species with a high information content (like first of all ozone) strongly determine the chemistry and accurate measurements of these species have a high priority.

H. Elbern discussed the assimilation of chemical observations and focused on the terms "observability", "representativity" and "controllability". Many critical species are not observed by the present satellites and ground networks, (e.g. N_2O_5, ClO and HCl in the stratosphere, and hydrocarbons in the troposphere). The current stratospheric observations provide strong constraints, but the troposphere is still largely undersampled. He also stressed the importance of "controllability": an *a-posteriori* validation of the covariances in the assimilation with the chi-square test.

K. Wargan discussed the impact of using flow-dependent error correlations in data assimilation with the DAO Ozone DAS. The flow dependence is computed by evaluating the covariances at the end of 24h back trajectories. Benefits are found especially in unobserved regions (e.g. polar night).

S. Migliorini gave a detailed discussion on the observation operator and covariances for the assimilation of MIPAS profiles. This work closely follows the retrieval formalism of Rodgers, and special focus was given to the use of averaging kernels and complications related to vertical interpolations.

V. Yudin provided an overview of the tropospheric tracer assimilation work done at NCAR using the MOZART-2 model. The first results were shown for the Version 3 CO retrievals from the MOPITT instrument. New ideas are proposed for an improved representation of the model error.

Q. Errera described the 4D-Var chemical analysis of MIPAS observations, based on the BASCOE stratospheric modelling and assimilation system. This is one of the first systems to analyse ENVISAT-MIPAS observations of H_2O, O_3, HNO_3, CH_4, NO_2 and N_2O on a quasi-operational basis (since September 2002). The comparisons with UARS-HALOE measurements show good agreement for ozone and NO_x. The water vapour and methane concentrations were found to be smaller than HALOE.

The 15 posters of the session discussed assimilation techniques, covariance modelling and analyses of satellite observations of the atmospheric composition based on measurements from GOMOS, MIPAS, SCIAMACHY, ODIN, GOME, and MOPITT.

AS 20 Session : Polar Stratospheric Clouds

Convenors: **K. Carslaw** (carslaw@env.leeds.ac.uk), **T. Deshler** and **J. Remedios**

The aim of this session was to synthesize the current state of knowledge of PSCs and to present results from the latest campaigns. The oral session started with three presentations on solid PSC formation. **T. Koop** reported on our current understanding of solid particle nucleation in the polar stratosphere, on experiments attempted to quantify

homogeneous and heterogeneous nucleation by freezing of $HNO_3/H_2SO_4/H_2O$ solutions, as well as on more recent ideas on solid particle formation by sedimentation out of 'mother clouds'. **K. Drdla** presented model calculations of the effect of variable concentrations of heterogeneous nuclei and compared them with observations. **O. Möhler** showed results from the AIDA chamber investigating the effect of heterogeneous nuclei on solid nitric acid particle formation. They have observed solid formation, but have yet to determine the molar composition of the particles. Overall, from these three presentations it can be concluded that solid PSCs could form heterogeneously, although the identity of possible nuclei in the stratosphere remains to be identified. **R. Spang** showed early observations of PSCs from MIPAS on ENVISAT, demonstrating the capability of the instrument to detect the temporal evolution of PSC cloud top height. **M. Fromm** showed an extensive record of POAM PSC observations, including the 2002/3 SOLVE II-VINTERSOL campaign. The PSC occurrence frequency changed through the winter, possibly in response to denitrification. **G. Mann** presented 3-D simulations of denitrification using the Leeds DLAPSE model and described the factors that appear to control the severity of denitrification. The 2002/3 winter was fairly strongly denitrified, though not as much as in 1999/2000. **H. Schlager** showed observations of denitrification from the NO_y instrument on board the Geophysica during the EUPLEX campaign, with a distinctive signature of de- and re-nitrification that agrees reasonably well with the DLAPSE model. Finally, in his solicited talk **K. Mauersberger** presented a very personal view of the discovery and significance of NAT particles. His work spans the full range of discoveries related to NAT, from the first laboratory determination of NAT thermodynamic properties to the first detection of NAT in the stratosphere by using balloon-borne instruments.

AS26 Session: Water vapour and its isotopic composition in the UT and stratosphere

Main Organizer: **K. Boering** (boering@cchem.berkeley.edu)

The goal was to discuss the latest developments in the measurement, modelling, and interpretation of water and its isotopic compositions (i.e. the deuterium, tritium and oxygen-18 content).

A. Gettelman opened the session by introducing the topic of water vapour and its isotopic fractionation in the tropical tropopause layer (TTL); he compared new results from both trajectory-based and 3D global CTMs. **K. Rosenlof** presented observations from HALOE in the 100-70 hPa tropical region, as well as NOAA CMDL frost-point balloon observations in the LS, which show a significant decrease in water vapour over the past two years. She discussed the possible links both to decreases in tropical tropopause temperatures, as well as to increases in stratospheric CH_4 due to a widening of the tropical upwelling region. **M. Dameris** discussed the use of cloud-screened microwave limb-sounder data of relative humidity to produce the global distribution of ice-supersaturated regions at 147 and 215 hPa. **M. Geller** investigated the 3D-structure of temperatures in the tropical tropopause region and defined a "dehydration index" based on the volume of the atmospheric region with temperatures colder than a reference temperature. Linking the dehydration indices with tropical upwelling can explain the observation of the beating of 3 frequencies from the annual cycle in temperature and the temperature variations associated with the QBO and ENSO.

G. Toon (in absentia with assistance from **R. Salawitch**) presented ATMOS observations of HDO and H_2O using recently measured spectral lines that enable extension into the TTL. The isotopic composition remains quite constant in the TTL, despite a decrease in water vapour mixing ratios by a factor of 5 with altitude within the TTL. The null isotopic gradient requires that a major role must be played by convective processes. **J.A. Smith** discussed the incorporation of isotope microphysics into both a parcel model and a large eddy simulation in order to quantify the source of deuterium for the TTL; **D. Murtagh** presented new measurements of HDO and $H_2{}^{18}O$ from the Odin satellite.

C. Webster presented in situ measurements of HDO, $H_2{}^{16}O$, $H_3{}^{18}O$, and $H_2{}^{17}O$ in the UTLS from the ALIAS instrument aboard the WB-57. High isotopic variability was observed, from near-Rayleigh distillation to highly enriched. **A. Dessler** showed model results for water vapour in the TTL including HDO and predicting that lofted ice is important in simulating the recently observed null gradient in isotopic composition. **A. Zahn** extended modelling of water vapour isotopic compositions into the middle and upper troposphere, where the oxidation of CH_4 (as well as isotope exchange reactions for the oxygen isotopes) become an important influence beyond the isotopic compositions determined by fractionation in the TTL.

The posters included: *(a) water vapour observations* by **P. Mote** (on subseasonal variability in the tropical tropopause region); **G. Vaughan** (on comparison of water vapour in the UT from radiosondes and two hygrometers); **M. Coffey** (on the long-term change in stratospheric water vapour from a reanalysis of column measurements from IR spectra); **S. Nyeki** (on column water vapour using a PFR radiometer at a high-Alpine site); and **E. Chiou** (on the upcoming SAGE II and SAGE III water vapour datasets); *(b) observations of water vapour isotopes* by **N. Lautie** (by Odin/SMR measurements); **K. Jucks** (on far-IR remote sensing from balloons); **K. Boering** (on the annual mean D/H ratio of water vapour entering the stratosphere inferred from high precision CH_4 and H_2 isotope measurements from the ER-2); and **F. Rohrer** (on the longest-lived mode of stratospheric tracer distributions from the relaxation of tritiated water vapour after the thermonuclear test explosions in the 1960s); *(c) development of new instrumentation for measuring water isotopes* by **T. Hanisco** (by aircraft-based instrumentation for *in situ* measurements in the UTLS using a new water photolysis system with the pre-existing OH instrument); **P. Franz** (on continuous-flow isotope ratio mass spectrometry to measure very small stratospheric water samples); **J.-L. Bertaux** (on "SOIR" – solar occultation in the infrared); and **M. Andres-Hernandez** (on water vapour in the 920-950 nm range using cavity ringdown spectroscopy); and *(d) modelling of water vapour and/or its isotopes in the UT and stratosphere* by **H. Wernli** (on troposphere-to-stratosphere transport and implications for water vapour in the extratropical lowermost stratosphere based on a Langrangian climatology for the ECMWF 15-year reanalysis period); **M. Bonazzola** (on transport and dehydration in the tropical tropopause from 3-month back trajectories); **H. Hatsushika** (on a stratospheric "sprinkler" over the maritime continent from a trajectory analysis of 3D-AGCM-simulated 3D-wind and temperature); **J. Lyons** (on the mass-independent fractionation in stratospheric water using a midlatitude box model); **E. Moyer** (on 3D-NCAR MATCH CTM of seasonal variation in isotopic compositions); and **G. Schmidt** (3D-GISS GCM modeling of $H_2{}^{18}O$, HDO, and HTO).

Future SPARC and SPARC-related Meetings

2003

04 November: Jim Angell 80th Birthday Symposium, Silver Spring, Maryland, USA. (http://www.arl.noaa.gov/ss/climate/AngellSymposium.html) A one-day symposium honouring and celebrating the career of Dr. James K. Angell. Organizer: D. Seidel (dian.seidel@noaa.gov)

05 November: SPARC Workshop on Understanding Seasonal Temperature Trends in the Stratosphere, Silver Spring, Maryland, USA. (http://www.arl.noaa.gov/ss/climate/SPARCWorkshop.html) A one-day workshop organized by the SPARC Stratospheric Indicators of Climate Change initiative. Organizing committee: V. Ramaswamy (V.Ramaswamy@noaa.gov) and W. Randel (randel@ucar.edu)

17-19 November: Workshop on Process-orientated validation of coupled chemistry-climate models, Grainau/Garmisch-Partenkirchen, Germany. (http://www.pa.op.dlr.de/workshops/ccm2003/index.html)
Chair: N. Harris (Neil.Harris@ozone-sec.ch.cam.ac.uk)

18-19 December: Joint UTLS Ozone and CWVC Workshop "Aerosols in the UTLS", St Hugh's College, Oxford, UK. Organizer (manager@utls.nerc.ac.uk): R. Grainger

2004

10-14 January: AGU Chapman Conference on Gravity Waves Processes and Parameterization, Kohala Coast, Hawaii, USA. (http://www.agu.org/meetings/cc04acall.html) Chair: K. Hamilton (kph@soest.hawaii.edu)

15-20 March: 34th Saas-Fee Advanced Course: "The Sun, Solar Analogs and the Climate", Davos, Switzerland (http://www.pmodwrc.ch/pmod.php?topic=saas_prelim) Chair: M. Lockwood

01-08 June: Quadrennial Ozone Symposium "Kos 2004", Kos, Greece. (http://lap.physics.auth.gr/ozone2004/) Chair: C. S. Zerefos (ozone2004@geol.uoa.gr)

07-12 June: 3rd Workshop on Long-term trends in the atmosphere, Sozopol, Bulgaria. Chair: K. Georgieva (kgeorg@bas.bg)

18-25 July: 35th COSPAR Scientific Assembly, Paris, France. (http://www.cospar2004.org/gb_welcome.htm)
Chair: M.-L. Chanin (chanin@aerov.jussieu.fr)

- Interdisciplinary lectures (relevant of SPARC):
  - **21 July:** P. Crutzen "First ENVISAT Results"
  - **23 July:** C. Fröhlich "Solar Radiation and Climate"
- SPARC co-sponsored sessions:
  - **A 1.1 -** Atmospheric Remote Sensing: Earth's Surface, Troposphere, Stratosphere and Mesosphere. Chair: J. Burrows
  - **C.2.3 -** Long-term Changes of Greenhouse Gases and Ozone and their Influence on the Middle Atmosphere. Chair: D. Chakrabarty
  - **C.2.5. -** Structure and Dynamics of the Arctic and Antarctic of the Middle Atmosphere. Chair: M. Rapp
  - **D 2.1/C2.2/E 3/1 -** Influence of the Sun's Radiation and Particles on the Earth's Atmosphere and Climate. Chair: J. Pap

Deadline for Abstract Submission: February 15, 2004.

01-06 August: 3rd SPARC General Assembly 2004, Victoria Conference Centre, Victoria (BC), Canada. (http://sparc.seos.uvic.ca/)
Chairs: A. Ravishankara (ravi@al.noaa.gov) and T. Shepherd (tgs@atmosp.physics.utoronto.ca)

- Stratospheric climate and indicators of climate change
- Stratospheric data assimilation
- Transport and mixing in the stratosphere and between stratosphere and troposphere
- Gravity-wave processes and their parameterization
- Stratospheric and upper tropospheric water vapour
- Chemistry, radiation, aerosols and dynamics in the UT/LS
- Chemistry-climate modelling of the stratosphere

A particular emphasis for this General Assembly will be chemistry-climate coupling.
Deadline for Abstract Submission: January 31, 2004.

09-12 August: 12th SPARC SSG Meeting, Canada.

04-09 September: 8th International IGAC Conference, Christchurch, New Zealand (http://www.IGAConference2004.co.nz/)
Chairs: U. Lohmann (ulrike@fizz.phys.dal.ca) and P. Rasch (pjr@ucar.edu)
The focus of the 2004 IGAC Conference will be Atmospheric Chemistry in the Environment

Edited by the SPARC Office

Service d'Aéronomie, CNRS, BP 3
91371 Verrières-le-Buisson cedex, France
Tel: +33- 1 64 47 43 15
Fax: +33- 1 64 47 43 16
Email: sparc.office@aerov. jussieu.fr
http://www.aero.jussieu.fr/~sparc/

Published by Météo-France -
Direction commerciale et de la communication

ISSN 1245-4680 - Dépôt légal 3ème trimestre 2003